

**DESIGN, CHARACTERIZATION
AND APPLICATION OF THE
MULTIPLE AIR-LIFT LOOP BIOREACTOR**

Wilfried A.M. Bakker

Promotor: dr. ir. J. Tramper
hoogleraar in de bioprocestechnologie

Co-promotoren: dr. ir. C.D. de Gooijer
universitair docent bij de sectie Proceskunde
dr. H.H. Beeftink
universitair docent bij de sectie Proceskunde

NN08201, 2029

Wilfried A.M. Bakker

**Design, characterization and application of the
Multiple Air-lift Loop bioreactor**

Proefschrift

ter verkrijging van de graad van doctor
in de landbouw- en milieuwetenschappen
op gezag van de rector magnificus,
dr. C.M. Karssen,
in het openbaar te verdedigen
op dinsdag 19 december 1995
des namiddags te vier uur in de Aula
van de Landbouwuniversiteit Wageningen

ISBN: 919514

ISBN 90-5485-479-0

BIBLIOTHEEK
LANDBOUWUNIVERSITEIT
WAGENINGEN

Cover: Scheme of the Multiple Air-lift Loop bioreactor

STELLINGEN

1. Het optellen van de verdunningssnelheden, in plaats van de verblijftijden, van in serie geschakelde reactoren leidt tot grove overschattingen van de prestaties van een serieschakeling van reactoren ten opzichte van die van een enkelvoudige reactor met eenzelfde totaal volume.

Lee, J.M.; Pollard, J.F.; Coulman, G.A. 1983. Ethanol fermentation with cell recycling: computer simulation. *Biotechnol. Bioeng.* 25: 497-511.

2. Het fileleed in Nederland kan worden voorkomen door, analoog aan de succesvolle invoering van de wisselstrook tussen 't Gooi en Amsterdam, het samenvoegen van beide weghelften van alle rondwegen om steden tot één wisselstrook, waarbij 's ochtends tegen de klok in wordt gereden en 's avonds omgekeerd.
3. Almere zou nooit binnen 20 jaar meer dan 100000 inwoners hebben gehad als niet eerst Lelystad was gebouwd.
4. De dunne darm is een uitstekend voorbeeld van een propstroom-bioreactor.
5. Nieuwe AIO's zouden hun nieuwe, snelle en vaak onderbezette PC's moeten ruilen tegen die van oudere AIO's zodat zij allen, gedurende de hele promotie, gemiddeld over een vlotte PC beschikken.
6. De constatering dat voor een belegger één goed idee per jaar voldoende is, geeft een onderzoeker stof tot nadenken over een omscholingscursus.
7. Het herhaaldelijk laten uitlopen van nachtelijke wegwerkzaamheden geeft blijk van een grove minachting voor de werkzaamheden van anderen.
8. Fokker is een duur 'speelgoed'; in plaats van de voortdurende steun met miljarden is het voordeliger dit bedrijf te sluiten en elke werknemer een ton per jaar te geven.

9. Het is merkwaardig om te moeten constateren dat de huizenprijzen in Flevoland niet passen bij de status als ontwikkelingsgebied waarvoor EG subsidies worden ontvangen.
10. In verband met de gevolgen van het broeikaseffect is het raadzaam om bij het plannen van nieuw land en een vliegveld in zee alvast rekening te houden met het smelten van de poolkappen en een mediterraan klimaat.
11. Het concheerproces is een cruciale stap in de chocoladebereiding.
12. De afgelopen jaren is bewezen dat de parlementaire enquête een prima bezigheids-therapie voor politici is; mogelijk heeft het correctieve referendum een zelfde heilzame werking.

Stellingen behorende bij het proefschrift: 'Design, characterization and application of the Multiple Air-lift Loop bioreactor'.

W.A.M. Bakker

Wageningen, 19 december 1995

Voor Stephanie en Marijn

VOORWOORD

Dit proefschrift is tot stand gekomen door de medewerking van zeer veel mensen. Die wil ik hierbij allemaal bedanken. Enkele personen wil ik hier met name noemen.

Hans Tramper die mij grote vrijheid gaf, en mij veel heeft geleerd. In een adem kunnen daarbij *Kees de Gooijer* en *Rik Beeftink* worden genoemd. Alle drie bleken zij onmisbaar. Heren, ga zo door!

Mijn mede dierlijke celkwekers *Fred van den End*, *Frank van Lier* en *Arie van Oorschot* waren een steun en toeverlaat voor alles en nog wat. De leden van de nitrificatie groep, *Imke Leenen*, *Vitor Santos*, *Jan Hunik* en *René Wijffels*, leerden mij immobiliseren en leverden de benodigde bacteriën en apparatuur. *Henk van Sonsbeek* voorzag mij van zijn stimulerende commentaar en adviezen. Verder leverde *Arthur Oudshoorn* een inbreng in alle werkbesprekingen.

Veel dank ben ik verschuldigd aan de studenten die zich hebben ingezet voor mijn onderzoek. In volgorde van opkomst: *Joost Knitel*, *Eric van Can*, *Harold van Rijswijk*, *Marcel den Hertog*, *Marjolein Bakker*, *Isabel Araújo*, *Maria Karadima*, *Mariët van de Noort*, *Mohd. Ali Hassan*, *Pieter Pelders*, *Bert Dijkink*, *Thomas Schäfer*, *Patrick Kers* en *Pieter Overdevest*. Jullie optimisme, toewijding en daadkracht hebben een belangrijke bijdrage geleverd aan dit proefschrift.

Zonder de hulp van *Serge Lochtman* en *Arie van Oorschot* was het verzorgen van het practicum 'Opschaling Dierlijke Celkweek' onmogelijk geweest.

Mijn kamergenoten, en de overige medewerkers van Proceskunde, zorgden voor een, bijna legendarische, prettige werksfeer met ook veel activiteiten naast het werk. Daarin passen zeker de vele potjes tennis met Kees (zelfs tot hoog in de Zwitserse Alpen), waarin elk punt met volle overgave werd bevochten. Het is moeilijk toe te geven, maar uit mijn archieven bleek dat, sinds oktober 1991, Kees 13 volledig uitgespeelde sets heeft gewonnen tegen 11 voor mij.

In het verre Groningen waren *Leo van der Pol* en *Gerben Zijlstra* altijd bereid wat bevroren of reeds groeiende hybridoma's te leveren, of monoclonalen te laten analyseren.

Tenslotte bedank ik de medewerkers van de glasblazerij, automatisering, electronica, werkplaats, fotolocatie, tekenkamer, en het chemicaliënmagazijn voor de vakkundige ondersteuning.

ABSTRACT

Bakker, W.A.M., 1995. Design, characterization and application of the Multiple Air-lift Loop bioreactor. Ph.D. thesis, Wageningen Agricultural University, The Netherlands (174 pp., English and Dutch summaries).

Key words: Hydrodynamics, mixing, oxygen transfer, reactor series, modeling, optimization, hybridomas, *Nitrobacter agilis*, invertase.

A new bioreactor is introduced: the Multiple Air-lift Loop reactor (MAL). The MAL consists of a series of air-lift loop reactors within one vessel. With the MAL, a new type of geometry for air-lift reactors with an internal loop is introduced. This new geometry was characterized with respect to hydrodynamics, mixing and oxygen transfer. The hydrodynamics were described by an existing model. Hydrodynamics, mixing and oxygen transfer in the new reactor configuration were comparable to that in conventional air-lifts with an internal loop.

The design and use of the MAL as a reactor cascade, to approximate plug-flow behaviour, were studied. Biological model systems were used to compare the reactor series to a single vessel. These model systems included immobilized invertase and nitrifying bacteria. With the immobilized invertase it was shown that a three-compartment MAL gives an improved substrate conversion when compared to a single vessel of the same overall volume. This could be described with a previously developed model. Also for the immobilized nitrifying bacteria improved substrate conversion was shown in the comparison between a series and a single vessel. Free suspended hybridomas were used for monoclonal antibody (MAb) production. It was shown that reactor series can be useful research tools for kinetic studies. In the second vessel in the series conditions were obtained that can hardly be reached in a single vessel. Not only growth, but also death could be studied under stable conditions. A model was derived that describes hybridoma growth and their MAb production.

Vessels in a series can be of equal volume, but very often unequal volumes can be more advantageous. Therefore, choosing the appropriate reactor volumes is an important design step, which is discussed for different applications. Finally, a general procedure for choosing the optimal bioreactor cascade configuration for any application is given.

CONTENTS

1. INTRODUCTION TO THE MULTIPLE AIR-LIFT LOOP BIOREACTOR 1

Physical characterization

2. HYDRODYNAMICS AND MIXING IN A MULTIPLE AIR-LIFT
LOOP REACTOR 7

3. OXYGEN TRANSFER IN A MULTIPLE AIR-LIFT LOOP REACTOR 31

Theoretical considerations

4. BIOREACTORS IN SERIES: AN OVERVIEW OF DESIGN PROCEDURES
AND PRACTICAL APPLICATIONS 47

Biological modelsystems

5. SUCROSE CONVERSION BY IMMOBILIZED INVERTASE IN A
MULTIPLE AIR-LIFT LOOP BIOREACTOR 95

6. HYBRIDOMAS IN A BIOREACTOR CASCADE: MODELING AND
DETERMINATION OF GROWTH AND DEATH KINETICS 117

7. NITRIFICATION BY IMMOBILIZED *NITROBACTER AGILIS* CELLS
IN AN AIR-LIFT LOOP BIOREACTOR CASCADE 145

Future trends

8. SERIAL AIR-LIFT BIOREACTORS FOR THE APPROXIMATION
OF AERATED PLUG-FLOW 157

Summary 169

Curriculum vitae 173

Bibliography 174

Part of this chapter 1 was used for the publication in chapter 8.

CHAPTER 1

INTRODUCTION TO THE MULTIPLE AIR-LIFT LOOP BIOREACTOR

INTRODUCTION

In this thesis a novel type of bioreactor is introduced: the Multiple Air-lift Loop reactor (MAL). The MAL consists of a series of air-lift loop reactors incorporated into one vessel. Serial reactors, like the MAL, can be used for many goals in biotechnology. In this introduction, bioreactor series will be described shortly, and then, more specifically, the MAL will be discussed briefly. This is followed by an outline of this thesis.

REACTOR SERIES

Reactor series find their application not only in chemical engineering, but also in food and bioprocess engineering. Multistep processes are not an uncommon feature in biotechnology. The subsequent conversion steps can be executed separately in a series

of vessels. An alternative use of the reactor cascade is to approximate plug-flow behaviour. Here one reaction step is applied repeatedly in each compartment of a serial bioreactor. This may be done when optimal bioreactor design with respect to a minimal total residence time at a given substrate conversion is the goal. In this thesis the design and applicability of bioreactor cascades for plug-flow approximations was studied.

THE MULTIPLE AIR-LIFT LOOP REACTOR

The MAL, which can both be used for scale-up of the majority of multi-step systems and for plug-flow approximations, consists of a series of internal-loop air-lift reactors within one vessel (Figure 1). The central MAL compartment is a conventional internal-loop air-lift reactor with aeration in the annulus. Subsequent compartments in the MAL are concentric. The annular-shaped compartments have a circular baffle which splits them into a riser and a downcomer section. Medium 'travels', driven by gravity, through the cascade via overflows. The advantages of the MAL compared to single air-lift loop reactors in series include:

- many configurations can be constructed for various applications *e.g.*:
 - supplying different gases to the subsequent compartments to, for example, carry out aerobic and anaerobic processes in series within one vessel,
 - remove the baffles to obtain a multiple bubble column,
 - direct the medium flow from the inside to the outside, or vice versa;
- no extra pumps or hoses are needed for medium transport;
- the reactor series can be sterilized as one reactor;
- old reactor vessels can be reused and upgraded to a MAL by placing walls, baffles and gas distributors;
- inner walls and baffles can be of simple construction because hydrostatic pressure acts on both sides.

and the disadvantages for the same comparison include:

- on a lab scale the compartments are narrow, which makes:
 - cleaning difficult and,

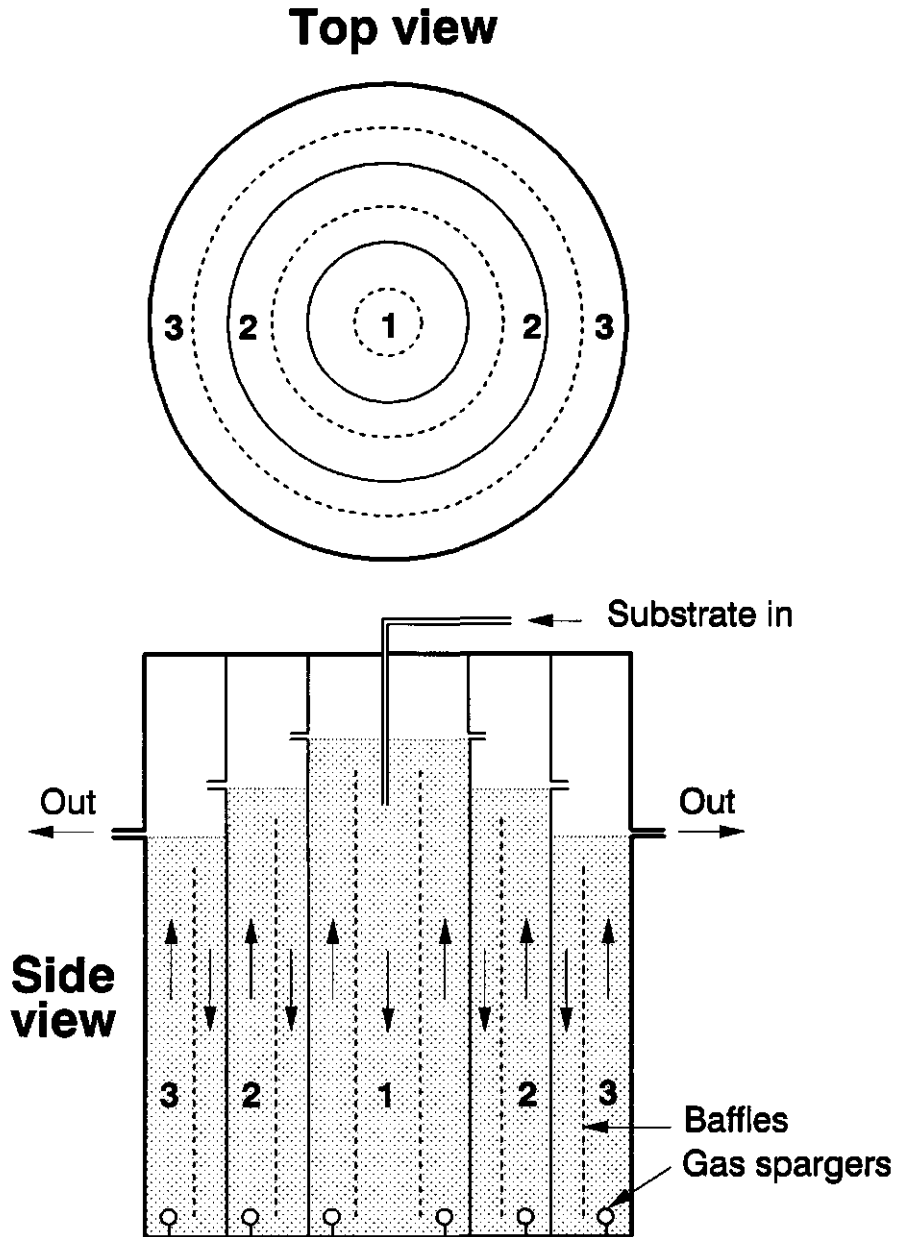


Figure 1. Three compartment Multiple Air-lift Loop bioreactor cross-sectional side and top view.

- leaves little space for electrodes and other inserts;
 - the gas distributor in the outer compartments is relatively complex.
- Nevertheless, there are several cases where the advantages outweigh the disadvantages, as shown in this thesis.

OUTLINE OF THIS THESIS

With the outer compartments of the MAL, a novel type of geometry for air-lift reactors with an internal loop is introduced. Hydrodynamic properties affect shear forces, mixing, and mass and heat transfer, which are all important aspects in the design of reactors for bioprocesses. Hydrodynamics are greatly influenced by reactor geometry. This made knowledge of the hydrodynamics necessary for designing a MAL, and thus a *Physical characterization* was carried out, which is described in the chapters 2 and 3. In these chapters the MAL is also described in more detail.

Vessels in a series can be of equal volume, but very often unequal reactor volumes can be more advantageous when optimal bioreactor design with respect to a minimal total residence time at a given substrate conversion is the goal. Therefore, choosing the appropriate reactor volumes is an important design step, which is discussed in the *Theoretical considerations* section (chapter 4) for different applications.

To investigate the applicability of the MAL in practice, and to evaluate the design steps known from the previous chapters (2 - 4), several *Biological modelsystems* were studied. These included freely suspended hybridoma cells for monoclonal-antibody production. Further, enzymes (invertase for sucrose conversion) and growing cells (nitrifying bacteria for nitrite conversion) were used as an immobilized biocatalyst. With the immobilized invertase it was shown in practice that a three-compartment MAL gives an improved substrate conversion when compared to a single vessel of the same overall volume (chapter 5). The hybridomas were grown in a series of two continuously-operated stirred vessels, instead of using a MAL, for practical reasons. Here, bioreactor series were shown to be useful tools for kinetic studies (chapter 6). Finally, in chapter 7, for immobilized nitrifying bacteria it was shown that a series of two air-lift loop reactors gives a better substrate conversion than

that in a single vessel of the same overall volume.

In chapter 8 the *Future trends* in the theoretical considerations discussed in chapter 4, with respect to the optimal design procedures, are addressed. Using the practical experience gained with the biological modelsystems (chapters 5 - 7) it was found that several prerequisites have to be fulfilled before a bioreactor optimization for plug-flow approximations can be carried out successfully. Also in this final chapter 8 the *Future trends* in physical characterization studies of air-lift reactors with an internal loop are given.

This chapter 2 has been published as: Bakker, W.A.M.; Van Can, H.J.L.; Tramper, J.; De Gooijer, C.D. 1993. Hydrodynamics and mixing in a Multiple Air-lift Loop reactor. *Biotechnol. Bioeng.* **42**: 994-1001.

CHAPTER 2

HYDRODYNAMICS AND MIXING IN A MULTIPLE AIR-LIFT LOOP REACTOR

SUMMARY

A new bioreactor, in which a series of air-lift reactors with an internal loop is incorporated into one vessel, is introduced. With this Multiple Air-lift Loop reactor (MAL) an approximation of an aerated plug-flow fermentor is strived for. Mixing, liquid velocity, and gas holdup were measured as a function of the gas flow rate in this new internal-loop reactor geometry. As a reference, hydrodynamics were also investigated in a conventional internal-loop reactor. A model description of the hydrodynamics in the second compartment of the MAL is given. This model is based on a two-phase, drift-flux model and a friction coefficient. Frictional losses were independent of the reactor bottom geometry, and were observed to increase with the gas flow rate as a result of the presence of stationary gas bubbles in the downcomer. The hydrodynamics and mixing of the second MAL compartment were comparable with those of conventional internal-loop reactors.

INTRODUCTION

The quest for new or optimal processes in biotechnology is still proceeding. Although the stirred-tank reactor (continuous or batchwise operated) dominates most bioprocess applications, the interest in alternative configurations is increasing. A promising alternative is the cascade of continuous stirred-tank reactors. The behavior of a series of ideal mixers approximates that of a plug-flow reactor [Levenspiel, 1972]. Such flexible reactor systems can be helpful tools for the optimization of bioprocesses [Hill and Robinson, 1989; Pirt, 1975; Shimizu and Matsubara, 1987].

The Multiple Air-lift Loop reactor (MAL) is a new type of Air-lift Loop Reactor (ALR). In this MAL, a series of ALRs with an internal loop is incorporated into one vessel. ALRs behave like nearly ideally mixed vessels [Verlaan *et al.*, 1989]. With the MAL, aerated plug-flow behavior can thus be approximated. A schematic side and top view of the MAL is given in Figure 1. The subsequent reactors in the MAL are concentrically placed, which introduces a new type of geometry for air-lift reactors with an internal loop. The torus-shaped compartments have a circular baffle that splits the compartment in a riser and downcomer. The central reactor is a conventional internal-loop reactor (ILR). Gasner [1974] suggested a rectangular MAL version for waste-water treatment; its geometry is, however, different from the MAL presented here.

Hydrodynamic properties affect shear forces, mixing, and mass and heat transfer. Hydrodynamics and mixing are greatly influenced by reactor geometry. Important design parameters are downcomer-to-riser area ratio [Bello *et al.*, 1984; Jones, 1985; Zuber and Findlay, 1965], the downcomer-to-bottom area ratio [Chisti *et al.*, 1988; Sukan and Vardar-Sukan, 1987], filling height above the draft tube [Chisti, 1989; Sukan and Vardar-Sukan, 1987; Weiland, 1984], and reactor height [Chisti, 1989]. This makes knowledge of the hydrodynamics necessary for designing a MAL, and thus this physical characterization study was started. The hydrodynamics and mixing for the new reactor geometry have been in particular studied in the second compartment of a MAL. Liquid velocity, gas holdup, and mixing time were measured as a function of the gas flow rate. Also the effect of downcomer-to-riser area ratio was investigated by varying the baffle diameter.

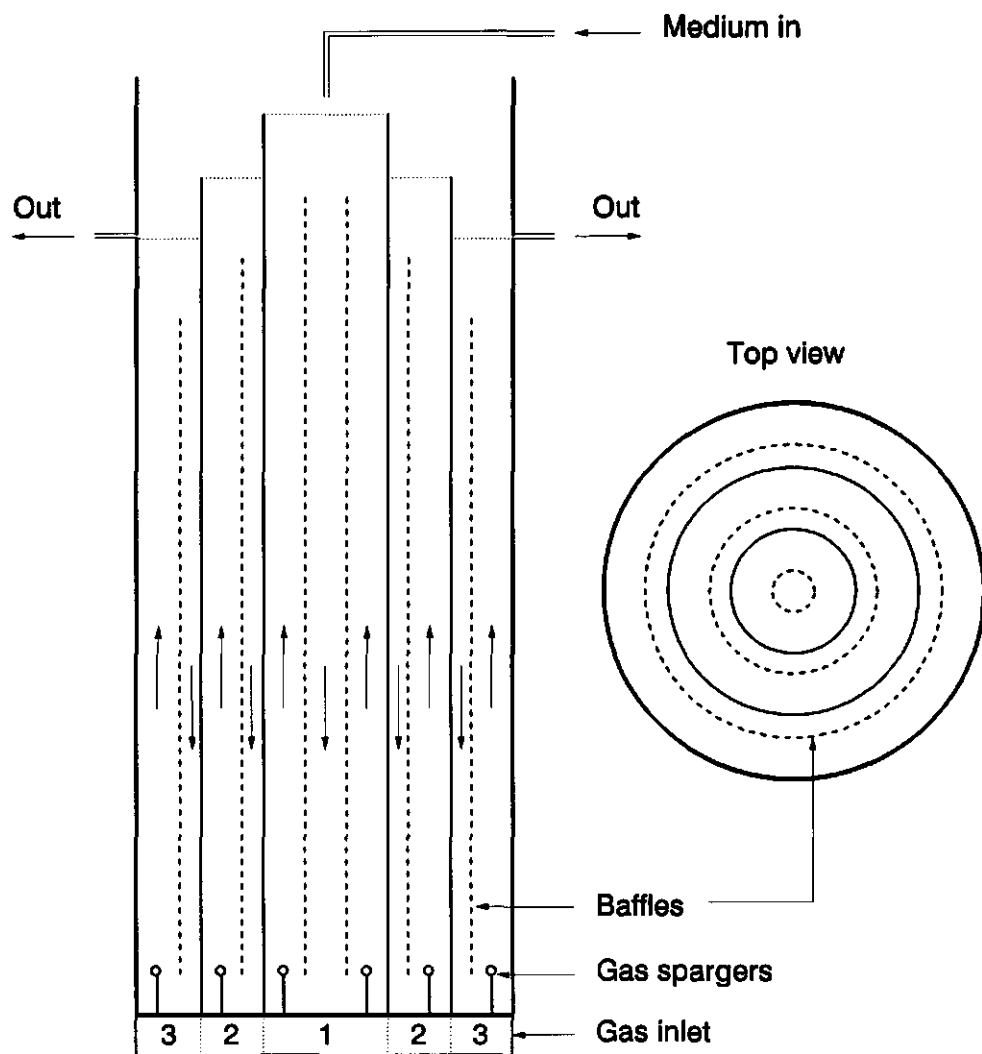


Figure 1. Three-compartment MAL, cross-sectional side and top view.

Consequently, the bottom area for flow under the baffle was also varied. To investigate the effects on hydrodynamics of varying the bottom area only, a conventional ILR was used. The ILR results are also compared with the hydrodynamics in the second MAL compartment.

A model description, in good agreement with the experimental data, of the hydrodynamics of the second MAL compartment, is given. The estimations are based on the two-phase, drift-flux model of Zuber and Findlay [1965], and on a friction coefficient derived from experimental data.

THEORY

In general, hydrodynamic models for ALRs are based on conservation laws of mass, momentum, and energy completed by empirical correlations. Van Sonsbeek [1992] reviewed the hydrodynamic models based on either momentum or energy conservation, and concluded that there is no advantage of using one approach over the other. The energy balance has been used frequently in recent literature [Chisti *et al.*, 1988; Garcia Calvo, 1989; Garcia Calvo and Letón, 1991; Jones, 1985]. A disadvantage of the energy balance approach is that all energy dissipation, which may be difficult to estimate, has to be accounted for. For applying the model based on the momentum conservation law, only a frictional loss coefficient is needed which can be determined from one-phase flow theory for external-loop reactors [Van Sonsbeek *et al.*, 1990; Verlaan *et al.*, 1986]. Because the momentum balance is straightforward, and has been applied successfully in various publications [Siegel *et al.*, 1986; Van Sonsbeek *et al.*, 1990; Verlaan *et al.*, 1986; Young *et al.*, 1991], it is also used in this work.

Liquid flow rate and gas holdup in ALRs depend on the gas flow rate. To model the relation between these quantities, two independent equations are required to calculate both dependent variables from the independent variable. The two equations used here are based on a momentum balance and on the two-phase, drift-flux theory of Zuber and Findlay [1965]. It is assumed that, in a steady state, the hydrostatic pressure difference between riser and downcomer (ΔP) is the driving force for liquid circulation:

$$\Delta P = (\alpha_r - \alpha_d) \Delta \rho g H \quad (1)$$

where α_r and α_d are the time average gas holdup in the riser and in the downcomer, respectively, $\Delta \rho$ the density difference between the liquid and gas phase, g the gravitational acceleration, and H the riser or downcomer length. Here, α_r , α_d , and $\Delta \rho$ are considered not to change over reactor height. The pressure drop due to overall frictional losses along the circulation loop is expressed as [Van Sonsbeek *et al.*, 1990; Verlaan *et al.*, 1986]:

$$\Delta P = K_f \cdot \frac{1}{2} \rho v^2 \quad (2)$$

where K_f is the overall frictional loss coefficient, ρ the liquid density, and v the average liquid velocity in an arbitrarily chosen reactor section. This velocity term, on which K_f is based, can be chosen arbitrarily, because the liquid velocities in all reactor sections are interrelated; the same liquid volume will flow through all reactor sections. Combination of Eqs. (1) and (2) leads to a stationary hydrodynamic force balance:

$$(\alpha_r - \alpha_d) \Delta \rho g H = K_f \cdot \frac{1}{2} \rho v^2 \quad (3)$$

In a steady state, the equation for momentum conservation is the same as for the force balance [Eq. (3)], as momentum is mass multiplied by velocity or force multiplied by time [Van Sonsbeek, 1992]. Thus, Eq. (3) is based on the momentum conservation law over the liquid phase.

With a known K_f and a relation between gas flow rate and liquid velocity, the ALR hydrodynamics (*i.e.* liquid velocity and gas holdup) can be predicted. Many authors [Clark and Flemmer, 1985; Lee *et al.*, 1987; Siegel *et al.*, 1986; Van Sonsbeek *et al.*, 1990; Verlaan *et al.*, 1986; Young *et al.*, 1991] based this relation on the Zuber and Findlay [1965] theory, which is also used here:

$$v_g = C \cdot (v_{gs} + v_{ls}) + v_{b\infty} \quad (4)$$

where v_g is the gas velocity in the riser, C is the distribution parameter, v_{gs} and v_{ls}

are the superficial gas and liquid velocity, respectively, and $v_{b\infty}$ is the terminal rise velocity of a bubble in an infinite stagnant medium. In Eq. (4), C accounts for radial distributions of gas concentration and liquid velocity for two-phase flow in circular tubes. Values for C approaching unity indicate flat flow and concentration profiles and, *e.g.*, $C = 1.5$ is found for a parabolic gas-concentration profile combined with a parabolic liquid-velocity profile. In Eq. (4), the gas velocity, v_g , in the riser is defined as:

$$v_g = \frac{v_{gs}}{\alpha_r} \quad (5)$$

From the continuity equation, liquid velocities in all reactor sections can be calculated:

$$v_{lr} A_r (1 - \alpha_r) = v_{ld} A_d (1 - \alpha_d) \quad (6)$$

in which v_{lr} and v_{ld} are average liquid velocities in the riser and downcomer, respectively. Superficial liquid velocities can be derived from these liquid velocities by:

$$v_{lsr} = v_{lr} (1 - \alpha_r) \quad \text{and} \quad v_{lsd} = v_{ld} (1 - \alpha_d) \quad (7)$$

where v_{lsr} and v_{lsd} are average superficial liquid velocities in the riser and downcomer, respectively.

MATERIALS AND METHODS

THE MAL

The vessel in study was the 0.034 m³ second compartment of a MAL with a glass outer wall (Figure 2). Three downcomer-to-riser area ratios could be configured by using interchangeable baffles with different diameters. Geometric data are given in Table I. One of the baffles consisted of non-transparent PVC and the other two of transparent perspex to allow visual observation of gas bubbles in the downcomer.

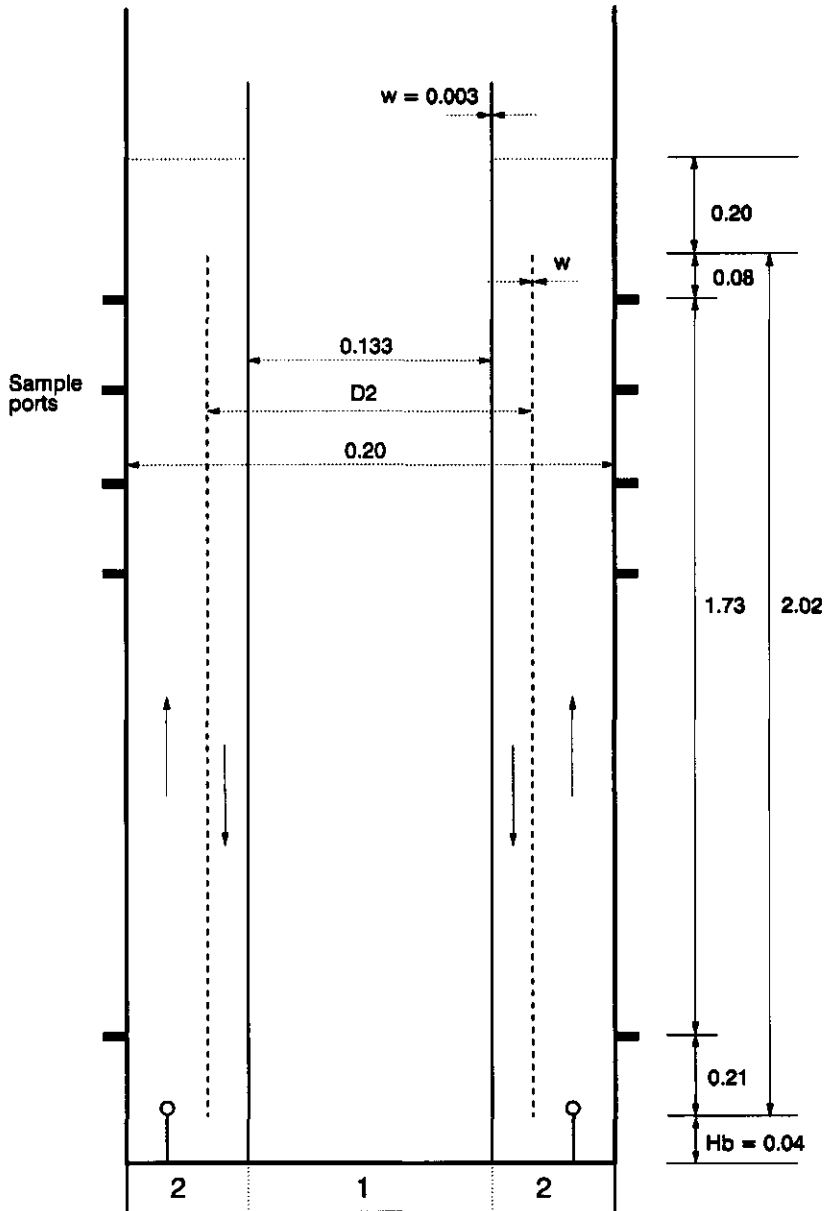


Figure 2. Schema of the second MAL compartment (not on scale). Inner diameters are given (m). Variable dimensions are summarized in Table I.

The tubular wall between the first and second compartment also consisted of transparent perspex.

THE ILR

A $1.5 \times 10^{-2} \text{ m}^3$ conventional ILR was constructed of glass cylinders. Inner diameters were $9.6 \times 10^{-2} \text{ m}$ and $6.8 \times 10^{-2} \text{ m}$ for the outer wall and the baffle, respectively. The baffle height was 2.0 m, and the liquid filling height above the baffle 0.10 m. Air was sparged in the central tube. The baffle height above the bottom of the ILR could be adjusted by interchangeable supports, resulting in different free areas for flow under the baffle (A_b). Geometric data are given in Table I.

Table I. Geometric data for MAL and ILR.

Config.	MAL			ILR			
	A	B	C	A	B	C	D
D_2 [m]	0.154	0.158	0.162	--	--	--	--
w [mm]	3.0	3.0	9.0	3.3	3.3	3.3	3.3
Hb [m]	0.04	0.04	0.04	0.031	0.052	0.081	0.102
A_d/A_r	0.31	0.43	0.91	0.78	0.78	0.78	0.78
A_d/A_b	0.18	0.22	0.27	0.70	0.29	0.27	0.21

SPARGERS

The ILR sparger consisted of sintered ceramic. The MAL sparger was made of a circular tube (stainless steel, $D = 5 \times 10^{-3} \text{ m}$) with 58 holes ($D = 5 \times 10^{-4} \text{ m}$) at equal distances. This sparger ring ($D = 1.85 \times 10^{-1} \text{ m}$) was connected by eight pipes ($D = 5 \times 10^{-3} \text{ m}$) to a gas inlet chamber to guarantee an equal distribution of air. Spargers for ILR and MAL were positioned at the riser entrance to prevent entrainment of bubbles into the downcomer due to turbulence in the bottom section.

EXPERIMENTAL CONDITIONS

A 20 mol.m^{-3} solution of KCl was used in all experiments to eliminate tracer effects on coalescence. Surface tension of the liquid was 73 mN.m^{-1} ; viscosity was

1.0 mPa.s. All experiments were carried out at $20 \pm 1^\circ\text{C}$.

HOLDUP

Gas holdup was registered by differential pressure measurement between two sample ports. Their distance was taken as large as possible in order to measure an average holdup. Sample ports were at least 0.08 m from the baffle top and bottom to eliminate entrance effects. Fully developed two-phase flow was assumed.

LIQUID VELOCITY

Liquid velocity was investigated by tracer response measurements. As a tracer, 10 cm³ of 2×10^3 mol.m⁻³ of either HCl or KOH was injected. This tracer was detected by two identical pH probes, which were positioned at a known distance from each other in the investigated reactor part. Tracer was injected at the entrance of the riser or downcomer for the ILR or MAL, respectively, and measured in the opposite reactor part. For practical reasons, liquid velocity was measured in the MAL riser. Superficial liquid velocities in the downcomer were calculated from these experimental data by using Eqs. (6) and (7). Friction coefficients were derived from these downcomer superficial liquid velocities to make the values comparable to the ILR data.

MIXING

Mixing behavior of the second MAL compartment was also studied by tracer responses. The experimental and calculation procedures are given by Verlaan *et al.* [1989]. Like for the velocity measurements, two electrodes were positioned in the riser. Tracer was injected 0.47 m below the upper electrode in the riser. The pH response was converted to ion concentrations as described by Verlaan *et al.* [1989]. Mixing time was defined as the time elapsed until the concentration deviated less than 5% from the calculated average for both electrodes.

RESULTS AND DISCUSSION

LIQUID VELOCITY AND HOLDUP

In Figure 3 downcomer liquid velocities and riser gas holdups are shown as a function of superficial gas velocity for four ILR configurations. Average values for the four ILR configurations are shown; effects from differences in bottom geometry on hydrodynamics were insignificant. Figures 4 and 5 show downcomer superficial liquid velocities and riser gas holdups at different superficial gas velocities for three MAL configurations.

The MAL and ILR results show the same trends. With increasing superficial gas velocities, liquid velocities rapidly became constant. From a certain gas velocity onward, the power supply was large enough for gas bubbles to flow completely through the downcomer (recirculation). From here onward, liquid velocities increased again with the gas flow rate. Obviously, for both reactor types, the downcomer relative gas-liquid velocity had to exceed the bubble terminal rise velocity before gas recirculation started. This value can vary due to variations in

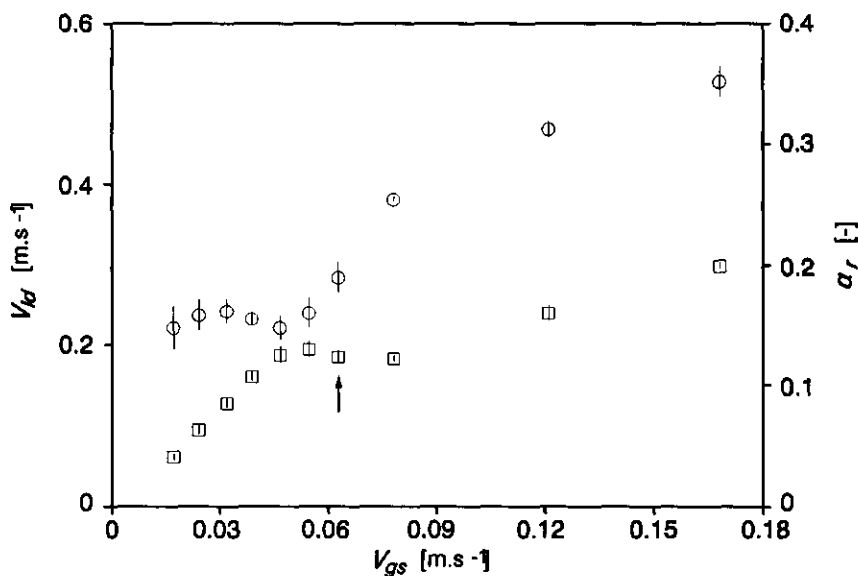


Figure 3. Average downcomer liquid velocity (O) and average riser holdup (□) for four ILR configurations (specified in Table I). Error bars give standard deviation. Arrow: onset of gas recirculation.

bubble sizes, but 0.25 m.s^{-1} is assumed to be the average value [Wallis, 1969]. Gas bubbles in the downcomer were observed to be larger than in the riser for both reactor types. The largest bubbles had the form of spherical caps and were formed by coalescence in the downcomer. Their rising velocity was in equilibrium with the downward flowing liquid and they were thus observed as stationary. When those bubbles grew further by coalescence they escaped upward.

Downcomer holdup was found to be a constant fraction of the riser holdup, at all gas flow rates, for all reactor configurations (Figure 6a and b). The average holdup ratio for the MAL configurations ($\alpha_d/\alpha_r = 0.875 \pm 0.006$), and for the ILR configurations ($\alpha_d/\alpha_r = 0.863 \pm 0.004$), were in agreement with earlier findings [Bello *et al.*, 1985; Chisti, 1989] ($\alpha_d/\alpha_r = 0.89$). Riser and downcomer holdup both increased with superficial gas velocity. This increase was less steep after the occurrence of gas recirculation in the ILR (Figure 3) than in the MAL (Figure 5). Furthermore, Figure 5 suggests pronounced geometric effects on gas holdup for the three MAL configurations. At all superficial gas velocities in Figure 5, lower riser gas holdups are observed with increasing downcomer-to-riser area ratio (A_d/A_r), this is going from MAL configuration A to C. However, comparable superficial gas velocities for different riser areas correspond to different gas flow rates. Plotting the holdup as a function of the gas flow rate (not shown) showed no such trend in holdup with different downcomer-to-riser area ratios (A_d/A_r) at the same gas flow rates for the three MAL configurations. These MAL results are comparable to findings for conventional ILRs [Bello *et al.*, 1985; Chisti, 1989].

Very low gas flow rates were not applicable for the MAL, because this resulted in an unequal distribution of gas over the sparger ring. This caused large irregular variations in liquid velocities. At higher gas flow rates with equal gas distribution, where the measurements were done, bubble coalescence in the riser probably caused local holdup differences that induced visually observed tangential liquid movements. Consequently, holdup measurements showed an increasing spread with an increasing gas flow rate. Holdup measurements however, could be replicated within 5% accuracy for both the MAL and the ILR.

For the MAL, the standard deviation in liquid-velocity measurements was 20%, probably due to irregularities in the tracer path between the electrodes. In spite of this limitation, the tracer-response method was used because those

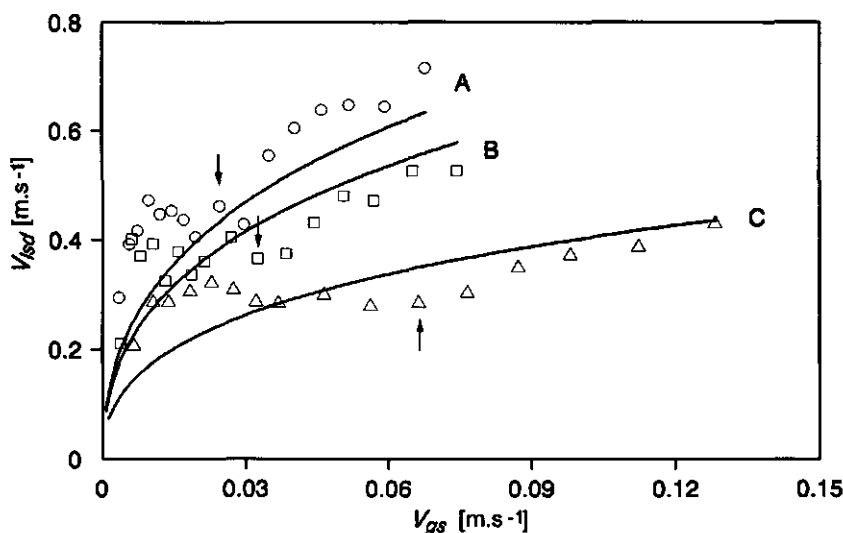


Figure 4. Superficial liquid velocity in the downcomer for three MAL configurations (specified in Table I): A (○), B (□) and C (Δ); solid lines: model estimations. Arrows: onset of gas recirculation.

deviations are inherent to the reactor type, and other methods also have their disadvantages. Liquid velocities in the ILR could be determined more accurately, within 10% standard deviation, which is acceptable in observing that Chisti [1989] reported variations of $\pm 30\%$ for liquid velocities in ILRs. The fluctuations were ascribed to gas entrainment in the downcomer, and comparable observations of fluctuating flows were described by Siegel *et al.* [1986] and were also seen in the present study.

FRICTION COEFFICIENTS

The model estimations were based on two input parameters: the gas flow rate, and the overall frictional-loss coefficient K_f . Theoretical K_f values for ILRs, derived from one-phase flow theory, were difficult to derive, because no accurate estimates of the frictional losses in the 180° turns at the top and bottom of the reactor could be made. Recent studies emphasize that entrance effects due to a flow which is not fully developed at the turns may cause additional frictional losses [Wachi *et al.*, 1991; Young *et al.*, 1991].

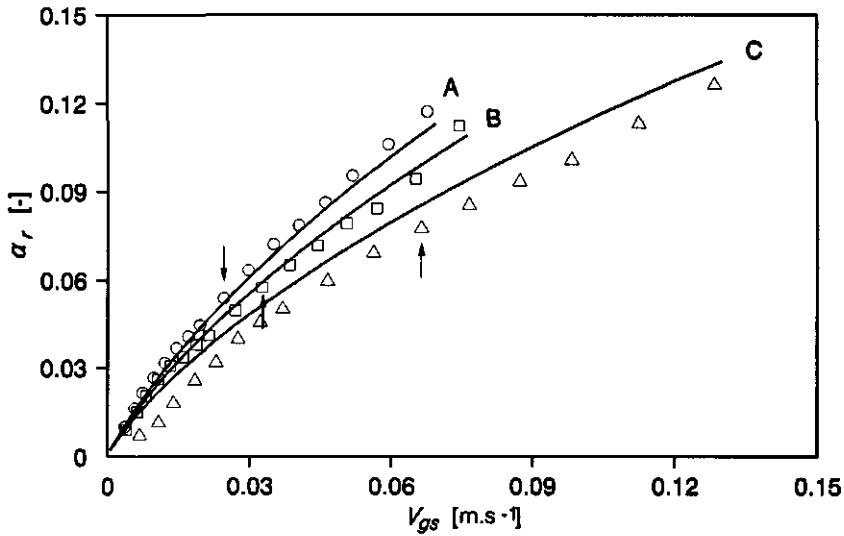


Figure 5. Riser gas holdup for three MAL configurations (specified in Table I): A (○), B (□) and C (△); solid lines: model estimations. Arrows: onset gas recirculation.

Friction coefficients were calculated from riser and downcomer holdup and superficial liquid velocity by using Eq. (3). The small difference between both holdups made this K_f determination very sensitive toward inaccuracies in experimental data. Nevertheless, the resulting K_f values show a clear positive trend with the superficial gas velocity for both the MAL and ILR (Figure 7a and b) up to the velocity where gas recirculation occurred. Linear regression on K_f as a function of superficial gas velocity in this range indeed showed a significant positive slope for each configuration - and also when K_f was calculated [Eq. (3)] on the basis of measured average liquid velocity instead of using superficial liquid velocities. This increase in K_f is not as expected from one-phase flow theory when applied to the current experimental conditions. During the experiments, the diameter of the described spherical-cap bubbles in the downcomer often was as large as the width of the downcomer torus. This flow regime is referred to as slug flow [Wallis, 1969]. Liquid velocity was approximately constant, and the flow regime turbulent at all gas flow rates. ($Re > 7000$ for all reactor configurations). For one-phase flow, this implies that wall friction coefficients should remain constant [Wallis,

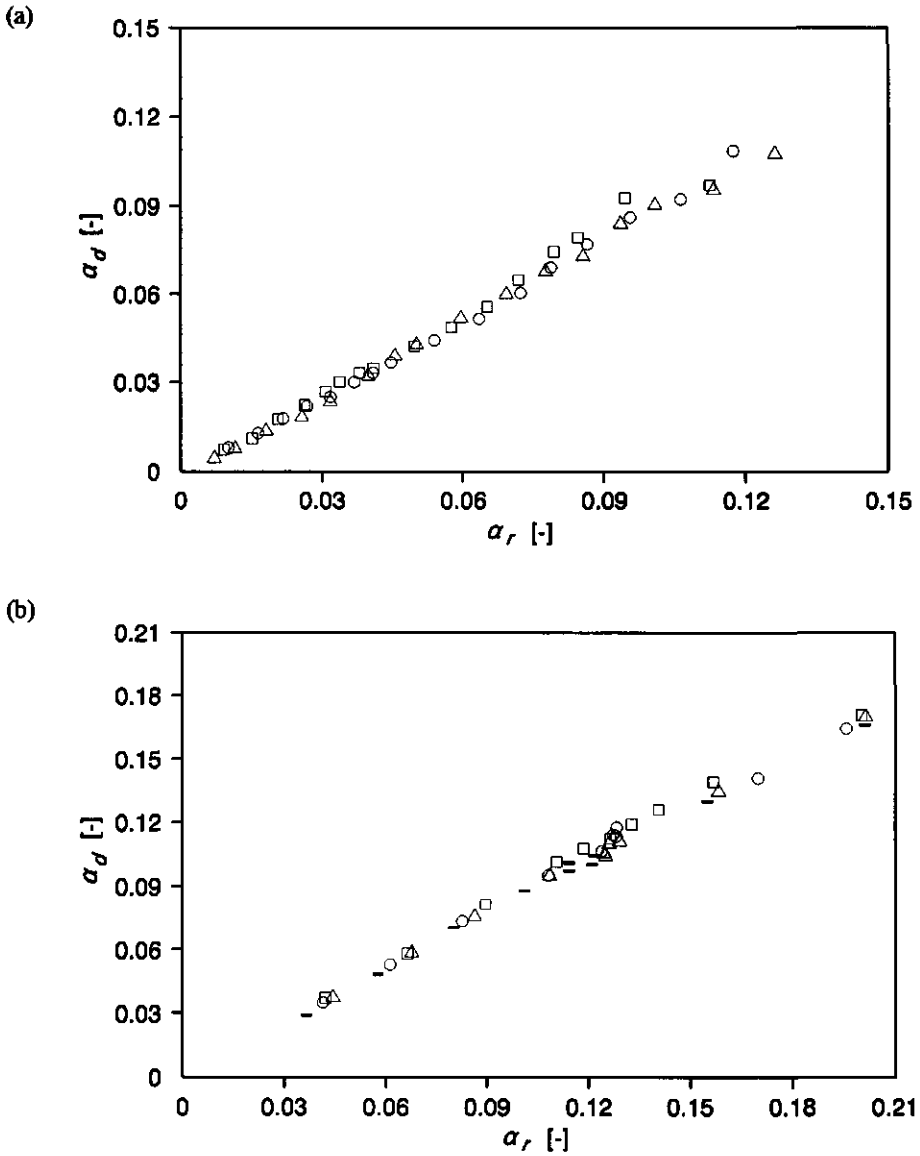


Figure 6. (a) Downcomer holdup versus riser holdup for three MAL configurations (specified in Table I): A (\circ), B (\square), and C (\triangle). (b) Downcomer holdup versus riser holdup for four ILR configurations (specified in Table I): A (\circ), B (\square), C (\triangle), and D ($-$).

1969], and not increase with superficial gas velocity. Frictional losses dropped again to lower values at higher liquid velocities after gas recirculation occurred. It is thus clear that no single K_f value can characterize the reactor hydrodynamics at all gas flow rates.

A mechanistic explanation for the increasing frictional losses can be given by considering the interfacial drag effects between gas bubbles and the surrounding liquid [Chisti and Moo-Young, 1988; Ishii and Zuber, 1979; Patel *et al.*, 1986; Young *et al.*, 1991]. Ishii and Zuber [1979] developed general drag-force relations for bubble, droplet and particle flow. Young *et al.* [1991] successfully adopted this model for the estimation of the frictional losses in the riser of their ALR with an external loop. For the present study, pressure drops were derived from drag-force estimations with the Ishii and Zuber [1979] relations. The increased pressure drop expressed in a higher K_f value, as found in practice for the MAL and ILR, could be calculated with Eq. (2). The pressure drops derived from drag-force estimations for the downcomer section were of the same order of magnitude. For more accurate estimations, and incorporation into the model calculations by introduction of a variable K_f , bubble-size distributions must be known at all gas flow rates. Concluding from the observations of the current study and literature [Chisti and Moo-Young, 1988; Ishii and Zuber, 1979; Patel *et al.*, 1986; Wachi *et al.*, 1991; Young *et al.*, 1991], three contributions to the total friction have thus to be distinguished: fully developed annular flow, entrance effects at turnarounds, and stationary bubbles.

In this study, the MAL and ILR were used to validate an empirical correlation [Chisti *et al.*, 1988]: $K_f = 11.4(A_d/A_b)^{0.79}$, relating K_f to the bottom clearance (A_d/A_b) for K_f values of different ILRs derived from literature with $0.2 \leq A_d/A_b \leq 2$. When valid, this correlation can be useful for model estimations of hydrodynamics in the MAL and other ILRs. In the MAL, A_d and A_b are not independent and thus varied at the same time (Table I). However, the four ILR configurations used in this study only differed in A_b (Table I), and are therefore useful to investigate the effect of changing A_b on K_f separately. For the three A_d/A_b ratios which are similar for the MAL and ILR, the experimental K_f was found to be considerably lower for the MAL (Table II) and, consequently, the empirical correlation, which should be applicable to different reactor geometries, does not

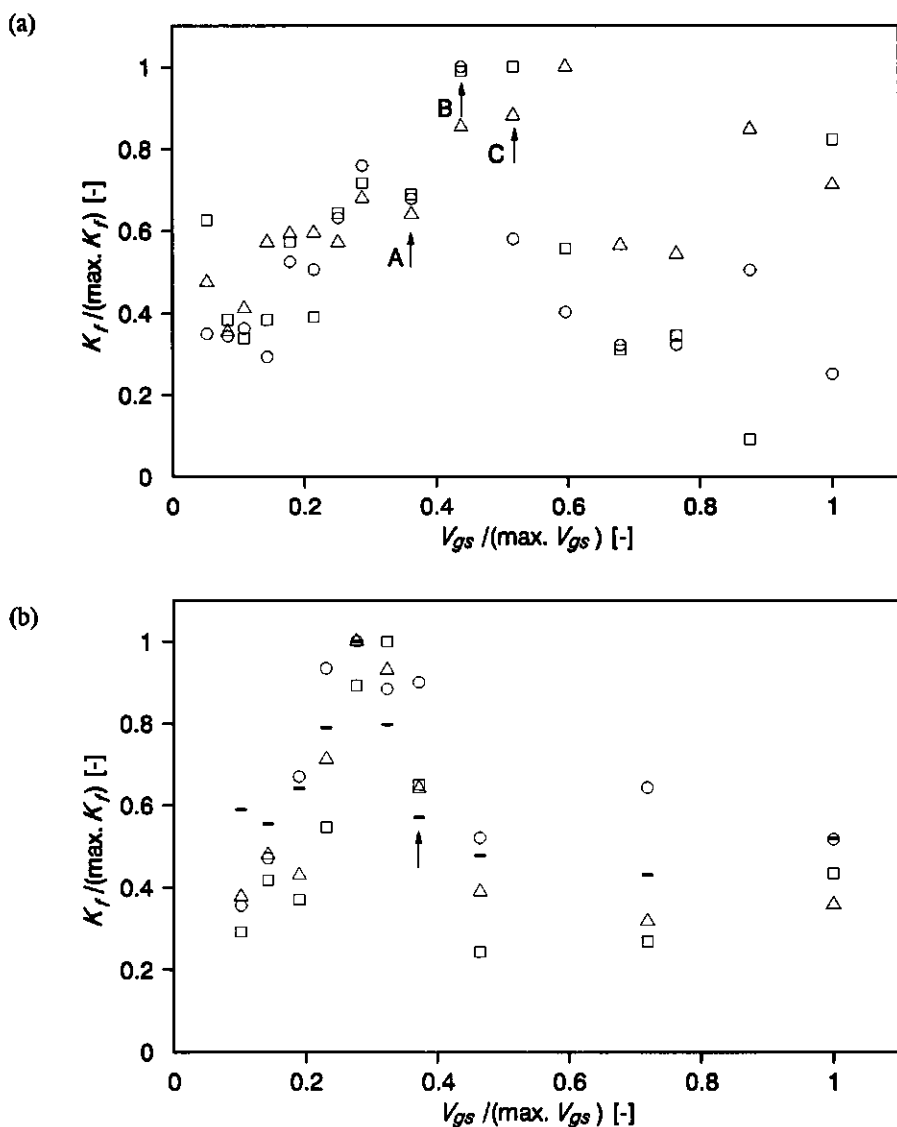


Figure 7. (a) Friction coefficient as a function of superficial gas velocity for three MAL configurations (specified in Table I): A (\circ), B (\square) and C (\triangle). Values normalized with respect to the maximum per configuration (see Table II). Arrows: onset of gas recirculation. (b) Friction coefficient as a function of superficial gas velocity for four ILR configurations (specified in Table I): A (\circ), B (\square), C (\triangle) and D ($-$). Values normalized with respect to the maximum per configuration (see Table II). Arrow: onset of gas recirculation.

apply. From these findings it can be concluded that K_f has to be determined experimentally for the MAL and other ILRs.

Table II. MAL and ILR experimental K_f values for the hydrodynamic model, and maximum K_f and v_{gs} values used for Figure 7a and b.

Config.	MAL			ILR			
	A	B	C	A	B	C	D
K_f [-]	1.32	1.53	3.31	7.74	8.58	11.5	10.0
Max. K_f [-]	2.57	2.66	5.48	10.4	14.4	17.7	14.2
Max. v_{gs} [m.s ⁻¹]	0.0678	0.0745	0.128	0.168	0.168	0.168	0.168

MODEL CALCULATIONS

For model calculations, the average K_f in the absence of gas recirculation was used (Table II), because K_f was shown to depend on the gas flow rate. This implies that the amount of measurements can influence the average value of K_f . Furthermore, model calculations in the absence of gas recirculation are the most interesting because these flow rates will be used for most practical applications.

Liquid-velocity and gas-holdup estimations were based on the two-phase, drift-flux model [Zuber and Findlay, 1965] [Eq. (4)]. For external-loop reactors, it has been shown that experimentally determined values for C and $v_{b\infty}$ can be explained by physical theory [Merchuk and Stein, 1981; Van Sonsbeek *et al.*, 1990; Verlaan *et al.*, 1986; Young *et al.*, 1991]. Furthermore, Siegel *et al.* [1986] showed the validity of the drift-flux model for ILRs. Clark and Flemmer [1985] investigated two-phase up and down flow in tubes; their results agreed with the drift-flux model.

From the drift-flux model [Eq. (4)] estimates for C and $v_{b\infty}$ can be obtained. Linear regression on v_g as a function of the total flow, $v_{gs} + v_{ls}$, gives values of C (slope) and $v_{b\infty}$ (intercept) that characterize the flow. For all configurations of the MAL and ILR, values obtained for C varied between 1.3 and 1.7, suggesting a positive correlation between liquid-velocity and holdup-concentration profile across the riser. The average $v_{b\infty}$ obtained for the three MAL configurations (0.25 ± 0.07 m.s⁻¹) agreed well with the assumed average value

[Wallis, 1969] of 0.25 m.s^{-1} ; the average $v_{b\infty}$ for all ILR configurations was considerably lower ($0.09 \pm 0.04 \text{ m.s}^{-1}$). This can be explained by nonideal circumstances at higher gas holdups. Such nonidealities are inevitable at the present experimental scale as the ducts for fluid flow in both model reactors were narrow compared with bubble size, thus causing wall effects [Wallis, 1969].

Bubble rise velocity decreased due to turbulence effects. This means that, at holdups exceeding 0.10, as found for the ILR, air bubbles start hindering each other in their flow [Ishii and Zuber, 1979]. In order to use only physically explainable parameters, and to show the general applicability of the drift-flux model, it was decided to take conservative estimates, $C = 1.3$ and $v_{b\infty} = 0.25 \text{ m.s}^{-1}$, for further model calculations for the three configurations of the current laboratory-scale MAL. Estimates for C and $v_{b\infty}$ in the downcomer could not be made, as the gas flow rate in the downcomer is not known.

The drift-flux model was originally developed for plug flow in vertical tubes [Zuber and Findlay, 1965]. Although the MAL geometry deviates from this, the model turns out to be applicable. Model calculations, based on mass flows, were made by an iterative calculation procedure [Verlaan *et al.*, 1986]. As the gas flow in the downcomer is not known, the average experimental holdup ratio ($\alpha_d/\alpha_r = 0.88$) was used for estimation of the downcomer gas holdup from the estimate for the riser. Local gas density differences were accounted for by a pressure correction halfway the column [Verlaan *et al.*, 1986].

Figure 4 shows model estimates for the superficial liquid velocity in the downcomer for three MAL configurations. Deviations were explained by the fluctuating flow due to downcomer gas holdup. On the whole, experimental data are approximated well, taking into account the deviations from ideality and the fact that parameter values explainable from physical theory were used. Estimates of gas holdup in the riser (Figure 5) and downcomer agreed well with the measurements. No correction was made for the unknown amount of recirculation gas flow.

MIXING

Mixing is an important feature for the MAL performance. For continuous operation, the residence time in each MAL compartment should exceed the mixing time per compartment to prevent short-cut flow of medium. For the second MAL

compartment, axial as well as tangential mixing may be expected. From the data for two MAL configurations (Table III), it is concluded that a large riser area (configuration A) entails a slightly better mixing. This is in agreement with data and correlations for conventional ILRs [Bello *et al.*, 1984; Chisti, 1989; Sukan and Vardar-Sukan, 1987; Weiland, 1984], of which the first (central) MAL compartment is an example. The tangential liquid movements in the second MAL compartment slightly enhanced liquid mixing; complete mixing was established within 3.4 liquid circulations.

Table III. Mixing and circulation times for two MAL configurations at different superficial gas velocities.

MAL config.	v_{gs} [m/s]	$\tau_m \pm SD$ [s]	τ_c [s]	τ_m/τ_c [-]
A	0.0074	49.5 ± 3.2	21.5	2.3
	0.0145	46.0 ± 2.0	19.4	2.4
	0.0297	40.4 ± 1.4	20.0	2.0
	0.0646	38.7 ± 3.0	11.3	3.4
B	0.0081	54.0 ± 1.2	18.8	2.9
	0.0160	52.3 ± 4.6	18.1	2.9
	0.0327	52.6 ± 1.3	18.4	2.8
	0.0710	39.2 ± 4.4	12.0	3.3

CONCLUSIONS

Tangential liquid movements were observed in the second MAL compartment. Otherwise, MAL hydrodynamics were similar to hydrodynamics in conventional ILRs. Downcomer holdup was a constant fraction of the riser holdup at all gas flow rates: α_d/α_r equaled 0.88 for the MAL and 0.86 for the ILR. Mixing in the MAL as a function of riser-to-downcomer area ratio was shown to be comparable with conventional ILRs. Tangential liquid movements slightly enhanced mixing.

Frictional losses were observed to increase with the gas flow rate. Stationary

bubbles could be regarded as obstacles causing additional friction. From both this observation and the literature [Chisti and Moo-Young, 1988; Ishii and Zuber, 1979; Patel *et al.*, 1986; Wachi *et al.*, 1991; Young *et al.*, 1991], three contributions to the total friction have to be distinguished: fully developed annular flow, entrance effects at turnarounds, and stationary bubbles.

A correlation for the frictional-loss coefficient based on reactor bottom geometry [Chisti *et al.*, 1988] could not be applied for both reactors under study. Frictional losses had to be determined experimentally, especially considering the fact that friction was shown to depend on the applied gas flow rate.

The hydrodynamic model based on the two-phase, drift-flux model [Zuber and Findlay, 1965], and on a friction coefficient derived from experimental data, describes the experimental data for the second MAL compartment well. For the chosen experimental setup, wall effects at higher gas holdups were inevitable. Model estimations can be improved, by using a variable K_f , when accurate drag-force estimations can be made.

ACKNOWLEDGEMENTS

This work was partly supported by Applikon Dependable Instruments B.V., Schiedam, The Netherlands. The authors thank H.M. van Sonsbeek for fruitful discussions. W.A. Beverloo and H.H. Beeftink are thanked for their suggestions during the manuscript preparation.

NOMENCLATURE

A_b	free bottom area	[m ²]
A_d	cross sectional downcomer area	[m ²]
A_r	cross sectional riser area	[m ²]
C	distribution parameter	[-]
D	diameter	[m]
$D2$	inner baffle diameter for the second MAL compartment	[m]

g	gravitational acceleration	$[m.s^{-2}]$
H	riser length	$[m]$
Hb	baffle height above reactor base	$[m]$
K_f	overall friction coefficient	$[-]$
ΔP	pressure difference	$[Pa]$
Re	Reynolds number	$[-]$
v	velocity	$[m.s^{-1}]$
$v_{b\infty}$	terminal rise velocity of a single bubble in an infinite stagnant medium	$[m.s^{-1}]$
v_g	gas velocity	$[m.s^{-1}]$
v_{gs}	superficial gas velocity	$[m.s^{-1}]$
v_{ld}	downcomer liquid velocity	$[m.s^{-1}]$
v_{lr}	riser liquid velocity	$[m.s^{-1}]$
v_{ls}	superficial liquid velocity	$[m.s^{-1}]$
v_{lsd}	downcomer superficial liquid velocity	$[m.s^{-1}]$
v_{lsr}	riser superficial liquid velocity	$[m.s^{-1}]$
w	baffle wall thickness	$[m]$
α_d	downcomer holdup	$[-]$
α_r	riser holdup	$[-]$
ρ	density	$[kg.m^{-3}]$
$\Delta\rho$	density difference	$[kg.m^{-3}]$
τ_c	circulation time	$[s]$
τ_m	mixing time	$[s]$

REFERENCES

- [1] Bello, R.A.; Robinson, C.W.; Moo-Young, M. 1984. Liquid circulation and mixing characteristics of airlift contactors. *Can. J. Chem. Eng.* **62**: 573-577.
- [2] Bello, R.A.; Robinson, C.W.; Moo-Young, M. 1985. Gas holdup and overall volumetric oxygen transfer coefficient in airlift contactors. *Biotechnol. Bioeng.* **27**: 369-381.
- [3] Chisti, M.Y. 1989. Airlift bioreactors. Elsevier, London, UK.

- [4] Chisti, M.Y.; Halard, B.; Moo-Young, M. 1988. Liquid circulation in airlift reactors. *Chem. Eng. Sci.* **43**: 451-457.
- [5] Chisti, M.Y.; Moo-Young, M. 1988. Gas holdup in pneumatic reactors. *Chem. Eng. J.* **38**: 149-152.
- [6] Clark, N.N.; Flemmer, R.L. 1985. Predicting the holdup in two-phase bubble upflow and downflow using the Zuber and Findlay drift-flux model. *AIChE. J.* **31**: 500-503.
- [7] Garcia Calvo, E. 1989. A fluid dynamic model for airlift loop reactors. *Chem. Eng. Sci.* **44**: 321-323.
- [8] Garcia Calvo, E.; Letón, P. 1991. A fluid dynamic model for bubble columns and airlift reactors. *Chem. Eng. Sci.* **46**: 2947-2951.
- [9] Gasner, L.L. 1974. Development and application of the thin channel rectangular air lift mass transfer reactor to fermentation and waste-water treatment systems. *Biotechnol. Bioeng.* **16**: 1179-1195.
- [10] Hill, G.A.; Robinson, C.W. 1989. Minimum tank volumes for CFST bioreactors in series. *Can. J. Chem. Eng.* **67**: 818-824.
- [11] Ishii, M.; Zuber, N. 1979. Drag coefficient and relative velocity in bubbly, droplet or particulate flows. *AIChE. J.* **25**: 843-855.
- [12] Jones, A.G. 1985. Liquid circulation in a draft-tube bubble column. *Chem. Eng. Sci.* **40**: 449-462.
- [13] Lee, C.H.; Glasgow, L.A.; Erickson, L.E.; Patel, S.A. 1987. Liquid circulation in airlift fermentors, In: *Biotechnology Processes* (Ho, C.S.; Oldshue, J.Y., Eds.), AIChE., New York, 50-59.
- [14] Levenspiel, O. 1972. Chemical reaction engineering. 2nd ed., Wiley, New York.
- [15] Merchuk, J.C.; Stein, Y. 1981. Local hold-up and liquid velocity in air-lift reactors. *AIChE. J.* **27**: 377-388.
- [16] Patel, S.A.; Glasgow, L.A.; Erickson, L.E.; Lee, C.H. 1986. Characterization of the downflow section of an airlift column using bubble size distribution measurements. *Chem. Eng. Comm.* **44**: 1-20.
- [17] Pirt, S.J. 1975. Principles of microbe and cell cultivation. Blackwell, Oxford, UK.
- [18] Shimizu, K.; Matsubara, M. 1987. Product formation patterns and the performance improvement for multistage continuous stirred tank fermentors. *Chem. Eng. Comm.* **52**: 61-74.
- [19] Siegel, M.H.; Merchuk, J.C.; Schügerl, K. 1986. Air-lift reactor analysis: interrelationships between riser, downcomer, and gas-liquid separator behaviour,

- including gas recirculation effects. *AIChE. J.* **32**: 1585-1596.
- [20] Sukan, S.S.; Vardar-Sukan, F. 1987. Mixing performance of air-lift fermenters against working volume and draft tube dimensions. *Bioproc. Eng.* **2**: 33-38.
- [21] Van Sonsbeek, H.M. 1992. Physical aspects of liquid-impelled loop reactors. Ph.D. thesis. Wageningen Agricultural University, The Netherlands.
- [22] Van Sonsbeek, H.M.; Verdurmen, R.E.M.; Verlaan, P.; Tramper, J. 1990. Hydrodynamic model for liquid-impelled loop reactors. *Biotechnol. Bioeng.* **36**: 940-946.
- [23] Verlaan, P.; Tramper, J.; Van 't Riet, K.; Luyben, K.Ch.A.M. 1986. A hydrodynamic model for an airlift-loop bioreactor with external loop. *Chem. Eng. J.* **33**: B43-B53.
- [24] Verlaan, P.; Van Eijs, A.M.M.; Tramper, J.; Van 't Riet, K.; Luyben, K.Ch.A.M. 1989. Estimation of axial dispersion in individual sections of an airlift-loop reactor. *Chem. Eng. Sci.* **44**: 1139-1146.
- [25] Wachi, S.; Jones, A.G.; Elson, T.P. 1991. Flow dynamics in a draft-tube bubble column using various liquids. *Chem. Eng. Sci.* **46**: 657-663.
- [26] Wallis, G.B. 1969. One-dimensional two-phase flow. McGraw-Hill, New York.
- [27] Weiland, P. 1984. Einfluss des Kernrohrdurchmessers auf das Betriebverhalten von Airlift-Schlaufenreaktoren. *Chem. -Ing. -Tech.* **56**: 64-65. (In German).
- [28] Young, M.A.; Carbonell, R.G.; Ollis, D.F. 1991. Airlift bioreactors: analysis of local two-phase hydrodynamics. *AIChE. J.* **37**: 403-428.
- [29] Zuber, N.; Findlay J.A. 1965. Average volumetric concentration in two-phase flow systems. *J. Heat Transfer* **87**: 453-468.

This chapter 3 has been published as: Bakker, W.A.M.; Den Hertog, M.; Tramper, J.; De Gooijer, C.D. 1995. Oxygen transfer in a Multiple Air-lift Loop reactor. *Bioproc. Eng.* 12: 167-172.

CHAPTER 3

OXYGEN TRANSFER IN A MULTIPLE AIR-LIFT LOOP REACTOR

SUMMARY

The Multiple Air-lift Loop reactor (MAL) is a new type of bioreactor, in which a series of air-lifts with internal loops is incorporated into one vessel. As such, the MAL is an approximation of an aerated plug-flow fermentor. Gas/liquid oxygen transfer was studied as a function of the gas flow rate in a MAL. The second MAL-compartment in the series was investigated in particular, and a Rectangular Air-lift Loop reactor (RAL) was used as a reference. Both a dynamic and a steady-state method were used for the determination of the overall volumetric oxygen-transfer coefficient. Both methods gave the same results. The oxygen transfer coefficient in the second MAL-compartment was low compared to that of conventional internal-loop reactors. Wall effects probably caused bubble coalescence and a reduction in the oxygen transfer. For the RAL it was found that oxygen transfer was comparable to that in a bubble column.

INTRODUCTION

The Multiple Air-lift Loop reactor (MAL) is a new type of bioreactor [De Gooijer, 1989]. In the MAL a cascade of Air-lift Loop Reactor (ALRs) with internal loops is incorporated into one vessel. Bioreactor series, like the MAL, can be used for the optimization of bioprocesses [Bakker *et al.*, 1993]. With the MAL, aerated plug-flow behavior can be approximated if sufficient ALRs, which behave like nearly ideally mixed vessels [Bakker *et al.*, 1993], are placed in the cascade. Aerated plug-flow reactors, like the MAL, have not been used in biotechnology until now.

A schematic side and top view of the MAL is given in Fig. 1. The subsequent reactors in the MAL are placed concentrically. This construction results in a new type of geometry for air-lift reactors with an internal loop, in this study represented by the second MAL-compartment. These annular-shaped compartments have a cylindrical wall to separate the riser and downcomer regions. The central reactor is a conventional internal-loop reactor.

Recently the MAL has been described and evaluated regarding its applicability for biotechnological processes. To that end sucrose conversion by immobilized invertase was studied in a three-compartment MAL and compared to that in a single, nearly ideally mixed, ALR. Indeed a higher degree of sucrose conversion was obtained in the MAL [Bakker *et al.*, 1994].

Now gas/liquid oxygen transfer is described for the same MAL configuration that previously was used for the hydrodynamics and mixing studies [De Gooijer, 1989]. A Rectangular Air-lift Loop reactor (RAL) was used as a single-vessel reference for the comparison of oxygen transfer in it with that in the second compartment of the MAL. Gasner [1974] suggested the use of a series of RALs for wastewater treatment, and characterized oxygen transfer in it. Others also used RALs for characterization studies [Chisti, 1989; Siegel and Merchuk, 1988], and reviewed the literature on oxygen transfer in ALRs with an internal loop [Bello, *et al.*, 1985; Chisti, 1989; Siegel and Merchuk, 1988].

Oxygen is a substrate in many bioconversions and therefore the gas/liquid oxygen transfer rate is an important parameter in the physical characterization of an aerated bioreactor. The product of the oxygen mass-transfer coefficient k_{La} and the

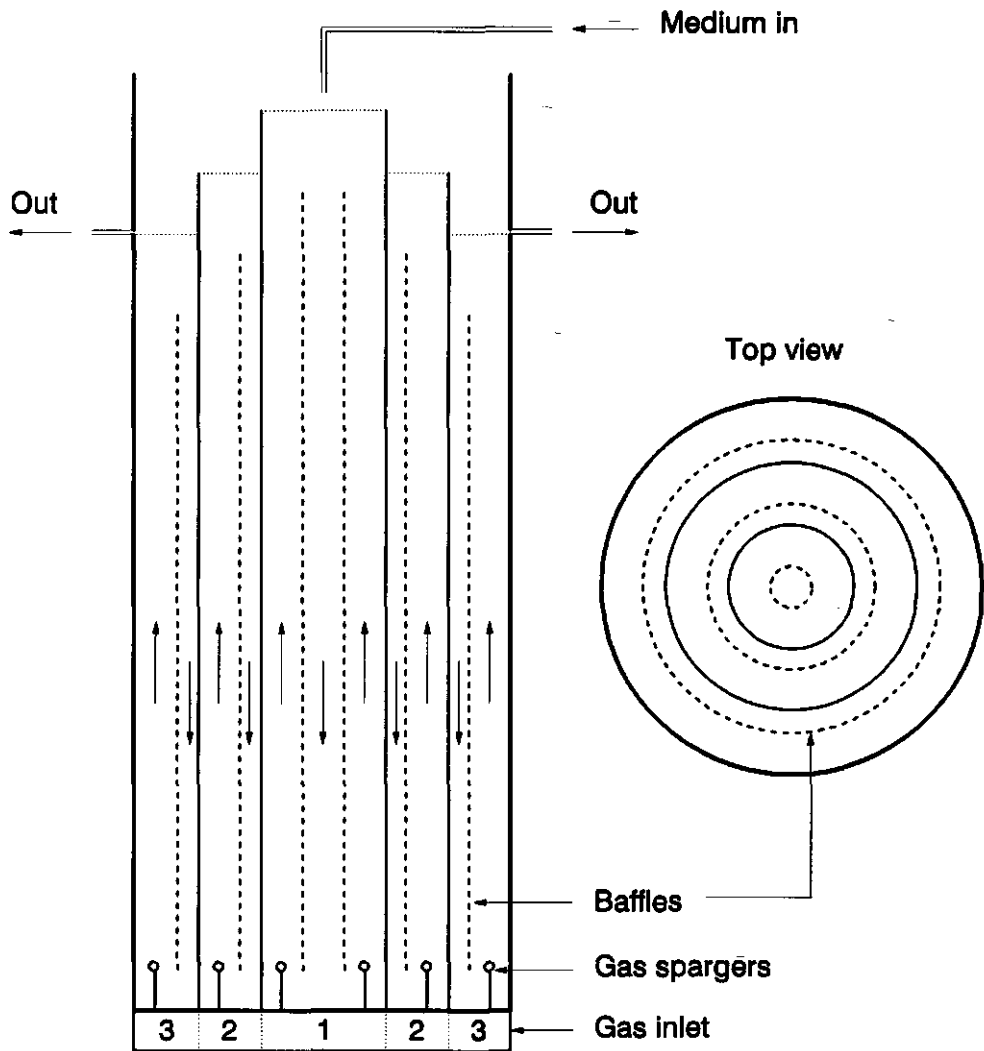


Figure 1. Three-compartment MAL, cross-sectional side and top view.

specific gas/liquid interfacial area a , known as the overall volumetric mass-transfer coefficient $k_o a$, was determined as a function of the gas flow rate in four different configurations of the second MAL-compartment. The four MAL-configurations differed in their downcomer-to-riser area ratio. In this study also two different methods to determine $k_o a$ in the second MAL-compartment were compared. The first is the frequently applied dynamic method [Van 't Riet, 1979]. The second method is the steady-state method [Van Sonsbeek *et al.*, 1991], based on de-oxygenation of the liquid phase outside the bioreactor.

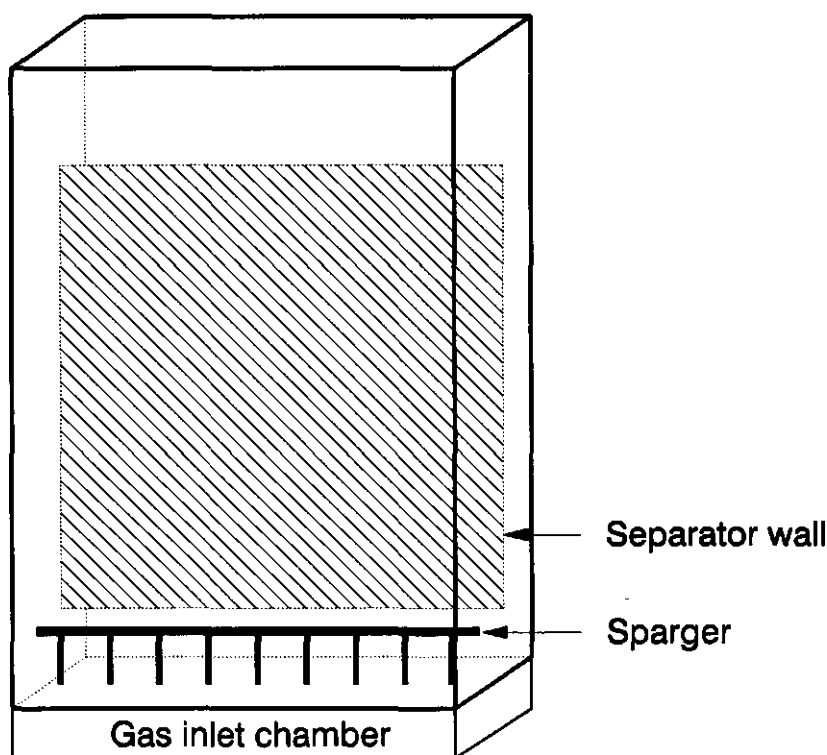


Figure 2. Scheme of the rectangular air-lift loop reactor (not on scale). Variable dimensions are summarized in Table I.

MATERIALS AND METHODS

THE MAL

The vessel in study was the previously described 0.034 m³ second compartment of a MAL [Bakker *et al.*, 1993]. The downcomer-to-riser area ratios were: $A_d/A_r = 0.31$ (configuration A); 0.43 (configuration B); and 0.91 (configuration C). In addition to that, the vessel was also operated as a bubble column (without separator wall; configuration BC): $A_d/A_r = 0$. Geometric data are given in Table I. Gas-holdup data were determined earlier [Bakker *et al.*, 1993].

Table I. Geometric data and bubble-diameter estimations for the MAL and the RAL. Values for the k_{oi}/d_b ratio are from a non-linear fit of Eq. (4) to the data for the MAL and the RAL, as illustrated in Figures 7 and 8. Furthermore, average bubble sizes (d_b) were derived from the k_{oi}/d_b ratio assuming k_{oi} to be constant ($= 4 \times 10^{-4}$ m.s⁻¹) for bubbles larger than 6 mm.

Config.	MAL				RAL			
	BC	A	B	C	A	B	C	D
Geometric data:								
R_2 [m]	--	0.077	0.079	0.081	--	--	--	--
w [mm]	--	3.0	3.0	9.0	3.0	3.0	3.0	3.0
H_w [m]	--	2.06	2.06	2.06	0.75	1.25	0.75	1.25
H_i [m]	2.26	2.26	2.26	2.26	0.85	1.34	0.85	1.34
A_d/A_r	0	0.31	0.43	0.91	0.98	0.98	0.42	0.42
Bubble-diameter estimations:								
k_{oi}/d_b [s ⁻¹]	0.039	0.025	0.032	0.022	0.071			
d_b [mm]	10	16	13	18	5.6			

THE RAL

The 0.115 m³ RAL consisted of transparent perspex (Fig. 2), with metal support bars on the outside to prevent the walls from bending. Dimensions were $l \times b \times h = 0.8 \times 0.1 \times 1.5$ m. The downcomer-to-riser area ratio could be changed by choosing a different position of the separator wall. Also, the height of the separator wall could be adjusted. Liquid height above the separator wall was 0.10 m, and the

height of the separator wall above the bottom was 0.05 m. Variable geometric data are given in Table I. The straight sparger construction was comparable to that for the MAL [Bakker *et al.*, 1993]. Gas was injected in a gas inlet chamber, from there it was distributed over the straight sparger tube. Overall gas holdup was determined by measuring the dispersion height over the unaerated liquid.

EXPERIMENTAL CONDITIONS

As previously [Bakker *et al.*, 1993] a 20 mol.m⁻³ solution of KCl was used for all experiments. The k_{oa} values measured were converted to those at standard conditions of 20°C with [Heijnen and Van 't Riet, 1984; Siegel and Merchuk, 1988]: $k_{oa}(20^\circ\text{C}) = k_{oa}(T)/(1.024)^{T-20^\circ\text{C}}$, where T is the actual temperature (°C). Surface tension of the liquid was 73 mN.m⁻¹; viscosity was 1.0 mPa.s.

DYNAMIC METHOD

The general equation for the oxygen transfer rate from a gas to a well mixed bulk liquid is [Van 't Riet, 1979]:

$$\frac{dc_l}{dt} = k_{ol}a(c_s - c_l) \quad (1)$$

where k_{ol} is the overall oxygen transfer coefficient, a the specific gas/liquid interfacial area, c_s the saturation oxygen concentration in the liquid phase and c_l the actual oxygen concentration in the liquid phase. Integration of Eq. (1) for constant c_s gives:

$$\frac{c_s - c_l(t)}{c_s - c_l(0)} = e^{-k_{ol}a \cdot t} \quad (2)$$

Eq. (2) is suitable for the determination of the lumped parameter $k_{ol}a$ by the dynamic method; the aqueous oxygen concentration has to be measured in time after a step-wise change in the gas inlet oxygen concentration.

The constraints to this method [Van 't Riet, 1979] were found to be met. The response time (63% of full scale) of the polarigraphic electrodes was $6.3 \pm$

1.5 s, which is low compared to $1/k_a a$. Linear regression on $\ln(\{c_i - c_i(0)\}/\{c_i - c_i(t)\})$ between $0.25c_s < c_i(t) < 0.75c_s$ as a function of time [see Eq. (2)] yielded $k_a a$ [Van 't Riet, 1979]. Each dynamic measurement was done at least two times and averaged to give $k_a a$.

STEADY-STATE METHOD

The central MAL-compartment (*i.e.* the first vessel in the series) was operated as a bubble column, with nitrogen supply, for the de-oxygenation during the steady-state measurements (Fig. 3). Liquid was pumped from the bottom of the second MAL compartment downcomer to the de-oxygenation vessel. From there liquid returned to the reactor via natural overflow. Measurements were done up to superficial gas flow rates of 0.04 m.s^{-1} where no gas was entrained in the tubing (MAL configuration A). Gas holdup in the external circuit should be known, or avoided, as it can contribute to the oxygen transfer [Van Sonsbeek *et al.*, 1991]. Oxygen concentrations were measured in both the reactor and in the de-oxygenation vessel.

In a steady-state the net transport of oxygen in the de-oxygenation circuit will be equal to the oxygen transfer in the reactor, and to the oxygen transfer in the de-oxygenation vessel [Van Sonsbeek *et al.*, 1991]:

$$\Phi_l (c_{l,in} - c_{l,out}) = V_r (k_{ol} a)_r (c_{s,r} - c_{l,r}) = V_d (k_{ol} a)_d c_{l,d} \quad (3)$$

where Φ_l is the liquid flow rate to the de-oxygenation vessel, V is the liquid volume, $c_{l,in}$ and $c_{l,out}$ are the oxygen concentrations in the incoming and outgoing liquid of the de-oxygenation vessel, respectively. Furthermore, the subscripts r and d refer to the reactor and the de-oxygenation vessel, respectively.

For this method two constraints have to be taken into account [Van Sonsbeek *et al.*, 1991]: (i) both reactor and de-oxygenation vessel are assumed to be perfectly mixed, in other words, the mixing time $\tau_{m,r} < V_r/\Phi_l$, resulting in $c_{l,in} = c_{l,r}$ and $c_{l,out} = c_{l,d}$, respectively, (ii) the oxygen concentration should agree with $c_{l,d}/c_{l,r} < 0.8$ and $c_{s,r}/c_{l,r} < 0.8$ for accurate measurements. Both constraints were found to be met.

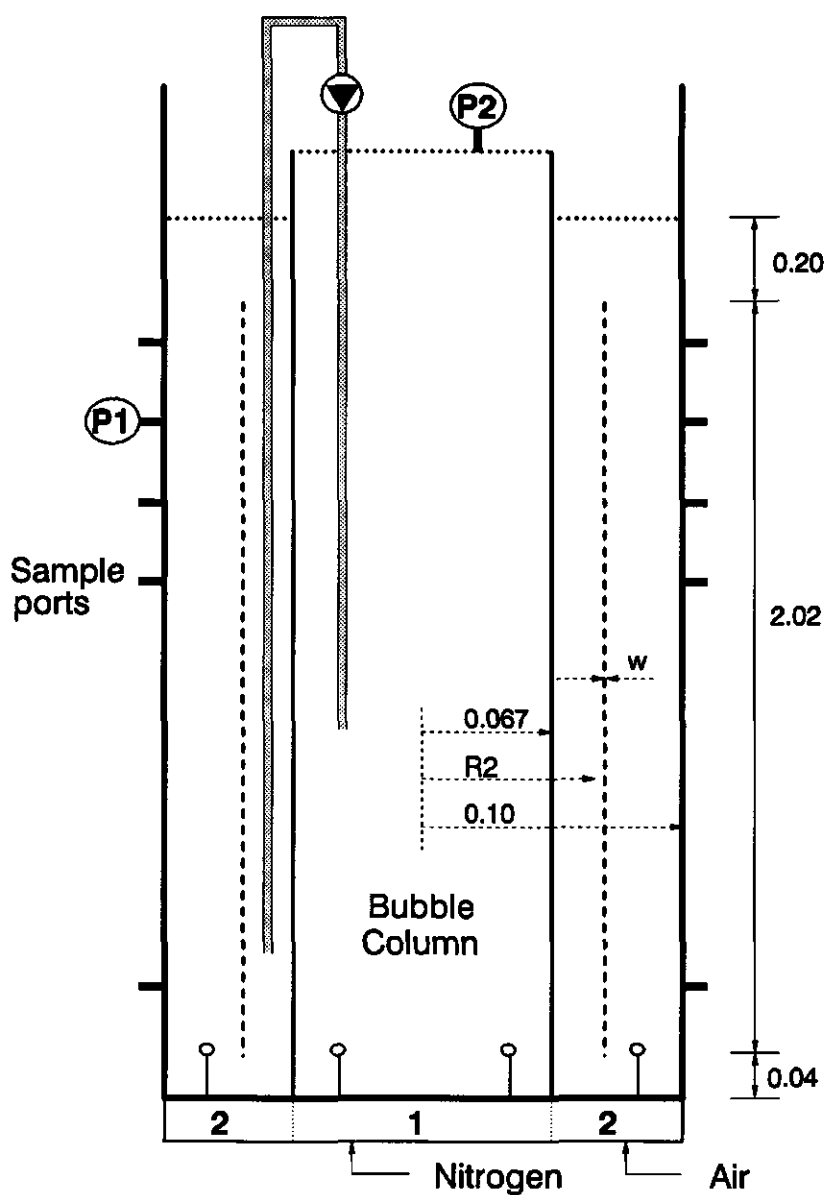


Figure 3. Scheme of the second MAL compartment (not on scale), and experimental setup for the steady-state method. Inner diameters are given (m). Variable dimensions are summarized in Table I. P1 = probe 1 and P2 = probe 2.

RESULTS AND DISCUSSION

OXYGEN TRANSFER IN THE MAL

The $k_a a$ was determined from the dynamic measurements at different superficial gas velocities for four configurations of the second MAL compartment. Figure 4 shows that, for all MAL configurations, $k_a a$ increased with the superficial gas velocity v_{gs} (defined as the division of gas flow rate by A_r). Furthermore, the $k_a a$ decreased with increasing downcomer-to-riser area ratio (from $A_d/A_r = 0$ to 0.91) at every superficial gas velocity, although configurations A and B show comparable results. This effect, a lower $k_a a$ with increasing A_d/A_r , was also observed by other investigators for air-lift loop reactors with an internal loop [Bello *et al.*, 1985; Chisti, 1989].

In Figure 4, a solid line is drawn using an empirical correlation for bubble columns [Heijnen and Van 't Riet, 1984] ($k_a a = 0.32 v_{gs}^{0.7}$) to make a comparison to the MAL. The $k_a a$ values for the present bubble column ($A_d/A_r = 0$; configuration BC) were somewhat lower (Fig. 4) but they approach this correlation, for which deviations of about 30% are acceptable [Van 't Riet and Tramper, 1991]. For all air-lift configurations (A, B and C), the experimental $k_a a$ values were somewhat lower than those for the bubble column, which is normally observed in such a comparison [Bello *et al.*, 1985; Chisti, 1989; Van 't Riet and Tramper, 1991]. This is because the contact time between gas and liquid phase in an ALR is always smaller than in a BC under the same experimental conditions.

In Figure 5, the results of measurements from the steady-state method are compared with those of the dynamic method for MAL configuration A. Good agreement between both methods of $k_a a$ -determination was observed, which was also found for a liquid-impelled loop reactor [Van Sonsbeek *et al.*, 1991]. The steady-state method is a useful alternative if problems associated with the dynamic method can not be avoided [Van Sonsbeek *et al.*, 1991; Van 't Riet, 1979]. For example, the presence of a third phase in which oxygen dissolves can cause large inaccuracies in the dynamic $k_a a$ determination.

OXYGEN TRANSFER IN THE RAL

The RAL was used as a reference, and may be seen as an approximation of an

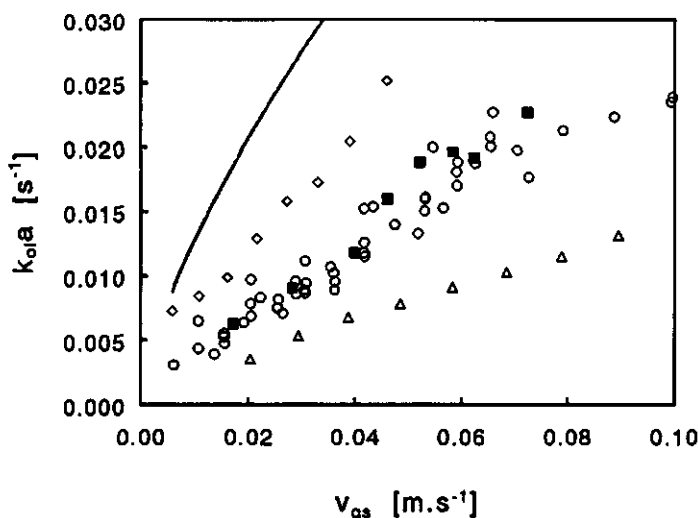


Figure 4. The k_{oa} as a function of the superficial gas velocity v_{gs} for four MAL configurations: A (\circ), B (\blacksquare), C (\triangle), and BC (\diamond). Solid line: empirical correlation for bubble columns [Heijnen and Van 't Riet, 1984]: $k_{oa} = 0.32v_{gs}^{0.7}$.

outer compartment of a large-scale MAL. Four extreme configurations were used to observe the effects of varying A_d/A_r , and reactor height, on k_{oa} . The results of the dynamic measurements at relatively low superficial gas velocities as compared to the MAL experiments, are shown in Figure 6. Reactor height did not affect k_{oa} , but still larger height differences might show an increased volumetric mass-transfer coefficient with increasing liquid height [Chisti, 1989; Onken and Weiland, 1983]. The effect of varying A_d/A_r on k_{oa} was comparable to that in the MAL where k_{oa} decreased with increasing A_d/A_r .

In the RAL, liquid circulation cells were observed in the downcomer. This is probably caused by low liquid velocities at the edges of the downcomer section; entrained gas bubbles moved to the edges and coalesced there, and then escaped upward. Therefore the hydrodynamic behavior of the RAL downcomer was bubble-column like because it was not possible to obtain complete bubble recirculation through the RAL downcomer. This holds for a wide range of power inputs per unit of reactor volume, and different A_d/A_r -ratios, which both were in the same range as applied in the MAL (results not shown). This is in contrast with findings of Siegel

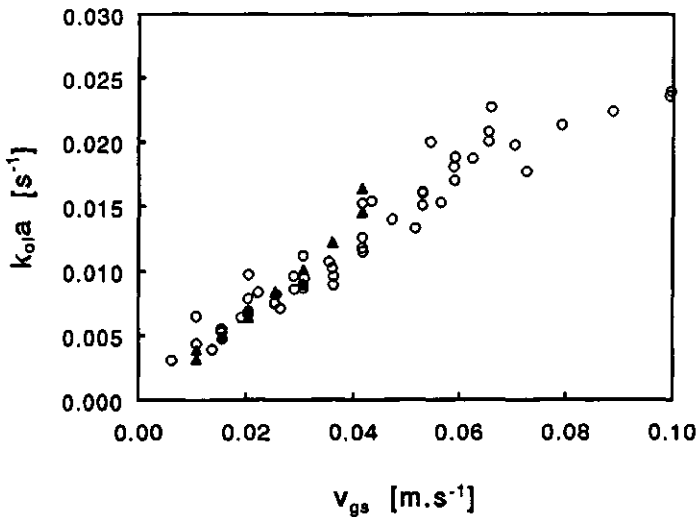


Figure 5. Comparison of the $k_o a$ -values measured with the steady-state method (Δ) to those obtained with the dynamic method (\circ) for MAL configuration A.

and Merchuk [1988] for a RAL with different (more slender) dimensions, where bubble recirculation could easily be established.

In Figure 6 a solid line is drawn using the same empirical correlation for bubble columns [Heijnen and Van 't Riet, 1984] again ($k_o a = 0.32 v_{gs}^{0.7}$), to make a comparison to the RAL. The oxygen transfer in the RAL was found to be comparable to that in bubble columns (Fig. 6). Others also reported high aeration efficiencies for different RALs [Chisti, 1989; Gasner, 1974; Siegel and Merchuk, 1988]. From these findings it was concluded here that the RAL was not a good model reactor for hydrodynamics and oxygen transfer in the second MAL-compartment where bubble recirculation can easily be established [Bakker *et al.*, 1993], and no liquid circulation cells were observed.

BUBBLE-SIZE ESTIMATIONS

For a mechanistic comparison of oxygen transfer in the MAL to that in the RAL and in other ALRs with internal loops, the total gas holdup and the bubble diameter are important parameters. Gas holdup and the bubble diameter together determine

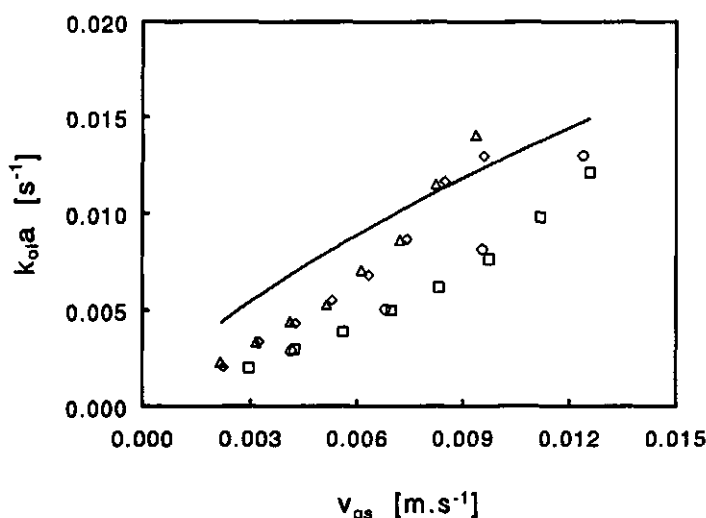


Figure 6. The $k_{ol}a$ as a function of the superficial gas velocity v_{gs} for four RAL configurations: A (\circ), B (\square), C (Δ), and D (\diamond). Solid line: empirical correlation for bubble columns [Heijnen and Van 't Riet, 1984]: $k_{ol}a = 0.32v_{gs}^{0.7}$.

the gas/liquid interfacial area for oxygen transfer. The $k_{ol}a$ can be related [Chisti, 1989; Van 't Riet and Tramper, 1991] to the overall gas holdup α , and the mean bubble size d_b :

$$k_{ol}a = \frac{6k_{ol}}{d_b} \cdot \frac{\alpha}{(1-\alpha)} \quad (4)$$

From a non-linear fit of Eq. (4) to $k_{ol}a$ as a function of the overall gas holdup, the k_{ol}/d_b ratio was estimated for all MAL and RAL configurations as shown in Figures 7 and 8, respectively (see Table I for the k_{ol}/d_b ratios). In this analysis, effects from different RAL geometries were insignificant (*t*-test), and thus one k_{ol}/d_b ratio was obtained.

The k_{ol}/d_b -values for the MAL were lower than the average 0.053 s^{-1} reported by Chisti [1989] for various ALRs with internal loops under similar conditions. This indicated that reduced gas/liquid interfacial area was present in the second compartment of the MAL, even in the bubble-column configuration. The

k_{α}/d_b ratio of 0.071 s^{-1} for the RAL (Fig. 8 and Table I) was higher than the ratio of 0.058 s^{-1} reported by Chisti for a bubble column [1989]. For bubble columns k_{α}/d_b may be estimated to be 0.067 s^{-1} by assuming bubbles with equilibrium diameter ($d_b = 6 \text{ mm}$) [Wallis, 1969], and $k_{\alpha} = 4 \times 10^{-4} \text{ m.s}^{-1}$ [Heijnen and Van 't Riet, 1984; Kawase and Moo-Young, 1992]. This k_{α}/d_b value is in agreement with the experimental results for the RAL (Table I).

In order to explain the difference between the MAL and the RAL, bubble sizes were estimated from the assumption that $k_{\alpha} = 4 \times 10^{-4} \text{ m.s}^{-1}$. The k_{α} itself is dependent on d_b , but for a rough estimate k_{α} was assumed to have this constant value for bubbles larger than 6 mm [Heijnen and Van 't Riet, 1984; Kawase and Moo-Young, 1992]. The large bubble sizes obtained (Table I) were in agreement with the visual observation of bubbles with diameters larger than 6 mm in the MAL riser and downcomer [Bakker *et al.*, 1993]. The occurrence of those bubbles could be explained by observing the scale of the MAL. The ducts for fluid flow were narrow compared to bubble size, thus causing bubble/wall interactions, bubble/bubble interactions, and bubble coalescence [Bakker *et al.*, 1993; Wallis,

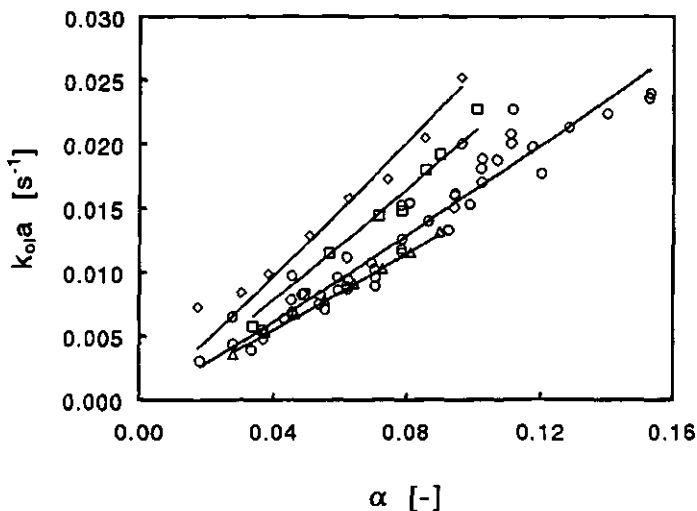


Figure 7. The $k_{\alpha}a$ as a function of the overall gas holdup α for four MAL configurations: A (\circ), B (\square), C (\triangle), and BC (\diamond). Solid lines: non-linear fit with Eq. (4). Resulting k_{α}/d_b -values are given in Table I.

1969].

CONCLUSIONS

Oxygen transfer in the MAL was low compared to that in the RAL. Hydrodynamics and oxygen transfer in the RAL were comparable to that in bubble columns. Therefore the current RAL was found not to be a good model reactor for studying the second MAL-compartment. Those compartments were earlier found to behave like conventional ALRs with an internal loop [Bakker *et al.*, 1993].

If oxygen transfer in the MAL has to be comparable to that in conventional ALRs with an internal loop, the MAL has to be of a larger scale than the current one to prevent bubble coalescence due to wall effects.

The steady-state method for $k_a a$ determination was shown to be a good alternative for the dynamic method as both methods gave comparable results.

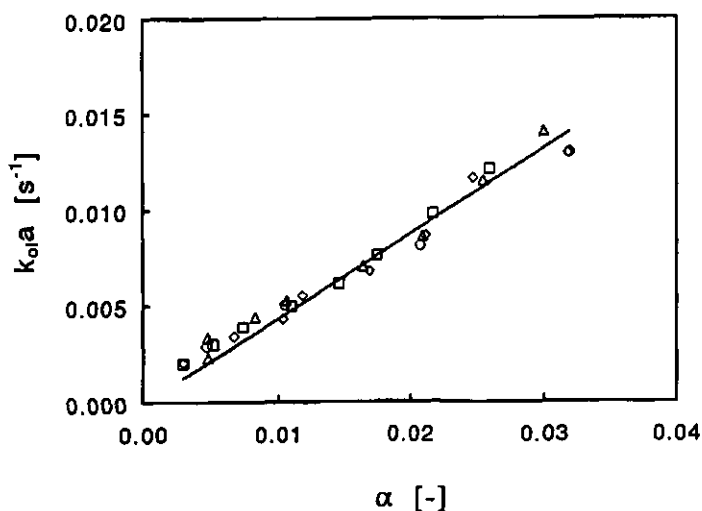


Figure 8. The $k_a a$ as a function of the overall gas holdup α for four RAL configurations: A (○), B (□), C (△), and D (◇). Solid line: non-linear fit with Eq. (4). The resulting k_a/d_b -value is given in Table I.

ACKNOWLEDGEMENTS

The authors thank H.L. van Rijswijk for his contribution to the experiments. W.A. Beverloo and H.H. Beftink are thanked for carefully reading the manuscript. This work was partly supported by Applikon Dependable Instruments B.V., Schiedam, The Netherlands. The research was carried out in a PBTS project, nr. 89069, initiated by the Dutch Ministry of Economic Affairs.

NOMENCLATURE

A_d	cross-sectional downcomer area	[m ²]
A_r	cross-sectional riser area	[m ²]
a	specific gas/liquid interfacial surface area	[m ² .m ⁻³]
c_l	actual oxygen concentration in the liquid	[mol.m ⁻³]
c_s	saturation oxygen concentration	[mol.m ⁻³]
d_b	mean bubble diameter	[m]
H_w	separator-wall height	[m]
H_l	liquid height above reactor base	[m]
k_{ol}	overall oxygen transfer coefficient	[m.s ⁻¹]
R_2	inner radius for the separator wall in the second MAL compartment	[m]
T	temperature	[°C]
t	time	[s]
v_{gs}	superficial gas velocity	[m.s ⁻¹]
w	separator-wall thickness	[m]
α	overall gas holdup	[-]
ρ	density	[kg.m ⁻³]
τ_m	mixing time	[s]
Φ_l	liquid flow rate	[m ³ .s ⁻¹]

Subscripts:

d	= de-oxygenation vessel	r	= reactor
in	= incoming	out	= outcoming

REFERENCES

- [1] Bakker, W.A.M.; Van Can, H.J.L.; Tramper, J.; De Gooijer, C.D. 1993. Hydrodynamics and mixing in a Multiple Air-lift Loop reactor. *Biotechnol. Bioeng.* **42**: 994-1001.
- [2] Bakker, W.A.M.; Knitel, J.T.; Tramper, J.; De Gooijer, C.D. 1994. Sucrose conversion by immobilized invertase in a Multiple Air-lift Loop bioreactor. *Biotechnol. Prog.* **10**: 277-283.
- [3] Bello, R.A.; Robinson, C.W.; Moo-Young, M. 1985. Gas holdup and overall volumetric oxygen transfer coefficient in airlift contactors. *Biotechnol. Bioeng.* **27**: 369-381.
- [4] Chisti, M.Y. 1989. Airlift bioreactors. Elsevier, London, UK.
- [5] De Gooijer, C.D. 1989. Dutch patent application. Nr.: 89.01649. (In Dutch).
- [6] Gasner, L.L. 1974. Development and application of the thin channel rectangular air lift mass transfer reactor to fermentation and waste-water treatment systems. *Biotechnol. Bioeng.* **16**: 1179-1195.
- [7] Heijnen, J.J.; Van 't Riet, K. 1984. Mass transfer, mixing and heat transfer phenomena in low viscosity bubble column reactors. *Chem. Eng. J.* **28**: B21-B42.
- [8] Kawase, Y.; Moo-Young, M. 1992. Correlations for liquid-phase mass transfer coefficients in bubble column reactors with Newtonian and non-Newtonian fluids. *Can. J. Chem. Eng.* **70**: 48-54.
- [9] Onken, U.; Weiland, P. 1983. Airlift fermenters: construction, behavior, and uses. *Adv. Biotechnol. Proc.* **1**: 67-95.
- [10] Siegel, M.H.; Merchuk, J.C. 1988. Mass transfer in a rectangular air-lift reactor: effects of geometry and gas recirculation. *Biotechnol. Bioeng.* **32**: 1128-1137.
- [11] Van Sonsbeek, H.M.; Gielen, S.J.; Tramper, J. 1991. Steady-state method for k_a measurements in model systems. *Biotechnol. Techn.* **5**: 157-162.
- [12] Van 't Riet, K. 1979. Review of measuring methods and results in nonviscous gas-liquid mass transfer in stirred vessels. *Ind. Eng. Chem. Process Des. Dev.* **18**: 357-364.
- [13] Van 't Riet, K.; Tramper, J. 1991. Basic bioreactor design. Marcel Dekker, New York.
- [14] Wallis, G.B. 1969. One-dimensional two-phase flow. McGraw-Hill, New York.

This chapter 4 has been accepted for publication as: De Gooijer, C.D.; Bakker, W.A.M.; Beeftink, H.H.; Tramper, J. 1995. Bioreactors in series: an overview of design procedures and practical applications. *Enzyme Microb. Technol.*

CHAPTER 4

BIOREACTORS IN SERIES: AN OVERVIEW OF DESIGN PROCEDURES AND PRACTICAL APPLICATIONS

"If one fermenter gives good results,
two fermenters will give better results and three fermenters better still.
This is sometimes true, but often false."

Herbert, D., 1964a

INTRODUCTION

Over the last decades, many papers described the design or application of series of bioreactors. Usually, these bioreactors in series are of the continuous stirred tank reactor (CSTR) type. This most widely used bioreactor is easy to operate, of simple construction, and replacement of biocatalysts and maintenance is not troublesome [Hill, 1977].

The pertinent processes described in literature can be divided into two main

groups: processes with a constant overall reaction stoichiometry that can be described by a single kinetic equation, and processes where the stoichiometry is variable and the descriptive kinetic equation changes. The first group consists of those bioprocesses that may well be performed in one bioreactor, but where segregation into two or more bioreactors may lead to a higher product concentration, a larger degree of conversion, or a higher volumetric productivity (also known as space-time yield), or a combination of these factors. The second group is by nature heterogeneous in time or space, and is characterized by two or more independent reactions each governed by its own kinetics, as in biogas production or nitrification/denitrification.

For processes with a fixed overall reaction stoichiometry, this paper first will present a general theoretical outline that enables one to decide *if* a series of bioreactors is favourable. After that, the question of *how* such a series should be designed will be addressed. Subsequently, the general theory will be applied to catalytic reactions (enzymatic conversions), and also to autocatalytic reactions (cells in suspension). This will be done for different types of kinetics. After each theoretical treatise, a number of applications of series of bioreactors will be presented.

For processes with a variable stoichiometry some examples will be presented, since up to now no design rules exist for series with these types of processes. The paper concludes with a short description of bioreactors suitable for bioprocesses in series, both with constant and variable stoichiometry.

The descriptions of a single plug-flow type bioreactor with the tanks-in-series model [Powell and Lowe, 1964; Kleinstreuer, 1987] are omitted, as well as the numerous papers devoted to this subject in the field of chemical engineering. This paper will also solely focus on single-feed series of bioreactors.

CONSTANT STOICHIOMETRY PROCESSES

Processes with a constant overall reaction stoichiometry may show a higher product concentration, a higher degree of conversion, a higher volumetric productivity, or a combination of those if executed in a series of CSTR's when compared to a single bioreactor.

THEORY

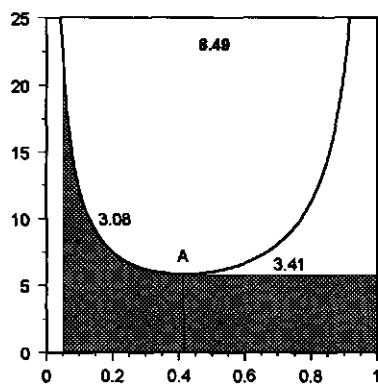
As a process with a constant stoichiometry, Bischoff [1966], citing Herbert [1964a], describes an optimal series for biomass production, consisting of a CSTR followed by a plug-flow reactor. Such a system may be conceived of as one large CSTR, followed by an infinite number of infinitesimally small CSTR's (Figure 1A; for the calculations underlying Figure 1 see appendix). This combination of a CSTR followed by a PFR has the lowest total residence time to achieve a certain degree of conversion (Figure 1A-G). Since for biomass production in most cases oxygen is required, and an aerated PFR does not exist, an alternative to this combination is a series of CSTR's with equal volume (Figures 1B and 1C), or a series of unequal-volume CSTR's (Figures 1D and 1E).

Implicitly, Figure 1, which holds with no biomass in the influent, imposes that the desired degree of conversion of the process determines whether a series of bioreactors is favourable or not: if the substrate concentration at the exit of the series is to the left-hand side of point A in Figure 1A (a high degree of conversion) then a series is favourable, if it would be to the right-hand side of point A (a low degree of conversion), a single CSTR would be the best solution. It should be noted, as also stated by Moser [1985], citing Topiwala [1974], that the PFR/CSTR volume ratio for such an optimal configuration is strongly dependent on the ratio $\kappa = K_s/S_0$, with K_s the Monod constant (mol.m^{-3}) and S_0 the substrate concentration at the inlet of the series (mol.m^{-3}) (Figure 2). For Monod kinetics, and a quite common influent concentration $\kappa = 0.01$ [Van 't Riet and Tramper, 1991], the minimum in Figure 1C is attained at $\alpha = S/S_0 = 0.1$, indicating that up to conversions of 90% a single CSTR (without any PFR) would perform optimally.

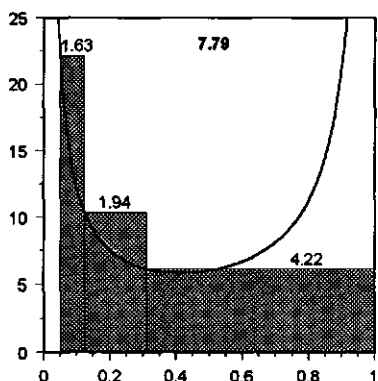
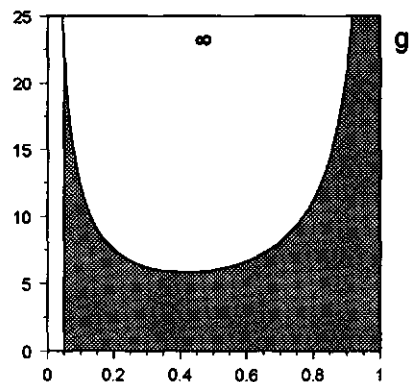
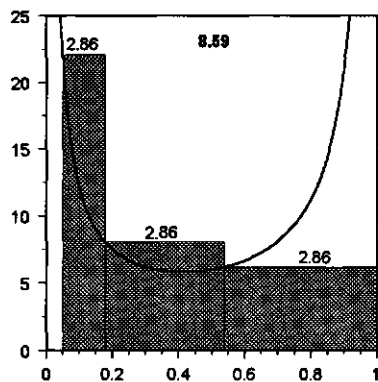
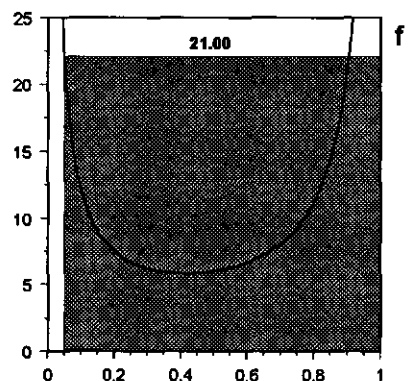
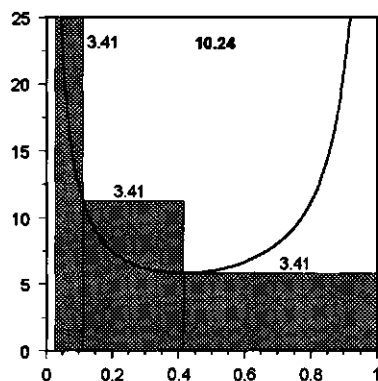
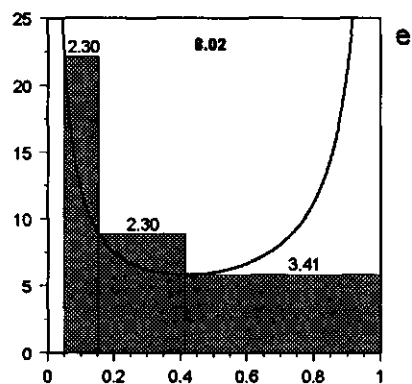
As far as the design of a reactor series is concerned, a distinction has to be made between the design of a series of equal volume CSTR's, and a series of non-equal volume CSTR's, the latter also referred to as optimal design.

Design of a finite equal-volume series. The theory of a series of equal-sized CSTR's was first treated by Herbert [1964B], and later cited by Moser [1988]. Two performance criteria were defined: biomass productivity ($\text{kg.m}^{-3}.\text{s}^{-1}$), and effective yield, defined as the ratio of biomass concentration at the outlet and the substrate concentration at the inlet of a bioreactor system. For the first criterion he showed that

Reciprocal rate $1/\rho$ (-)



Reciprocal rate $1/\rho$ (-)



Substrate concentration α (-)

Substrate concentration α (-)

Figure 1. (See the opposite page). For a continuous-flow system with a autocatalytic processes (microbial reaction, Monod kinetics, single feed and no biomass in the influent), at a fixed stoichiometry, optimal design is inferred from a plot of the reciprocal dimensionless rate ($1/r = \mu_{max}S_0/r_s$) versus the dimensionless concentration ($\alpha = S/S_0$). Due to the existence of a minimum in the curve, minimalization of overall holding time may require a CSTR and a PFR in series. Shaded areas: holding times. A 95% degree of conversion is aimed for, and $\kappa = K_s/S_0 = 1$. The number listed at the top of the graph is the total dimensionless holding time of each configuration.

- A:** one CSTR followed by a Plug-flow reactor. Point A is the minimum of the curve, corresponding to α_{crit} .
- B:** series of 3 equal-sized CSTR's designed by the procedure described by Fiechter [1981]; the first vessel operates at the maximum rate. Note that more than 95% is converted.
- C:** series of three equal-sized CSTR's where the first vessel operates at less than the maximum rate.
- D:** series of three unequal-sized CSTR's, optimal design according to Hill and Robinson [1989].
- E:** series of three unequal-sized CSTR's, where the first vessel operates at the maximum rate and the subsequent vessels have an equal volume.
- F:** one single CSTR.
- G:** one single PFR.

for a single-stage system this productivity equals $D \cdot X$ with D the dilution rate (s^{-1}) and X the biomass concentration ($\text{kg} \cdot \text{m}^{-3}$), whereas for a two-stage system this is $X_2 \cdot D_{ave}$, with $D_{ave} = D_2/2$ (or, in general terms, $D_{ave} = F/(NV)$, with V the volume (m^3) of each vessel in the series of N reactors, and F the flow rate ($\text{m}^3 \cdot \text{s}^{-1}$)). For single-feed series, three conclusions could be drawn, as illustrated in Figure 3:

- i) the maximum possible overall productivity is higher in a single-stage system,
- ii) at lower dilution rates the overall productivity of a two-stage system is slightly larger than that of a single-stage system, and, derived from this,
- iii) at lower dilution rates, the effective yield (or the utilization of substrate) is slightly higher in a two-stage system.

Herbert [1964b] also stated that more than two bioreactors in series have no practical advantage as far as the volumetric productivity is concerned. However, later stages might improve product quality, since the endogenous metabolism will continue in a third stage, leading to changes in the chemical and physiological state of the cells. Note that this in fact implies a change in stoichiometry.

For multiple-feed series of bioreactors, Fencel *et al.* [1969, 1972] showed that under certain conditions the productivity can be higher than for a single CSTR. Herbert [1964b] gives mathematical descriptions of a multiple-feed reactor system. For an extensive theoretical treatise of series with multiple-feed operation we refer to Fencel [1966].

Fiechter [1981], citing Fencel [1966], and Deindoerfer and Humphrey [1959], describes a four-step graphical procedure for the design of a series of chemostats of equal volume for biomass production. The first vessel should, in their view, operate at the maximal volumetric productivity, and subsequently the number of (equal-sized) vessels is determined in order to achieve a certain degree of conversion or biomass concentration (Figure 4):

- i) Obtain $d\chi/d\mu_{max}t$ as a function of χ , the dimensionless biomass concentration $X/Y_{xs}S_0$ with Y_{xs} the yield of biomass on substrate ($\text{kg} \cdot \text{mol}^{-1}$), from a batch experiment or from mass balances over substrate and biomass if the parameters in the kinetic equation are known;
- ii) Plot $d\chi/d\mu_{max}t$, with μ_{max} the maximum specific growth rate (s^{-1}) and t the time (s) versus χ ;
- iii) Draw a line from $\chi = 0$ to $\chi = \chi_I$, the dimensionless concentration of biomass

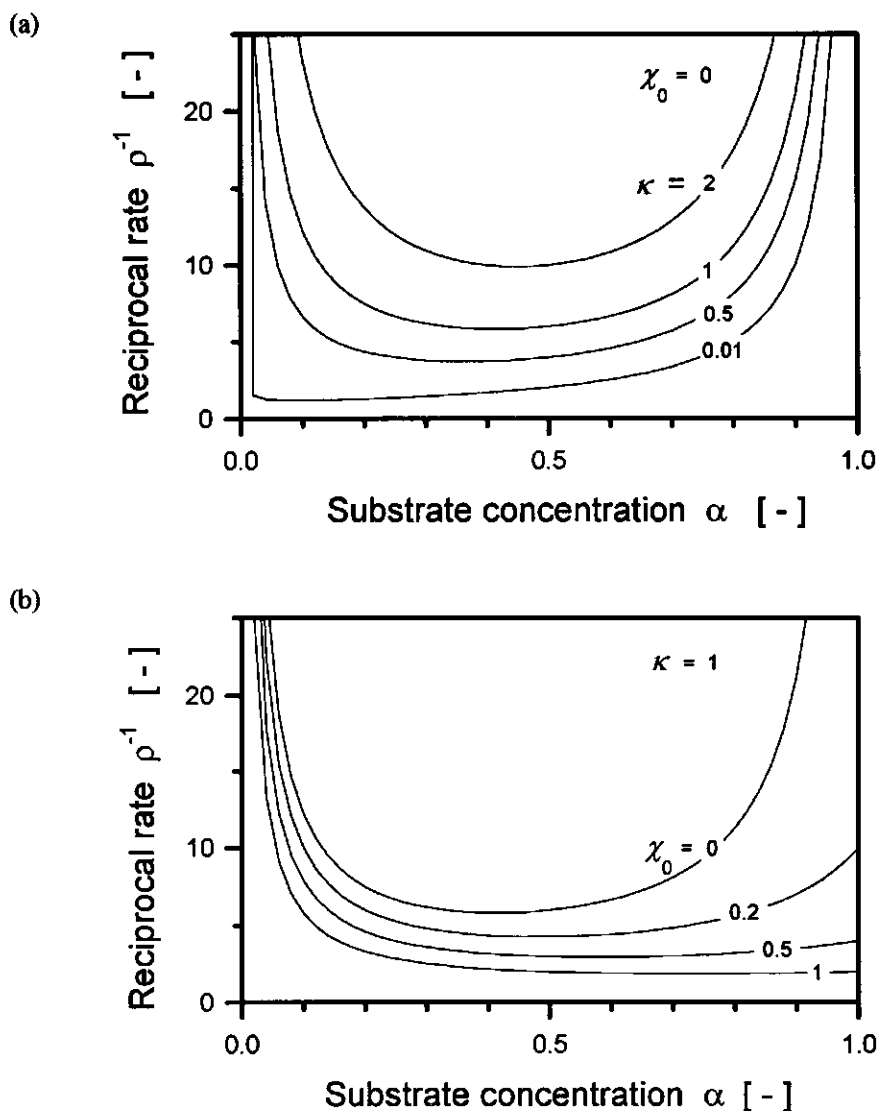


Figure 2. Dimensionless rate ($1/r = \mu_{max}S_0/r_s$) versus the dimensionless concentration ($\alpha = S/S_0$). (a) parameter $\kappa = K_s/S_0$, with no biomass in the influent ($\chi_0 = 0$). At low κ , the minimum in the curves (α_{crit}) decreases to a low value, indicating that a single CSTR performs best for most exit concentrations. (b) parameter $\chi_0 = X_0/Y_{xs}S_0$, with $\kappa = 1$. At high biomass concentrations at the inlet of the series, the minimum of the curves (α_{crit}) shifts to 1, indicating that series of CSTR's perform best for all exit concentrations.

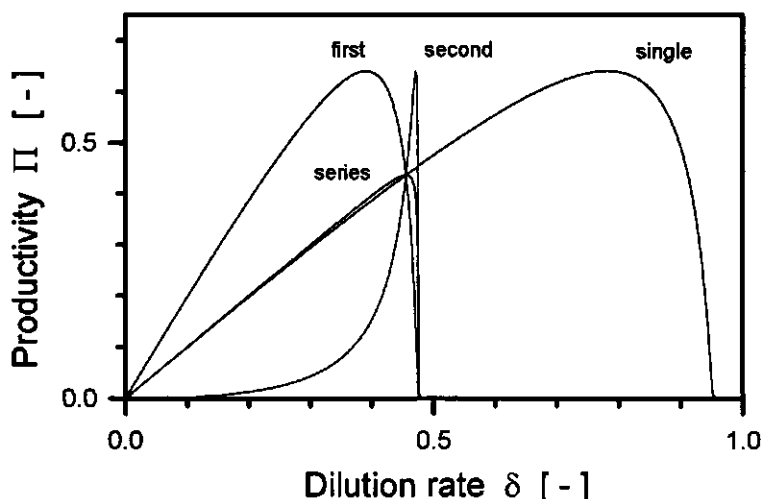


Figure 3. Dimensionless production rate per unit of reactor volume ($\Pi = D \cdot X / \mu_{\max} Y_{xs} S_0$) in an equal-volume two-stage series versus dimensionless dilution rate ($\delta = D / \mu_{\max}$) as compared to a single CSTR. Each reactor on itself (the first and second reactor in the series, and the single CSTR) shows the same maximum in productivity. At low overall dilution rates, the series shows a slightly higher overall productivity; maximum productivity is attained in a single reactor at high dilution rates. Monod kinetics, with $\kappa = K_s / S_0 = 0.05$.

in the first stage, which is found at the maximum of the curve. The slope of this line is equal to F/V_i ;

- iv) Keep the slope of this line constant, start at $\chi = \chi_I$ and determine χ_2 , and so forth.

Similarly, if product formation is the aim of the process, dP/dt versus the product concentration P ($\text{mol} \cdot \text{m}^{-3}$) can be plotted, as applied by Tyagi and Ghose [1980] for the design of an ethanol fermentation with cellulose hydrolysate as substrate. For enzymatic conversions the latter procedure is also adequate.

As shown in Figures 1B and 1C, this procedure may lead to a higher degree of conversion than needed. The alternative design of series of equal-sized CSTR's can be done iteratively, starting with a desired rate of conversion calculating back along the series, or by means of a zero-finding routine, solving the set of equations for each CSTR in the series, in a similar way as will be discussed below.

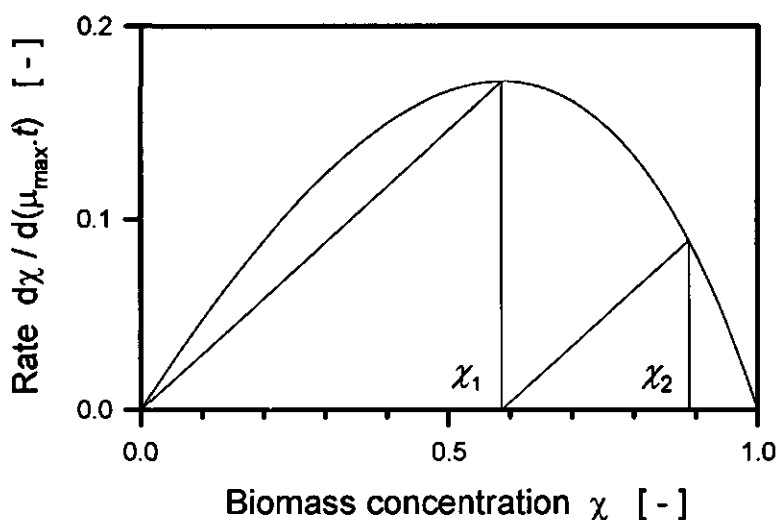


Figure 4. For a cascade of equal-volume CSTRs and a microbial reaction with Monod kinetics, the number of vessels in the series may be determined from a dimensionless rate vs. dimensionless concentration plot according to Fiechter [1981]. Slopes represent dilution rates; the first reactor operates at the maximum rate. See text for details.

Optimal design of a finite series of non-equal-volume-CSTR's. The theory on cascade design may be quite perplexing, due to the plethora of performance criteria and kinetic equations (and combinations thereof). Although quite relevant, economic criteria will be ignored here in favour of an engineering measure: Luyben and Tramper [1982] defined optimal design of a finite series of CSTR's as that configuration that has the minimal total holding time at a given degree of conversion in a series consisting of N reactors. This means that the volumes for all reactors along the series are varied, with a subsequent change in the intermediate substrate concentrations, until a minimal total volume is reached. Mathematically this leads to:

$$\frac{\partial \left[\sum_{j=1}^N \tau_j \right]}{\partial \alpha_i} = 0 \quad i = 1, 2, \dots (N-1) \quad (1)$$

where α_i is the dimensionless substrate concentration in the i -th vessel, S/S_0 , so $\alpha_0 = 1$,

N is the pre-defined number of vessels, and τ_j is the dimensionless residence time in the j -th vessel. τ is defined as $V_i v_{max} e / FS_0$ for enzymes with v_{max} the maximum specific velocity per unit amount of enzyme ($\text{mol.kg}^{-1}.\text{s}^{-1}$) and e the enzyme concentration (kg.m^{-3}), and as $V_i \mu_{max} / F$ for autocatalytic reactions. Although Luyben and Tramper [1982] defined this optimal design for a dissolved enzyme following Michaelis-Menten kinetics, Eq. (1) is independent of the kinetics involved, and has been used by many authors [Malcata, 1988; Hill and Robinson, 1989; De Gooijer *et al.*, 1989; Malcata and Cameron, 1992; Lopes and Malcata, 1993; Paiva and Malcata, 1993].

For autocatalytic systems (suspended micro-organisms), Schügerl [1987] and Hill and Robinson [1989] introduced the concept of a dimensionless critical effluent substrate concentration α_{crit} . At dimensionless effluent concentrations up to or equal to α_{crit} , the optimal "series" is the single tank. This critical concentration can be found by assuming that the dimensionless effluent concentrations of the first and the second vessel in the optimal series are the same, or $\alpha_1 = \alpha_2 (= \alpha_{crit})$, meaning that the volume of the second vessel is zero. If it is found that the desired dimensionless effluent concentration α_N is smaller than α_{crit} , an optimal design is feasible. In Figure 1 and 2, α_{crit} is the minimum of the curve.

Below, the α_{crit} concept and the optimal design of a series will be described for both autocatalytic and catalytic processes. To further classify the latter group, a division is made between non-growing and growing biocatalysts. Within each division, a subclassification is made between freely suspended and immobilized biocatalysts.

AUTOCATALYTIC SYSTEMS

In this section papers dealing with growing cells (Figures 1-4), freely suspended or immobilized, will be reviewed.

Theory. The design of a reactor cascade for autocatalytic reactions depends on the optimization criterion. The minimum overall residence time at an arbitrary but fixed exit substrate concentration will be used as a criterion. To investigate if a series is worth considering, the critical effluent concentration at which the reaction order changes from positive to negative (point A in Figure 1A) and at which the optimal cascade in fact is a single tank (α_{crit}), may be obtained from a procedure given by Hill

and Robinson [1989] and by Schügerl [1987], as discussed below.

A generalized form of the growth equation is used:

$$\frac{\mu}{\mu_{\max}} = \frac{p\alpha + q\alpha^2}{f + g\alpha + h\alpha^2} \quad (2)$$

Here p , q , f , g , and h are dimensionless parameter groups depending on the particular kinetic equation (Table I). Combining the specific growth rate μ (s^{-1}) with the yield factor Y_{xs} ($kg.mol^{-1}$) and the biomass concentration X ($kg.m^{-3}$), the substrate consumption rate r_s ($mol.m^{-3}.s^{-1}$) is obtained:

$$r_s = \frac{\mu}{Y_{xs}} X \quad (3)$$

A general mass balance over a single CSTR in a series yields:

$$\theta_i = \frac{V_i}{F} = \frac{(\alpha_{i-1} - \alpha_i)}{r_{s,i} / S_0} \quad (4)$$

where θ_i is the residence time in the i -th reactor (s). Substituting Eqs. (2) and (3) in Eq. (4) results in an expression for the dimensionless residence time for each vessel in the series in terms of substrate concentrations and kinetic parameters:

$$\tau_i = \frac{V_i \mu_{\max} X_i}{F S_0 Y_{xs}} = \frac{(\alpha_{i-1} - \alpha_i) (f + g\alpha_i + h\alpha_i^2)}{p\alpha_i + q\alpha_i^2} \quad (5)$$

which, with the result of a mass balance over all vessels in the series:

$$X_i = Y_{xs} (S_0 - S_i) + X_0 \quad (6)$$

can be written as :

Table I. Values of the parameters f , g , h , p and q in the general rate equation for autocatalytic reactions, and the critical substrate concentration α_{crit} at which an optimally designed series of bioreactors consists of a single vessel. For lethal product inhibition kinetics the implicit equation for α_{crit} has to be used, for all other kinetics a more convenient expression can be found, as shown.

	Monod	Substrate inhibition	Non-lethal product inhibition	Lethal product inhibition
$\frac{\mu}{\mu_{max}} =$	$\frac{S}{K_S + S}$	$\frac{S}{K_S + S + (S^2/K_I)}$	$\frac{S}{K_S + S} \cdot \frac{1}{1 + (P/K_P)}$	$\frac{S}{K_S + S} \left[1 - \frac{P}{K_P} \right]$
	$\frac{p\alpha + q\alpha^2}{f + g\alpha + h^2}$			
p	1	1	1	$1 - \frac{P_0}{K_P} - \frac{Y_{PS}S_0}{K_P}$
w	0	0	0	$Y_{PS}S_0/K_P$
f	$\frac{K_S}{S_0}$	$\frac{K_S}{S_0}$	$\left[1 + \frac{P_0}{K_P} + \frac{Y_{PS}S_0}{K_P} \right] \frac{K_S}{S_0}$	$\frac{K_S}{S_0}$
g	1	1	$1 + \frac{P_0}{K_P} + \frac{Y_{PS}S_0}{K_P} \left[1 - \frac{K_S}{S_0} \right]$	1
h	0	$\frac{S_0}{K_i}$	$\frac{Y_{PS}S_0}{K_P}$	0
α_{crit} (implicit)	$(1 - \alpha_{crit}) \left[1 + \frac{(1 + \chi_0 - \alpha_{crit})(g + 2h\alpha_{crit})}{(f + g\alpha_{crit} + h\alpha_{crit}^2)} - \frac{(1 + \chi_0 - \alpha_{crit})(p + 2q\alpha_{crit})}{(p\alpha_{crit} + q\alpha_{crit}^2)} \right] = 0$			
α_{crit}	$\sqrt{f^2 + f(1 + \chi_0)} - f$	$\frac{\sqrt{f^2 + f(1 + \chi_0)(1 + h(1 + \chi_0))} - f}{1 + h(1 + \chi_0)}$	$\frac{\sqrt{f^2 + f(1 + \chi_0)(g + h(1 + \chi_0))} - f}{g + h(1 + \chi_0)}$	

$$\tau_i = \frac{V_i \mu_{max}}{F} = \frac{(\alpha_{i-1} - \alpha_i)(f + g\alpha_i + h\alpha_i^2)}{(1 + \chi_0 - \alpha_i)(p\alpha_i + q\alpha_i^2)} \quad (7)$$

For a two-reactor cascade [$N = 2$ in Eq. (1)], operated at a fixed, arbitrary effluent concentration α_2 , optimization requires:

$$\frac{d(\tau_1 + \tau_2)}{d\alpha_1} = 0 \quad (8)$$

and from this equation, an optimal α_1 value is obtained as a function of the effluent concentration chosen (α_2). Implicitly, the volumes of both reactors are defined by this result.

In order to answer the question as to whether or not an optimally designed series is worthwhile, in other words if the desired effluent concentration is to the left of point A in Figure 1A, the minimum of this curve has to be found. Substituting Eq. (7) in Eq. (8), and applying $\alpha_1 = \alpha_2 = \alpha_{crit}$ for this general case of 2 reactors in series, results in the following implicit equation:

$$(1 - \alpha_{crit}) \left(1 + \frac{(1 + \chi_0 - \alpha_{crit})(g + 2h\alpha_{crit})}{(f + g\alpha_{crit} + h\alpha_{crit}^2)} - \frac{(1 + \chi_0 - \alpha_{crit})(p + 2w\alpha_{crit})}{(p\alpha_{crit} + w\alpha_{crit}^2)} \right) = 0 \quad (9)$$

Table I shows the expression for α_{crit} for different types of kinetics. If indeed two reactors in series are superior to a single vessel, that is $\alpha_2 < \alpha_{crit}$, then this procedure may be used to show the favourability of multi-reactor cascades [Hill and Robinson 1989]. This means that:

- i) if two reactors in series are superior to a single vessel then any series of reactors will be superior, and
- ii) the optimization of the design requires an infinite number of vessels that are increasingly smaller along the series, or, the optimal reactor configuration is a single CSTR followed by a PFR.

It can be derived from Table I that a cascade is particularly suited for product-

inhibited autocatalytic reactions: increasing the severity of the inhibition (*i.e.* decreasing K_p , the inhibition constant (mol.m^{-3})), results in an increase in α_{crit} , thus widening the feasibility range for a cascade. This may also be clarified by taking the limit for K_p to zero of α_{crit} . To find this expression, the relation for α_{crit} from the bottom row in Table I is used, and appropriate expressions for f , g , h , p , and q are substituted. Thereby, for the sake of simplicity, it is assumed that both the biomass and product concentration are zero at the inlet of the first reactor ($\chi_0 = 0$ and $P_0 = 0$). For non-lethal product inhibition it can then be found that:

$$\lim_{K_p \rightarrow 0} \alpha_{crit} = \lim_{K_p \rightarrow 0} \frac{(K_p + Y_P S_0) K_S + \sqrt{K_S K_P (K_P + Y_P S_0) (K_S + S_0)}}{S_0 (Y_P K_S - K_P)} = 1 \quad (10)$$

Hence at very strong inhibition (K_p approaching zero) a cascade becomes superior at all effluent concentrations (α_{crit} approaching one).

In case of substrate inhibition, the reverse is true: low K_i values entail low α_{crit} values, or, the more severe the substrate inhibition is, the less favourable series of reactors will become.

Now having the answer to the question *if* a series is worthwhile, that is after the determination of α_{crit} , the optimal design of the series according to Eq. (1) (*how*) can generally be done as suggested by Hill and Robinson [1989]. For N reactors in series, $N-1$ equations with $N-1$ unknown substrate concentrations can be derived by substituting Eq. (7) in Eq. (1) and taking the differentiation:

$$\frac{B(g + 2h\alpha_i) - A}{CD} + \frac{BA}{C^2 D} - \frac{BA(p + 2q\alpha_i)}{CD^2} + \frac{(f + g\alpha_{i+1} + h\alpha_{i+1}^2)}{(1 + \chi_0 - \alpha_{i+1})(p\alpha_{i+1} + q\alpha_{i+1}^2)} = 0 \quad (11)$$

with

$$A = f + g\alpha_i + h\alpha_i^2; \quad B = \alpha_{i-1} - \alpha_i; \quad C = 1 + \chi_0 - \alpha_i; \quad D = p\alpha_i + q\alpha_i^2 \quad (12)$$

and $i = 1..N-1$.

This set of equations can be solved by a suitable algorithm with a zero-finding routine on a PC. Alternatively, for the first two reactors in series, a more convenient design equation can be found for all kinetics with $q = 0$ (all kinetics except lethal product inhibition), and no biomass in the influent of the series ($\chi_0 = 0$). Substitution of Eq. (7) in Eq. (8) will then lead to an expression for α_1 in terms of α_2 :

$$\alpha_1^2 = \frac{f\alpha_2(1 - \alpha_2)}{\alpha_2(h + g) + f} \quad (13)$$

which is the same as found by Hill and Robinson [1989]. Hence, for a two-reactor cascade, Eq. [13] is sufficient, and if the series consist of more than two reactors, Eq. (13) combined with Eqs. (11) and (12) has to be used. After determination of the intermediate substrate concentrations, the required residence times are easily obtained through Eq. (7).

Hill and Robinson [1989] showed for Monod kinetics, Aiba kinetics (product inhibition) and Haldane kinetics (substrate inhibition) that if indeed a series design is favourable (*i.e.* if $\alpha_N < \alpha_{crit}$), three optimally designed non-equal volume CSTR's will provide an overall residence time that is close to the possible minimum, *i.e.* the CSTR-PFR sequence suggested by Bischoff [1966]. Also, it was shown that if three equal-sized CSTR's are used, the decrease in overall residence time is less than with an optimally designed series of non-equal-volume-CSTR's. If a series of equal-sized CSTR's is used, one should consider washout problems in the first vessel. It is also pointed out that although for substrate inhibition kinetics one would intuitively choose a single CSTR, depending on α , series of CSTR's might still be advantageous (Table I). A complication is the fact that with for example Haldane kinetics, the first reactor in the series operating at a substrate concentration beyond that concentration where the rate is maximal becomes inherently unstable (operating at a point to the right from point A in Figure 5: a small increase in the substrate concentration will result in washout, whereas a small decrease will result in an operating point to the left of point A at the same rate).

In the theory above, the assumption was made that all reactors in the series can be described by the same kinetic parameters. Lo *et al.* [1983] discuss the situation where the parameters of the Monod equation are non-identical in the different vessels

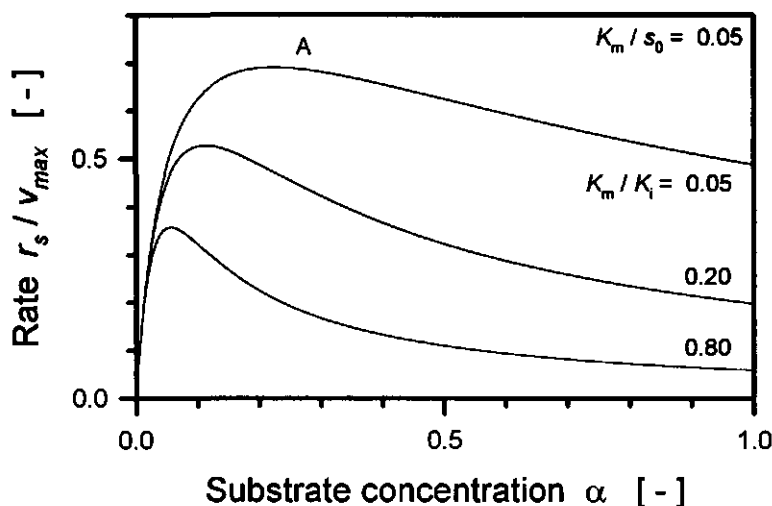


Figure 5. Dimensionless rate (r_s/v_{max}) versus dimensionless substrate concentration ($\alpha = S/S_0$) for substrate inhibition kinetics. The dimensionless substrate concentration at which the maximum rate is attained (point A) equals α_{crit} ; it decreases with increasing severity of the inhibition (*i.e.* lower K_i values).

of the series. They showed, for that case, with the use of two equal-sized bioreactors in series, that design according to the rules discussed above is no longer possible.

Cells in suspension. In this section some examples of freely suspended cells will be discussed, whereas quantitative data on ethanol production are given in Table II, and a review of other processes described in literature is given in Table III.

For the production of lactic acid from whey permeate Aeschlimann *et al.* [1990] conclude that the dilution rate of the series affects all important fermentation parameters. In a single vessel, a maximum volumetric productivity of $2.3 \times 10^{-3} \text{ kg.m}^{-3}.\text{s}^{-1}$ could be reached at a dilution rate of $1.1 \times 10^{-4} \text{ s}^{-1}$ with a degree of conversion of 50%. The addition of a second (non optimally designed) bioreactor resulted in an increase of the degree of conversion, but also in a decrease of the volumetric productivity, due to the additional reactor volume, which is consistent with theory (Figure 3). From their data of the first reactor only, plotted as r_s^{-1} versus S (compare Figure 1D), they simply searched for the minimum area under the curve for

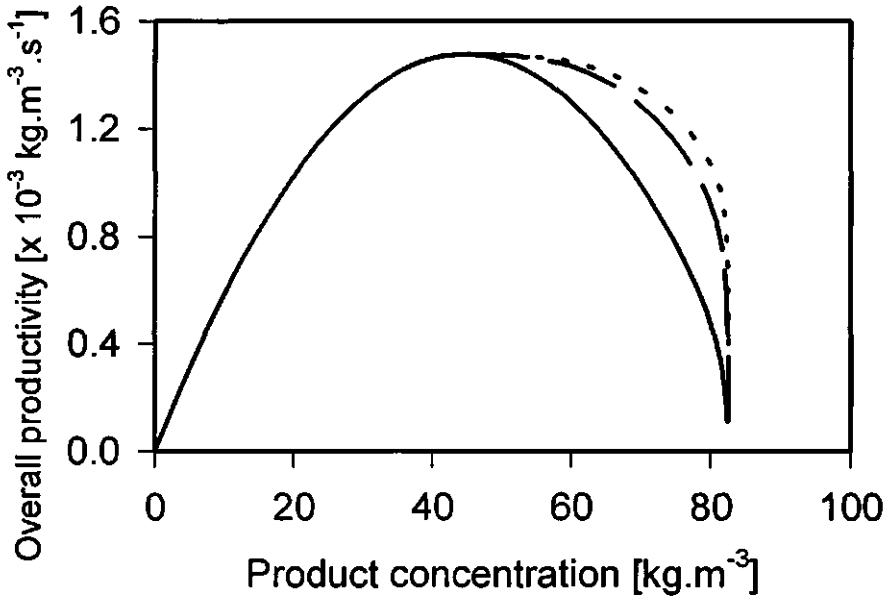


Figure 6. Volumetric productivity of an ethanol fermentation versus product concentration. Solid line = 1, dashed line = 2, dotted line = 3 reactors in series, respectively. Parameter values were as used by Shimizu and Matsubara [1987], with $K_s = 1.6 \text{ kg.m}^{-3}$, $\mu_m = 6.7 \times 10^{-5} \text{ s}^{-1}$, $Y_{xs} = 0.06$, $Y_{xp} = 0.16$, $P_m = 90 \text{ kg.m}^{-3}$, and $S_0 = 220 \text{ kg.m}^{-3}$. Note that at a product concentration of 82.5 kg.m^{-3} all substrate is converted.

two reactors in series, which is a correct approach. Further assuming that the data of the first reactor should also be valid for the second reactor, they conclude that for their case the total reactor volume may be reduced by almost 50% as compared to one fermentor (overall residence times of $3.2 \times 10^4 \text{ s}$ for the series as compared to $5.9 \times 10^4 \text{ s}$ for the single vessel, for a degree of conversion of 98%). They further report values for μ_{max} , S_0 , and S_N of $1.9 \times 10^{-4} \text{ (s}^{-1}\text{)}$, 49.2, and 0.9 (kg.m^{-3}), respectively. In order to be able to illustrate the design procedure discussed above, Monod kinetics were assumed, and a value for K_s was obtained from a fit to their r_s^{-1} versus S plot for the first vessel in the series: $11.6 \text{ (kg.m}^{-3}\text{)}$. Using Table I (Monod kinetics) a value of α_{crit} of 0.3 can be calculated, indicating that indeed a series is favourable. Subsequently, α_1 is found through Eq. (13) to be 0.13 ($\alpha_2 = 0.018$, fixed by the desired degree of conversion). Eq. (7), for the case of Monod kinetics, reduces to $V_2\mu_{max}/F = (\alpha_1 - \alpha_2)(K_s/S_0 + \alpha_2)/((1 - \alpha_2)\alpha_2)$ and $V_1\mu_{max}/F = (K_s/S_0 + \alpha_1)/\alpha_1$ for

the second and first vessel of the series, respectively. This then enables the calculation of the residence times: 1.5×10^4 and 0.8×10^4 s for the first and second vessel in the series, respectively. This results in an overall residence time of 2.3×10^4 s. If $\alpha_I = 0.018$ is substituted in the latter derivation of Eq. (7), the residence time in a single vessel can be calculated to be 7.1×10^4 s. The differences in residence times found here compared to those found by Aeschlimann *et al.* [1989; 1990] may be explained by the organism not completely obeying Monod kinetics. This shows that one should take care on how kinetic data are obtained and used.

An interesting theoretical study of the application of series of CSTR's (up to three reactors) for ethanol production is presented by Shimizu and Matsubara [1987]. They use production kinetics with absolute inhibition ($1-P/P_m$), in combination with either growth-associated or non-growth-associated production, and the condition of a zero-maintenance level. Based on the kinetics and parameter values of Shimizu and Matsubara [1987], the productivity as a function of the product concentration of one, two and three reactors in series was calculated, as shown in Figure 6. Obviously it is not possible to enhance the product concentration beyond P_m if this type of kinetics is involved. However, an improved volumetric productivity is possible at higher degrees of conversion by using more than one reactor. Note that, although the differences are marginal, for product concentrations below the point where the productivity is maximal, one single CSTR has the highest volumetric productivity. In other words, for substrate concentrations above α_{crit} , a single vessel is superior, as expected.

Shama [1988] reviewed the reactor development for fuel ethanol production. For a batch process with glucose as substrate and *Saccharomyces cerevisiae* as microbial strain, volumetric productivities of $2.8 - 6.7 \times 10^{-4}$ kg.m⁻³.s⁻¹ are typical, whereas 19.4×10^{-4} kg.m⁻³.s⁻¹ can be achieved in continuous processes. As can be seen from Table II, continuously operated series of bioreactors can lead to much higher productivities combined with high degrees of conversion, as for example the studies of Klein and Kressdorf [1983, 1986] showed: at almost complete conversion productivities of $158.3 - 300 \times 10^{-4}$ kg.m⁻³.s⁻¹ were reported. Also, compared to a batch process, the ease of control, and the absence of peak loads upon up- and downstream processes favour continuous processes.

Few papers could be found dealing with animal cells, whereas theoretically (an

autocatalytic system with growth-associated production, and very often by-product inhibition) series of bioreactors can be used advantageously for monoclonal-antibody production by hybridomas [Venables *et al.*, 1993; Reuveny *et al.*, 1986; Shimizu and Matsubara, 1987; Pirt 1975]. Reuveny *et al.* [1986] found that for a semi-continuous two-stage system with an extra feed of glucose and glutamine in the second stage, both the monoclonal-antibody concentration and the productivity doubled in the two-stage system as compared to the single semi-continuous bioreactor.

Immobilized growing cells. By immobilization, high cell densities and high volumetric productivities can be achieved. Immobilization also introduces simultaneous diffusion, consumption of substrates, and growth, which is troublesome to relate mathematically to design of a series. Therefore, it is not surprising that no papers could be found that deal with the theory of optimal design of series of CSTR's with immobilized growing cells. However, one paper presents a graphical procedure to provide design rules and estimation of kinetic constants for activated sludge processes for waste-water treatment [Braha and Hafner, 1985].

Godia *et al.* [1987] present a thorough review of the use of immobilized cells for continuous ethanol production. Table II shows experimental data on production of ethanol with series of immobilized-cell bioreactors. With ethanol production, three goals have to be met (preferably simultaneously):

- i) high volumetric productivities to reduce reactor costs,
- ii) high product concentrations to reduce downstream processing costs, and
- iii) high conversion degrees to reduce feed costs.

In a single vessel, these three goals can hardly be met simultaneously. Godia *et al.* [1987] show for example, that in a single vessel a productivity of $150 \times 10^{-4} \text{ kg.m}^{-3}.\text{s}^{-1}$ was obtained at a degree of conversion of 63%, whereas $25 \times 10^{-4} \text{ kg.m}^{-3}.\text{s}^{-1}$ was observed at a degree of conversion of almost 100%. It is still, however, a considerable improvement when compared with the review data of Shama [1988] where typical productivities of $2.8 - 6.7 \times 10^{-4}$ and $19.4 \times 10^{-4} \text{ kg.m}^{-3}.\text{s}^{-1}$ were reported for batch and continuous processes with freely suspended cells. From Table II it is clear that the use of series of reactors with immobilized cells are the most promising prospect to meet the three goals for ethanol production [Klein and Kressdorf, 1983; 1986].

Table II. Quantitative data on ethanol fermentation by several species of *Saccharomyces* and *Zymomonas*. N is the number of vessels in the series, X_a is the attained degree of conversion (%), P is the product concentration ($\text{kg} \cdot \text{m}^{-3}$), and Q_p is the reported volumetric productivity ($10^{-3} \text{ kg} \cdot \text{m}^{-3} \cdot \text{s}^{-1}$).

N	X_a	P	Q_p	Immob. Techn.	S^a M	Substrate	Micro- organism	Reference
2	-	106	1.4/5 ^b	-	S	glucose	<i>Z. mobilis</i>	Charley <i>et al.</i> (1983)
2	97	60	0.8	-	M	sugar beet molasses	<i>Z. mobilis</i>	Park & Baratti (1992)
10	99	90	-	-	S	glucose	<i>S. sake</i> , <i>S. c</i> UG5, <i>S. bayanus</i>	Bovee & Sevely (1982)
2	80	90	1.1	-	S	glucose	<i>S. cerevisiae</i>	Lee <i>et al.</i> (1983)
6	99	80	-	-	M	glucose	<i>S. bayanus</i>	Dourado <i>et al.</i> (1987)
4	86	98	-	-	S	glucose	<i>S. cerevisiae</i> UG5	Chattaway <i>et al.</i> (1988)
8	-	-	0.4	-	S	glucose	<i>S. cerevisiae</i> UG5	Moreno & Goma (1979)
- ^e	96	78	-	alginate	S	cane molasses	<i>S. formosensis</i> M111	Fukushima & Hanai (1982)
5 ^e	92	85.4	1.4	-	M	cane molasses	<i>S. uvarum</i>	Chen & Mou (1992)
3/5	81	-	-	-	M	cane molasses	<i>S. uvarum</i>	Chen (1990)
2	80	-	13.4	sintered glass	S	hydrolyzed waste starch	<i>Z. mobilis</i>	Weuster <i>et al.</i> (1990)
2	95	-	8.3	sintered glass	S	hydrolyzed waste starch	<i>Z. mobilis</i>	Weuster <i>et al.</i> (1990)
3	98	74	15.8	alginate	S	glucose	<i>Z. mobilis</i> DSM424	Klein & Kressdorf (1983)
3 ^d	100	72	30	alginate	S	glucose	<i>Z. mobilis</i>	Klein & Kressdorf (1986)
2	97	81	5.6	flocc.	S	cane molasses	<i>S. cerevisiae</i> HA2	Kida <i>et al.</i> (1990)
2 ^f	99	93	2.6	flocc.	M	cane molasses	<i>S. cerevisiae</i> IR-2	Kuriyama <i>et al.</i> (1993)
8 ^e	98	93	3.9	alginate	S	glucose	<i>S. carlsbergensis</i>	Tzeng <i>et al.</i> (1991)
82	77	4.7						
6	-	130	1.1	wood chips	S	glucose	<i>S. carlsbergensis</i> STV89	Ryu <i>et al.</i> (1982)

Remarks to Table II: a) S is Single feed at the entrance of the series, M is multiple feed in all reactors, b) 5×10^{-3} is with cell recycle, c) if a batch reactor requires 100 capital investment and 100 running costs, they calculate 62 and 89 for their series, respectively, d) two fluidized beds with recirculation followed by a plug-flow reactor, e) multistage fluidized bed with sieve plates, f) both vessels with settler and recycle.

Table III. Examples of autocatalytic processes described in literature. *N* is the number of reactors in series. a) a theoretical study. b) 2 CSTR's followed by one PFR, galactose is added to the PFR.

Product	Substrate	Biocatalyst	<i>N</i>	Reference
Lactic acid	Lactose	<i>Streptococcus cremoris</i> 2487	3	Mulligan <i>et al.</i> (1991)
Lactic acid	Lactose		7	Kulozik <i>et al.</i> (1992)
Lactic acid	Whey permeate	<i>Lactobacillus helveticus</i>	2	Aeschlimann <i>et al.</i> (1990)
Monoclonal Antibodies	-	Hybridoma cells	2	Reuveny <i>et al.</i> (1986)
Monoclonal Antibodies	-	Hybridoma cells	2	Venables <i>et al.</i> (1993)
Streptomycin	Glucose	<i>Streptomyces griseus</i>	3	Sikyta <i>et al.</i> (1959)
Protease	-	<i>Bacillus pumilus</i>	2	Fabian (1969)
3-ketosteroid- Δ^1 -dehydrogenase	Glucose	<i>Arthrobacter simplex</i>	2	Ryu & Lee (1975)
Biomass	Ethanol	<i>Candida utilis</i> IAM 4215	3	Goto <i>et al.</i> (1973)
Biomass	Ethanol	<i>Candida utilis</i> IAM 4215	3	Paca & Gregor (1979a, 1979b), Paca (1980, 1982)
Biomass	Molasses	<i>Torula utilis</i>	2	Fencel <i>et al.</i> (1961), Fencel (1964)
Biomass	D-Sorbitol	<i>Acetobacter suboxydans</i>	2	Ritica (1969)
Biomass	-	<i>Streptococci</i>	2	Holström & Rose (1964)
Biomass	Sugar	<i>Saccharomyces cerevisiae</i>	8	Prokop <i>et al.</i> (1969)
Biomass	Glucose	<i>Aspergillus niger</i>	2	Fencel <i>et al.</i> (1980)
Biomass	Glucose or ethanol	<i>Hansenula polymorpha</i> CBS4732	3, 10	Schügerl (1982)
Biomass	Glucose	<i>Escherichia coli</i> ATCC 11105	3, 10	Schügerl (1982)
Gramicidin S ^{a)}	-	-	3	Blanch & Rogers (1972)
α -galactosidase ^{b)}	Glucose, galactose	<i>Monascus</i>	3	Imanaka <i>et al.</i> (1973)
Acetone, Butanol	Glucose	<i>Clostridium acetobutylicum</i>	2	Bahl <i>et al.</i> (1982)
Wine	Koshu-grape must	<i>Saccharomyces cerevisiae</i> 2HY-1	5	Ogbonna <i>et al.</i> (1989)
Mead	Honey mash	<i>Saccharomyces cerevisiae</i> , <i>Hansenula anomala</i>	2	Qureshi & Tamhane (1986)

CATALYTIC SYSTEMS

Non-growing biocatalysts may consist of enzymes, cell organelles, whole non-viable cells, or viable non-growing cells [Van 't Riet and Tramper, 1991]. In literature however, only reports based on free or immobilized enzymes, applied in bioreactor series, can be found.

Theory. The same optimization criterion as with autocatalytic processes is used: the minimization of the overall cascade residence time at a given final exit concentration of substrate [Eq. (1)]. A fixed reaction stoichiometry is assumed, and the enzyme concentration in each reactor is assumed to be equal and constant. A generalized rate expression is used to represent various types of kinetics (Table IV). As a result, the reaction rate per unit volume r_s equals:

$$r_s = v_{\max} e \frac{k + l\alpha + m\alpha^2}{f + g\alpha + h\alpha^2} \quad (14)$$

where parameters f , g , h , k , l , and m are kinetic characteristics depending on the kinetic equation (see Table IV).

Substitution of Eq. (14) in the general mass balance over a single CSTR in a series [Eq. (4)] yields:

$$\tau_i = \frac{V_i v_{\max} e}{F S_0} = \frac{(\alpha_{i-1} - \alpha_i)(f + g\alpha_i + h\alpha_i^2)}{k + l\alpha_i + m\alpha_i^2} \quad (15)$$

In order to answer the question if an optimally designed series is worthwhile, Eq. (15) is substituted in Eq. (8) for $N=2$, and $\alpha_1 = \alpha_2 = \alpha_{crit}$ is applied. For this general case of 2 reactors in series this results in:

$$\alpha_{crit} = \frac{hk - fm + \sqrt{(hk - fm)^2 + g^2 km - fgml - ghkl + fhl^2}}{gm - hl} \quad (16)$$

Evaluation of Eq. (16) for the different types of kinetics (Table IV) shows that for Michaelis-Menten kinetics, unimolecular-equilibrium kinetics, product-inhibition

kinetics, and first-order kinetics, an optimally designed series is superior to a single vessel at all effluent concentrations: the critical concentration for these kinetics equals the system influent (*i.e.* $\alpha_{crit} = 1$). For substrate inhibited reactions however (Figure 5), the series configuration may be superior, but only if the desired effluent concentration α_N is below α_{crit} *i.e.* below $K_m K_i / S_0^2$ (Table IV). Evaluation of this latter expression shows that for substrate inhibition the feasibility range for the application of a cascade decreases with the severity of the inhibition: α_{crit} decreases with decreasing K_i values. For a zero-order reaction, there is no difference in performance between any cascade and a single-vessel system.

Interestingly, α_{crit} can be found in an alternative way by taking the first derivative of the reaction rate equation with respect to the substrate concentration. If a value of α exists at which this first derivative equals zero, then this value of α is α_{crit} . In other words, as long as the enzymatic reaction rate per volume is monotonically increasing with α , a series of bioreactors will always be superior to a single vessel (Figure 7).

Now having the answer to the question *if* a series is worthwhile, that is after the determination of α_{crit} , the optimal design of the series according to Eq. (1) can generally be done in the same way as suggested by Hill and Robinson [1989] for autocatalytic processes. For the case of Michaelis-Menten kinetics, the final, surprisingly simple design equation following from Eq. (1) is [Luyben and Tramper, 1982]:

$$\alpha_i = \alpha_{i+1}^{i/(i+1)} \quad (17)$$

Starting with the known α_N , the intermediate substrate concentrations can easily be calculated by Eq. (17), if the total number of reactors in the cascade is known. Optimum design results in a monotonically decreasing reactor volume along the series. The decrease in required total holding time is the largest when going from 1 to 2 bioreactors. Also, this decrease is larger at higher desired degrees of conversion. Note that for first order kinetics, exactly the same result is obtained.

Table IV. Values of the parameters f, g, h, k, l, m in the general rate equation for enzyme catalysed reactions [Eq. (14)] and the critical substrate concentration α_{crit} at which an optimally designed series of bioreactors consists of a single vessel.

	Michaelis Menten	Unimolecular equilibrium	Substrate inhibition	Product inhibition	Zero order	First order
$\frac{v}{v_{max}e} =$	$\frac{S}{K_m + S}$	$\frac{S}{K_m} - \frac{v_{max,b}}{v_{max}} \frac{P}{K_p}$ $\frac{P}{1 + (S/K_m) + (P/K_p)}$	$\frac{S}{K_m + S + \frac{S^2}{K_i}}$	$\frac{S}{K_m + S} \cdot \frac{K_p}{K_p + P}$	1	$\frac{S}{K_m}$
	$\frac{k + la + m\alpha^2}{f + g\alpha + h\alpha^2}$					
k	0	$\frac{v_{max,b}}{v_{max}} \frac{K_m}{K_b} \left[\frac{P_0 + Y_P}{S_0} \right]$	0	0	1	0
l	1	$1 + \frac{v_{max,b}}{v_{max}} \frac{K_m}{K_b} Y_P$	1	1	0	1
m	0	0	0	0	0	0
f	$\frac{K_m}{S_0}$	$\frac{K_m}{K_b} \left[\frac{K_b + \frac{P_0}{S_0} + Y_P}{S_0} \right]$	$\frac{K_m}{S_0}$	$\frac{K_m}{K_p} \left[\frac{K_p + \frac{P_0}{S_0} + Y_P}{S_0} \right]$	0	$\frac{K_m}{S_0}$
g	1	1	1	$1 - (K_m + S_0) \frac{Y_P}{K_p} \frac{P_0}{K_p}$	0	0
h	0	$1 - (K_m Y_P / K_b)$	S_0 / K_i	$- Y_P S_0 / K_p$	0	0
α_{crit}	$\frac{hk - fm + \sqrt{(hk - fm)^2 + g^2 km - fgml - ghkl + fh l^2}}{gm - hl}$					
	1	1	$\sqrt{f/h} = (K_m K_i / S_0)$	1	all α	1

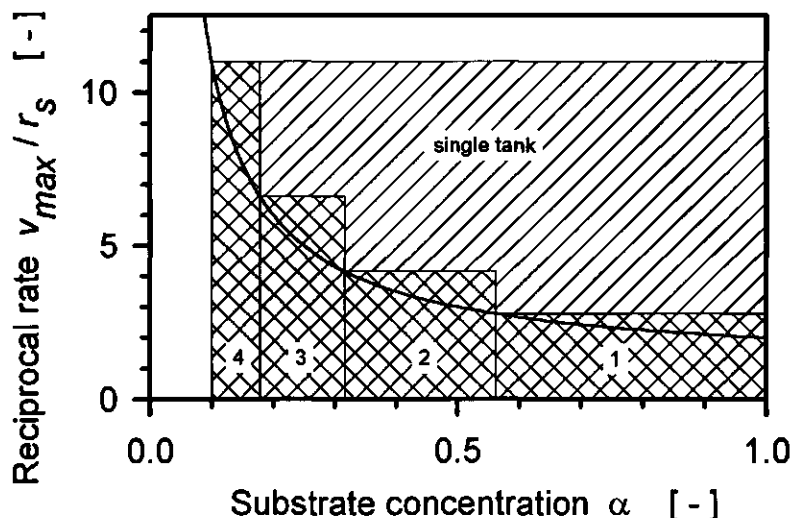


Figure 7. Overall residence times (shaded areas) for an enzymatic reaction with Michaelis-Menten kinetics in a single CSTR and in a cascade consisting of 4 CSTRs. For these kinetics, the curve decreases monotonically, and the cascade requires less holding time at all effluent concentrations.

Another way of assessing if a series of CSTR's is worthwhile is considering the difference between the residence time of a single CSTR and the residence time of a PFR. For Michaelis-Menten kinetics, the dimensionless residence time of a PFR can be described by [Luyben and Tramper, 1982]:

$$\tau_{pfr} = (\alpha_0 - \alpha_1) - \kappa \ln(\alpha_1) \quad (18)$$

with κ being the dimensionless Michaelis-Menten constant (K_m/S_0). The maximum attainable decrease in dimensionless residence times then becomes [Eqs. (4) and (18)]:

$$\xi = \frac{\tau_{pfr}}{\tau_{cstr}} = \frac{1 - \kappa \ln(\alpha_1) / (1 - \alpha_1)}{1 + \kappa / \alpha_1} \quad (19)$$

This equation indeed shows that for high degrees of conversion (α_1 approaching zero), ξ approaches zero, or the residence time of a single CSTR is infinite times higher than that of a PFR. This is in accordance with the findings of Luyben and Tramper [1982]. For the zero-order extreme of Michaelis-Menten kinetics (κ approaching zero) one can

find that ξ equals one (no difference in residence times), and for the first order extreme it can be found that:

$$\lim_{\kappa \rightarrow \infty} \xi = \frac{-\alpha_1 \ln(\alpha_1)}{1 - \alpha_1} \quad (20)$$

illustrating that at high degrees of conversion series of CSTR's might be worthwhile: with $\alpha_1 = 0.1$ and 0.01 , an ξ of 0.26 respectively 0.05 can be found, indicating that a single CSTR would be 4 or 20 times the volume of a PFR, respectively.

Enzymatic decay. First-order decay of enzymes is described by several authors [Lopes and Malcata, 1993; Paiva and Malcata, 1993; Vos, 1990; Yoon *et al.*, 1989; Furusaki *et al.*, 1980; Furusaki and Miyauchi, 1977]. Lopes and Malcata [1993] showed that as long as the time constant for decay is larger than the time constant for flow through the series (V_{tot}/F), a simple relation can be found that allows a good estimate for the reactor sizes in series of 3 and 4 bioreactors. If non-isothermal operation is considered, completely different optima can be found [Paiva and Malcata, 1993].

Vos [1990] describes a reactor system for the production of High Fructose Corn Syrup with immobilized glucose-isomerase. His reactor is a multiple fluidized bed, where intermittently the flow is stopped and the biocatalyst is refreshed top-down, by simply allowing the biocatalyst beads to pass the holes in the sieve plates between the different compartments and removing the beads from the bottom compartment. He concludes that HFCS could be produced 20% cheaper in such a reactor than in a single CSTR.

Yoon *et al.* [1989] describe three other strategies to address enzymatic decay in continuously operated bioreactors: i) change the feed rate for a constant degree of conversion which may affect mass-transfer properties in the bioreactor, ii) accept a decreasing degree of conversion at a constant feed rate, or iii) apply temperature control. For the case of a multi-stage immobilized-glucose-isomerase reactor, it is described that at least 10% higher specific productivities ($\text{mol.kg}^{-1} \text{ enzyme.s}^{-1}$) can be attained with optimal temperature control, and that three bioreactors in series perform better than two.

Dissolved enzymes. Dissolved enzymes are favourable if large throughputs are involved, the enzyme costs are not too high (since it has to be constantly added to the reactor), and residual enzymatic activity can be easily removed, *e.g.* by thermal treatment [Malcata and Cameron, 1992; Paiva and Malcata, 1993; Lopes and Malcata, 1993].

Penicillin acylase shows substrate inhibition, non-competitive 6-APA inhibition and competitive phenyl acetic acid inhibition. Karanth [1979] showed that for the case of hydrolysis of penicillin-G to 6-APA and phenyl acetic acid, 2 CSTR's in series are to be favoured over one batch reactor. In this analysis, at a degree of conversion of 98%, the volume of 1 CSTR would be 8.6 times the value of a batch reactor, and 2 CSTR's would require 1.5 times the batch volume, if the batch would have a zero downtime. If the downtime for the batch reactor would be 1 h with a reaction time of 2 h, the series of CSTR's would show a higher volumetric productivity. These results were confirmed by Noworyta and Bryjak [1993], where the superiority of a three-reactor series was shown over a single CSTR; the total residence time could be reduced by about 40%.

Malcata [1988, 1989] and Ong *et al.* [1986] extended the work of Luyben and Tramper [1982] with a description of the cost of scaleup by a power rule on the equipment capacity. The relation is only valid for a low number of reactors, and the extra costs (spare parts, cleaning) for differently sized bioreactors have to be carefully weighed. For a two-substrate reaction (ping-pong, obeying Michaelis-Menten kinetics) under application of the six-tenth-factor rule for capital investment, Malcata showed that the required volumes of the reactors in the series first decrease and after that increase again, and that never more than three reactors in the series are optimal with respect to reactor capital investment. This is in accordance with the findings of Blanch and Rogers [1972].

Using unimolecular equilibrium kinetics for the production of L-malic acid from fumaric acid, Malcata and Cameron [1992] showed that if the Monod constant K_s is close to the product inhibition constant K_p (Table IV), the optimal reactor series consist of equal-sized bioreactors.

Immobilized enzymes. Compared to dissolved enzymes, only a few papers can be found that describe series of bioreactors with immobilized enzymes. As a logic continuation of the work of Luyben and Tramper [1982], De Gooijer *et al.* [1989]

describe the optimum design of a series of CSTR's with invertase immobilized in alginate, obeying intrinsic Michaelis-Menten kinetics. The mathematical approach is the same as that of Luyben and Tramper [1982], except for the definition of the dimensionless holding time for each vessel: here the efficiency factor η appears in the denominator:

$$\tau_i = \frac{\eta_i V_i v_{\max} e}{FS_0} \quad (21)$$

Consequently, for optimal design the dimensionless concentrations can be calculated as if the enzyme were free [Eq. (17)], and after that for each intermediate substrate concentration along the series an effectiveness factor is determined. These effectiveness factors thus account for the extra volume required to compensate for both internal and external diffusion limitation caused by the immobilisation of the enzyme. Analogously, the same procedure can be applied for other kinetics. Hence, as for suspended enzymes, series of bioreactors are favourable for immobilized enzymes except for substrate inhibited kinetics. Note that for first-order kinetics, with negligible external diffusion limitation, there will be only a single internal effectiveness factor for all bioreactors in the series, since the Thiele modulus for that case is independent of the substrate concentration [Van 't Riet and Tramper, 1991].

In 1994, Bakker *et al.* made the experimental comparison between a single vessel and a three-vessel reactor series. They observed improved sucrose conversion by immobilized invertase to 83 % compared to 73 % in the single vessel with the same overall residence time.

CONCLUDING REMARKS

Theoretically, with respect to the overall residence time for a given degree of conversion, the use of more than one CSTR in series can be advantageous for any non-autocatalytic process that obeys non-zero order kinetics. For autocatalytic processes series of CSTR's can be favourable if a high product concentration combined with a high degree of conversion and an acceptable volumetric productivity is needed. However, one should always carefully weigh the practical and cost implications of more than one bioreactor to the possible advantages.

Few recent papers could be found that describe the use of series of bioreactors in industry. For an early review see Hospodka [1966], describing a few processes including the production of baker's yeast, ethanol (from sugar and starch), beer, and acetone/butanol. The largest scale recently described is of the pilot-plant type [Takahashi and Kyosai, 1991]. This may of course be caused by the reluctance of industry to publish regarding their source of income, but it may also be explained by a certain kind of conservatism in the implementation of the results of scientific research at an early stage [Tramper, 1993].

VARIABLE STOICHIOMETRY PROCESSES

Processes with a variable stoichiometry need a physical separation into two or more reactors (either in space, or time) by their nature. Some examples of such processes are discussed below.

INSECT CELLS

Insect-cell technology is a fast emerging tool for the expression of foreign genes. Also, due to the increase in strict regulations for chemical compounds for crop protection, the interest in the wild-type virus for use as a bioinsecticide emerges. Suspension cultures of insect cells can be generated by adapting cells of insects (*e.g.* *Spodoptera frugiperda*) via T-flasks to suspension cultures in spinner flasks or bioreactors. These cells are still susceptible to infection with the non-occluded form of a baculovirus (*e.g.* *Autographa californica* Nuclear Polyhedrosis Virus). After infection, cells will produce newly synthesized non-occluded viruses, and, subsequently, occluded viruses in the form of polyhedra, or recombinant proteins of foreign origin [Granados, 1976; 1980]. After this, the cells lyse. Therefore, if continuous production is desired, a physical separation has to be introduced, as suggested by Tramper and Vlak [1986]. Kompier *et al.* [1988] were the first to describe a successful experimental setup for such a process. They used a first CSTR to grow cells, followed by a second CSTR in series where infection takes place. Subsequently, Van Lier *et al.* [1990, 1992] investigated the optimization of the continuous production. It appeared that continuous production for prolonged periods

of time is hampered by the occurrence of the so-called passage effect, which manifests itself as a reduction in the number of non-occluded viruses and a decrease in the infectivity of these viruses. Based on an infection model, De Gooijer *et al.* [1992] suggested a pseudo-continuous mode of operation of the reactor series in the form of a repeated batch or fed-batch of the infection vessel, in order to reduce this passage-effect. The feasibility of such a process had already been demonstrated by Klöppinger *et al.* [1990] and was confirmed by Zhang *et al.* [1993].

WASTE-WATER TREATMENT

For waste-water treatment, reactor costs should be minimized under the constraint of high degrees of conversion. In the specialized journals in this field, numerous papers can be found describing reactor design. Some relevant studies are listed below.

Mitchell and Shuler [1978] studied the production of Single Cell Protein (SCP) for feedstuff purposes. Here, in a first vessel, carbohydrates and urea in poultry manure were converted. In a second stage, where the SCP was formed, glucose was added as additional carbon source, while the ammonia from urea was used as nitrogen source.

Aivisidis *et al.* [1989] described the anaerobic degradation of complex substrates to methane. In a first CSTR, acidogenic bacteria decomposed carbon sources into low-molecular-weight compounds with concomittant acidification of the waste-water to pH 3-4. In the second stage, for their case a fixed-bed loop reactor, methanogenic bacteria produced methane from these acids. This resulted in a more stable process with a lower occurrence of pathogens, but with a higher investment and a necessary pH control. A similar distribution of the subsequent steps in anaerobic degradation was found by Howgrave-Graham *et al.* [1994] for a three stage anaerobic digester with cellobiose as sole carbon source. Arora and Mino [1992] and Takahashi and Kyosai [1991] reported on the use of a series of bioreactors for treating domestic wastewaters for standard COD removal. With 5 reactors in series at pilot-plant scale, a conversion degree of 90% could be reached producing less sludge and without the need of a final settler tank. Yang *et al.* [1993] reported on the development of a cascade of 5 ponds in series, consisting of empty oil barrels, for treating swine waste water in tropical areas. Over 90% of all pollutants were removed well in this ultimately cheap series of bioreactors.

(DE)NITRIFICATION

Due to the low specific growth rate of nitrifying bacteria, the nitrifying capacities of traditional waste-water plants is often poor [Barnes and Bliss, 1983]. Taniguchi *et al.* [1988] described the use of two airlifts in series with sludge for simultaneous nitrification and denitrification, in which 80% of the ammonia was converted to nitrogen gas. Al-Haddad *et al.* [1991] used four aerated submerged fixed-film bioreactors in series to nitrify ammonia. Brauer and Annachhatre [1992a; 1992b] used three reciprocating jet bioreactors in series to remove ammonia from real-life waste water. A reciprocating jet bioreactor consists of a cylindrical vessel containing an assembly of sieve plates attached to vertical rods, which is given a reciprocatory motion. The first reactor was used to remove the majority of the carbon, the second did the nitrification, and the third the denitrification. In this process, 90% of the carbon was removed, and 85-95% of the ammonia was converted into nitrogen gas. For the denitrifying bacteria, methanol was used as additional carbon source. A similar process was suggested by Santos *et al.* [1993] in a multiple airlift-loop reactor (see the 'reactors' section).

RECOMBINANT MICRO-ORGANISMS

Barbotin *et al.* [1990] and Berry *et al.* [1990] described the improvement of apparent plasmid stability by immobilization of recombinant *Escherichia coli* in a two-stage bioreactor series. In the first stage, cells, immobilized in carrageenan, were grown. Released cells were fed to a second stage, where a temperature shock was used for derepression (*i.e.* production). This resulted in a five-fold production rate of catechol 2,3-dioxygenase. Fu *et al.* [1993] and literature cited therein described the continuous production and excretion of β -lactamase by genetically engineered *Escherichia coli* in suspension in a two stage-chemostat. The micro-organism was grown in the first chemostat, after which the expression of the protein was induced by isopropyl-b-D-thiogalactopyranoside in the second chemostat. Continuous production was possible for over 50 days, with the product accounting for 25% of the cellular protein. Due to cell death and the selection for *lac*⁻ cells this process fails in a single chemostat.

OTHER PRODUCTS

Already in 1959, Pirt and Callow suggested the use of a series of CSTR's to produce

penicillin. In the first vessel the mould would be grown at a pH below 7, in order to avoid the formation of aberrant hyphae, whereas in a second stage penicillin could be produced at pH 7.4 where the penicillin production is optimal.

Ricica [1964] showed that the biosynthesis of 6-azauracil (AzU) by *Escherichia coli* B was not feasible in a single CSTR since AzU inhibits cell growth. He successfully demonstrated the production in a series of four CSTR's, and also showed that the replacement of the last CSTR by a tubular reactor was not successful, which was attributed to a lack of oxygen in the latter reactor.

A rather important aspect of series was studied by Plevako [1964]. Baker's yeast was grown in a first CSTR, after which in a smaller second stage, under the condition of slight aeration, the residual substances in the medium were utilized, thus allowing the stabilization of the cell's enzyme system in maturing cells. It was reported that a high-quality, stable product with good keeping conditions was obtained.

Lelieveld [1984] described the continuous production of yoghurt (two strains) and buttermilk (three strains) with mixed cultures in a two-stage cascade. It was reported that in the first stage the lactic acid bacteria multiply whereas in the second stage they produced most of the desired (flavour) metabolites. He addressed the risk of the product being affected by the selection of a faster-growing mutant strain. If it is assumed that 1 mutant organism, having a 10% higher specific growth rate, is present at the very start of the fermentation, he showed that a continuous process can be run for 3.3 weeks for buttermilk cultures and for 1.1 weeks for yoghurt cultures if it is acceptable that 1% of the final microbial population is the mutant. The results from several years of full-scale production supported this conclusion.

For the removal of hexose and pentose sugars from agricultural waste streams, Grootjen *et al.* [1991] concluded that a physical separation between the two yeast strains used (*Pichia stipitis* for pentose sugars and *Saccharomyces cerevisiae* for hexose sugars) was necessary, since otherwise the yeasts will compete for oxygen, resulting in a low conversion of xylose.

Pfaff *et al.* [1993] described the use of two CSTR's in series for the removal of trichloroethylene (TCE) from drinking water. *Pseudomonas putida* was grown in the first chemostat, with ethanol as carbon source and phenol to induce the toluene dioxygenase enzyme system. In the second reactor, TCE was added. By the use of this second stage, the competition between phenol and TCE was minimised while the

biomass, inactivated by toxic TCE oxidation products, was replenished.

Series of bioreactors can also function as a research tool in itself: Molly *et al.* [1993] used five CSTR's of different volumes to successfully mimic the human gastro-intestinal tract. The small intestine was simulated by a two-step "fill-and draw" series (not continuously operated), the large intestine consisted of a continuously operated series of three CSTR's with different residence times.

A last small-scale application is the use of two bioreactors in tandem in a continuous-flow / stopped-flow sample / reagent processing setup for the determination of alkaline phosphatase activity in serum, as described by Raba and Mottola [1994]. With this analysis, co-immobilization of the enzymes involved (alkaline phosphatase and alcohol oxidase) would fail since the enzymes show mutual product inhibition, and buffer incompatibility. By physically separating the two enzymes, a successful assay was reported.

CONCLUDING REMARKS

Obviously, when the stoichiometry of the reaction changes with time in a batch process, a series of bioreactors is intrinsically favourable if a continuous process is aimed at. Some examples of such processes have been presented. The rules for deciding if a continuous process is more competitive than a classical (fed-) batch process, cannot be presented in a form analogous to the kinetically favourable series. Parameters involved in such a decision are the volumetric productivity, the stability of the organism, the acceptability of the risk of contamination, and the ease of construction and costs of a series compared to a single vessel.

REACTORS

The costs of series of conventional bioreactors form an important incentive to develop novel bioreactor types incorporating the principles of series. Many of those devices are patented. Only those patents that describe reactors that are relatively easy to scaleup are presented here. Almost all patents deal with cylindrical vessels in which compartments are formed by sieve plates [Lumb *et al.*, 1970; Kitai *et al.*, 1971; Blaß *et al.*, 1979; Caro, 1987]. Already in 1970, Lumb *et al.* patented a device consisting

of five compartments for the production of neomycin with *Streptomyces fradiae*. Blaß *et al.* [1979] patented the sieve plate itself: the holes in the plate should not occupy more than 15% of the bubble column area. Caro [1987] patented a cylindrical vessel with concentric cylinders inside to produce biogas from organic wastes. In the inner cylinder hydrolysis takes place, the middle stages show acidification, and in the outer stage methanogenesis occurs. The patent of Aivasidis *et al.* [1987] describes a fixed bed column for anaerobic decomposition processes, in which two or more compartments are stacked with open plates in between and a separate gas outlet for each chamber. Grobicki and Stuckey [1991] describe the Anaerobic Baffled Reactor (ABR) for waste-water treatment. These rectangular boxes, with working volumes of 8-10 dm³, are compartmentalized with alternately hanging and standing vertical baffles. ABR's with 4 to 8 compartments are described. As such, the ABR can be regarded as a series of upflow anaerobic sludge blanket reactors [Lettinga, 1980].

Recently, Bakker *et al.* [1993] presented results with a novel bioreactor [De Gooijer, 1989] consisting of a series of concentric airlift reactors with internal loop incorporated into one vessel. From the mixing behaviour it is shown that their prototype with three ALR's in series can be described by three ideal mixers in series, thus approximating an aerated plug-flow reactor [Levenspiel, 1972].

CONCLUSIONS

In this paper a classification is presented to decide if and when a series of bioreactors can be advantageously used, for both catalytic and autocatalytic processes. The optimization criterion used is the total holding time of the series compared to a single CSTR, at a given substrate concentration in the last vessel.

For autocatalytic processes there is no type of kinetics where a series is always superior to a single CSTR. With the critical substrate concentration concept as introduced by Hill and Robinson [1989], the feasibility of a series can be predicted. The first step to take is to calculate a critical substrate concentration at which the single vessel and a two-reactor cascade are equivalent. At desired effluent concentrations $\alpha_N < \alpha_{crit}$, a cascade is superior, and at desired effluent concentrations $\alpha_{crit} < \alpha_N < 1$ the single vessel is to be preferred.

For catalytic processes based on enzymes, it is shown that a series of bioreactors is always superior to a single CSTR if the rate of reaction is monotonically increasing with the substrate concentration (Michaelis-Menten, first order, product inhibition, and unimolecular equilibrium kinetics). For substrate inhibition kinetics, a single vessel may be superior. This superiority can also be determined by applying the α_{crit} concept. If a series is superior, the second step is to calculate the intermediate substrate concentrations. For the case of free or immobilized enzymes following Michaelis-Menten or first-order kinetics, these intermediary substrate concentrations can be calculated by a simple relation [Eq. (17)]. Furthermore, from the work of Malcata [1988, 1989], who evaluated the capital investment for series of bioreactors for enzymatic processes, and from the work of Blanch and Rogers [1972] and Hill and Robinson [1989], who evaluated series for autocatalytic processes, it can be concluded that the maximum number of bioreactors, when a series is worthwhile, is equal to three.

From the examples of the application of series of bioreactors found in literature it is clear that the use of series on an industrial scale is limited, and that most applications for kinetically favourable series can be found in ethanol production. As illustrated in Figure 1 and Table III, the combination of a high product concentration, a high degree of conversion, and a large volumetric productivity may well be attained in a series of bioreactors.

In the situation where use of a series is intrinsically favourable, that is virtually any process where the overall stoichiometry of the reaction changes with time, some interesting applications are presented, all on a laboratory scale.

The overview of the novel bioreactor types for series of CSTR's within one vessel shows that progress has been made in reactor development, which will lead to a possible reduction in cost for a series of reactors, and thus enhance the potential application of continuous processes on a larger scale.

APPENDIX A

A general mass balance for biomass in an ideally mixed bioreactor is:

$$V \frac{\partial X}{\partial t} = FX_0 - FX + VX\mu \quad (22)$$

which, under the assumption of steady state, and no biomass in the influent, reduces to:

$$\mu = \frac{F}{V} \quad (23)$$

A general mass balance for substrate is:

$$V \frac{\partial S}{\partial t} = FS_0 - FS + Vr_s \quad (24)$$

where r_s , the volumetric substrate uptake rate, is defined as:

$$r_s = \frac{\mu}{Y_{XS}} X \quad (25)$$

Again under steady state conditions, Eq. (24) can be simplified, and after combination with Eq. (23) this results in:

$$r_s = \mu (S_0 - S) \quad (26)$$

Introducing Monod kinetics, and combining Eq. (26) with the Monod equation, the result is:

$$\frac{r_s}{\mu_m} = \frac{S(S_0 - S)}{K_s + S} \quad (27)$$

which, with the introduction of the following dimensionless variables:

$$\rho = \frac{r_s}{\mu_m S_0}, \quad \kappa = \frac{K_0}{S_0}, \quad \alpha = \frac{S}{S_0} \quad (28)$$

can be rewritten to:

$$\frac{1}{\rho} = \frac{\kappa + \alpha}{\alpha - \alpha^2} \quad (29)$$

which is the equation that is depicted in Figure 1.

NOMENCLATURE

α	dimensionless substrate concentration (S/S_0)	[-]
χ	dimensionless biomass concentration ($X/Y_{xs}S_0$)	[-]
τ	dimensionless residence time in enzyme reactor ($V_i v_{max} e / FS_0$)	[-]
	or in autocatalytic reactor ($V_i \mu_{max} / F$)	[-]
κ	dimensionless Michaelis constant (K_m/S_0)	[-]
ρ	dimensionless substrate consumption rate ($r_s/\mu_{max}S_0$)	[-]
ξ	ratio of the residence times in a PFR and a CSTR	[-]
μ	specific growth rate	[s ⁻¹]
Θ	residence time	[s]
D	dilution rate	[s ⁻¹]
e	enzyme concentration	[kg.m ⁻³]
f	kinetic characteristic parameter (Table I and II)	[-]
F	flow rate	[m ³ .s ⁻¹]
g	kinetic characteristic parameter (Table I and II)	[-]
h	kinetic characteristic parameter (Table I and II)	[-]
k	kinetic characteristic parameter (Table II)	[-]
K	dimensionless monod constant ($K_s/(S_0 + X_0/Y_{xs})$)	[-]
K_b	kinetic constant, equilibrium reaction backwards	[mol.m ⁻³]
K_i	substrate inhibition constant	[mol.m ⁻³]

K_m	Michaelis constant	[mol.m ⁻³]
K_p	product inhibition constant	[mol.m ⁻³]
K_s	Monod constant	[mol.m ⁻³]
l	kinetic characteristic parameter (Table II)	[-]
m	kinetic characteristic parameter (Table II)	[-]
N	number of vessels in a series	[-]
p	kinetic characteristic parameter (Table I)	[-]
P	product concentration	[mol.m ⁻³ or kg.m ⁻³]
P_m	maximal product concentration	[mol.m ⁻³ or kg.m ⁻³]
q	kinetic characteristic parameter (Table I)	[-]
r_s	volumetric reaction rate	[mol.m ⁻³ .s ⁻¹]
S	substrate concentration	[mol.m ⁻³]
V	reactor volume	[m ³]
v_{max}	maximum reaction rate per unit amount of enzyme	[mol.kg ⁻¹ .s ⁻¹]
$v_{max,b}$	id., backward direction	[mol.kg ⁻¹ .s ⁻¹]
X	biomass concentration	[kg.m ⁻³]
X_a	degree of conversion	[-]
Y_p	yield of product on substrate	[kg.mol ⁻¹]
Y_{xs}	yield of biomass on substrate	[kg.mol ⁻¹]

Subscripts

0	inlet of a series
crit	critical effluent concentration at which a single vessel and a two-reactor cascade are equivalent
i	i -th vessel in a series
j	j -th vessel in a series
max	maximum
N	last vessel in a series

REFERENCES

- [1] Aeschlimann, A. 1989. Production of lactic acid from whey permeate by *Lactobacillus helveticus*. PhD thesis, Lausanne Federal Polytechnical University, Switzerland.
- [2] Aeschlimann, A.; Di Stasi, L.; Von Stockar, U. 1990. Continuous production of lactic acid from whey permeate by *Lactobacillus helveticus* in two chemostats in series. *Enzyme. Microb. Technol.* **12**: 926-932.
- [3] Aivasidis, A.; Wandrey, Ch.; Hilla, E. 1989. Studies on reaction techniques concerning reactor design for the anaerobic degradation of complex substrates with the example of methanation of effluents in the fermentation industry. *Bioproc. Eng.* **4**: 63-74.
- [4] Aivasidis, A.; Wandrey, Ch.; Pick, R. 1987. Fixed bed reactor column for anaerobic decomposition processes. U.S. Patent nr 4,670,140, 1987.
- [5] Al-Haddad, A.A.; Zeidan, M.O.; Hamoda, M.F. 1991. Nitrification in the aerated submerged fixed-film (ASFF) bioreactor. *J. Biotechnol.* **18**: 115-128.
- [6] Arora, S.; Mino, T. 1992. An experimental investigation of mechanism and operation conditions of multi-stage reversing-flow bioreactor (MRB) in treating domestic wastewater. *Wat. Sci. Tech.* **26**: 2469-2472.
- [7] Bahl, H.; Andersch, W.; Gottschalk, G. 1982. Continuous production of acetone and butanol by *Clostridium acetobutylicum* in a two-stage phosphate limited chemostat. *Eur. J. Appl. Microbiol. Biotechnol.* **15**: 201-205.
- [8] Bakker, W.A.M.; Knitel, J.T.; Tramper, J.; De Gooijer, C.D. 1994. Sucrose conversion by immobilized invertase in a multiple air-lift loop bioreactor. *Biotechnol. Prog.* **10**: 277-283.
- [9] Bakker, W.A.M.; Van Can, H.J.L.; Tramper, J.; De Gooijer, C.D. 1993. Hydrodynamics and mixing in a multiple air-lift loop reactor. *Biotechnol. Bioeng.* **42**: 994-1001.
- [10] Barbotin, J-N.; Sayadi, S.; Nasri, M.; Berry, F.; Thomas, D. 1990. Improvement of plasmid stability by immobilization of recombinant microorganisms. *Ann. New York Acad. Sci.* **589**: 41-53.
- [11] Barnes, D.; Bliss, P.J. 1983. Biological control of nitrogen in waste-water treatment. E.&F.N. Spon, London, U.K.
- [12] Berry, F.; Sayadi, S.; Nasri, M.; Thomas, D.; Barbotin, J-N. 1990. Immobilized and free cell continuous cultures of a recombinant *E. coli* producing catechol 2,3-

- dioxygenase in a two-stage chemostat: improvement of plasmid stability. *J. Biotechnol.* **16**: 199-210.
- [13] Bischoff, K.B. 1966. Optimal Continuous Fermentation Reactor Design. *Can. J. Chem. Eng.* **50**: 281-284.
- [14] Blanch, H.W.; Rogers P.L. 1972. Optimal conditions for gramicidin S production in continuous culture. *Biotechnol. Bioeng.* **14**: 151-171.
- [15] Blaß, E.; Wolf, C; Koch, K-H. 1979. Kontinuierliches Verfahren in einem Blasensäulen-Kaskadenreaktor. German patent nr. 2167070, Schering AG, Berlin, Federal Republic of Germany, (In German).
- [16] Bovee, J.P.; Sevely, Y. 1982. A new trend in alcoholic fermentation: modelling and optimal steady state for a continuous cascade ethanol production. In: *Modelling and Control of Biotechnical processes*. IFAC, Helsinki, Finland.
- [17] Braha, A.; Hafner, F. 1985. Use of Monod kinetics on multi-stage bioreactors. *Water res.* **19**: 1217-1227.
- [18] Brauer, H.; Annachhatre, A.P. 1992a. Nitrification and denitrification in a system of reciprocating jet bioreactor. *Bioproc. Eng.* **7**: 269-275.
- [19] Brauer, H.; Annachhatre, A.P. 1992b. Waste-water nitrification kinetics using reciprocating jet bioreactor. *Bioproc. Eng.* **7**: 277-296.
- [20] Caro, T. 1987. Mehrstufiges Verfahren und Apparatur zur Umwandlung von organischen und anorganischen Stoffen durch Katalysatoren. German patent nr. DE 3604415 A1, (In German).
- [21] Charley, R.C.; Fein, J.E.; Lavers, B.H.; Lawford, H.G.; Lawford, G.R. 1983. Optimization of process design for continuous ethanol production by *Zymomonas mobilis* ATCC 29191. *Biotechnol. Lett.* **5**: 169-174.
- [22] Chattaway, T.; Goma, G.; Renaud, P.Y. 1988. Modelling Ethanol and Secondary Inhibitions of Ethanol Fermentation in a Multistage Reactor. *Biotechnol. Bioeng.* **32**: 271-276.
- [23] Chen, H.C. 1990. Non-aseptic, Multi-stage, Multi-feeding, Continuous Fermentation of Cane Molasses to Ethanol. *Proc. Biochem. Internat.* **6**: 87-92.
- [24] Chen, H.C.; Mou, D.G. 1990. Pilot-Scale Multi-Stage Multi-Feeding Continuous Ethanol Fermentation Using Non-Sterile Cane Molasses. *Biotechnol. Lett.* **12**: 367-372.
- [25] De Gooijer, C.D. 1989. Werkwijze voor het uitvoeren van biotechnologische processen in meer-traps loopreactoren. Dutch patent application 89.01649, (In Dutch).
- [26] De Gooijer, C.D.; Hens, H.J.H.; Tramper, J. 1989. Optimum design for a series of

continuous stirred tank reactors containing immobilized biocatalyst beads obeying intrinsic Michaelis-Menten kinetics. *Bioproc. Eng.* **4**: 153-158.

- [27] De Gooijer, C.D.; Koken, R.H.M.; Van Lier, F.L.J.; Kool, M.; Vlak, J.M.; Tramper, J. 1992. A structured dynamic model for the baculovirus infection process in insect-cell reactor configurations. *Biotechnol. Bioeng.* **40**: 537-548.
- [28] Deindoerfer, F.H.; Humphrey, A.E. 1959. A logical approach to design of multistage systems for simple fermentation processes. *Ind. Eng. Chem.* **51**: 809-812.
- [29] Dourado, A.; Goma, G.; Albuquerque, U.; Sevely, Y. 1987. Modeling and Static Optimization of the Ethanol Production in a Cascade Reactor. I. Modeling. *Biotechnol. Bioeng.* **29**: 187-194.
- [30] Dourado, A.; Calvet, J.L.; Sevely, Y.; Goma, G. 1987. Modeling and Static Optimization of the Ethanol Production in a Cascade Reactor. II. Static Optimization. *Biotechnol. Bioeng.* **29**: 195-203.
- [31] Fabian, J. 1969. Protease synthesis of *Bacillus pumilus* grown in continuous culture. In: *Proc. 4th symp. contin. cult. microorganisms* (Malek, I., et al., Eds.). Academic press, New York, 489-495.
- [32] Fencel, Z. 1964. A comparative study of cell mass production in a single- and multistage cultivation. In: *Proc. 2nd symp. contin. cult. microorganisms* (Malek, I., et al., Eds.). Czechoslovak Academy of Sciences, Prague, CSSR, 109-119.
- [33] Fencel, Z. 1966. Theoretical analysis of continuous culture systems. In: *Theoretical and methodological basis of continuous culture of microorganisms* (Malek, I.; Fencel, Z., Eds.). Publishing house of the Czechoslovak Academy of Sciences, Prague, CSSR, 69-153.
- [34] Fencel, Z.; Machek, F.; Novak, M. 1969. Kinetics of product formation in multi-stage continuous culture. In: *Fermentation advances* (Perlman, D., Ed.). Academic Press, New York, 301-323.
- [35] Fencel, Z.; Ricica, J.; Kodesova, J. 1972. The use of the multi-stage chemostat for microbial product formation. *J. Appl. Chem. Biotechnol.* **22**: 405-416.
- [36] Fencel, Z.; Silinger, V.; Nusl, J.; Malek, I. 1961. Theory of semicontinuous and continuous cultivation applied to the yeast *Torula utilis*. *Folia Microbiol.* **6**: 94-103.
- [37] Fencel, Z.; Ujcova, E.; Machek, F.; Seichert, L.; Musilkova M. 1980. Continuous cultivation of fungi. In: *Proc. 7th symp. contin. cult. microorganisms* (Sikyta, B., et al., Eds.). Prague, CSSR, 49-62.
- [38] Fiechter, A. 1981. Batch and continuous culture of microbial, plant and animal cells. In: *Biotechnology: a comprehensive treatise in 8 vol.: Microbial fundamentals*.

- (Rehm, H.J.; Reed, G., Eds.). VCH, Weinheim, Federal Republic of Germany, 1: 455-504.
- [39] Fu, J.; Wilson, D.B.; Shuler, M.L. 1993. Continuous, high level production and excretion of a plasmid-encoded protein by *Escherichia coli* in a two-stage chemostat. *Biotechnol. Bioeng.* **41**: 937-946.
- [40] Fukushima, S.; Hanai, S. 1982. Pilot operation for continuous alcohol fermentation of molasses in an immobilized bioreactor. In: *Enzyme engineering*, vol. 6, (Chibata, I., et al., Eds.) Plenum, New York, 347-348.
- [41] Furusaki, S.; Matsuura, I.; Miyauchi, T. 1980. Effect of the cascade operation of enzymes in packed bed immobilized enzyme reactors. *J. Chem. Eng. Japan* **13**: 304-308.
- [42] Furusaki, S.; Miyauchi, T. 1977. Effect of the control of the residence time distribution for aging enzyme by a cascade operation -Michaelis-Menten kinetics-. *J. Chem. Eng. Japan* **10**: 247-249.
- [43] Godia, F.; Casas, C.; Sola, C. 1987. A survey of continuous ethanol fermentation systems using immobilized cells. *Process Biochem.* **4**: 43-48.
- [44] Goto, S.; Kitai, A.; Ozaki, A. 1973. Continuous yeast cell production from ethanol with a multi-stage tower fermenter. *J. Ferment. Technol.* **51**: 582-593.
- [45] Granados, R.R. 1976. Infection and replication of insect pathogenic viruses in tissue culture. *Adv. Virus Res.* **20**: 189-236.
- [46] Granados, R.R. 1980. Infectivity and mode of action of baculoviruses. *Biotechnol. Bioeng.* **22**: 1377-1405.
- [47] Grobicki, A.; Stuckey, D.C. 1991. Performance of the anaerobic baffled reactor under steady-state and shock loading conditions. *Biotechnol. Bioeng.* **37**: 344-355.
- [48] Grootjen, D.R.J.; Jansen, M.L.; Van der Lans, R.G.J.M.; Luyben, K.Ch.A.M. 1991. Reactors in series for the complete conversion of glucose/xylose mixtures by *Pichia stipitis* and *Saccharomyces cerevisiae*. *Enzyme Microb. Technol.* **13**: 828-833.
- [49] Herbert, D. 1964a. Multi-stage continuous culture. In: *Proc. 2nd symp. contin. cult. microorganisms* (Malek, I., et al., Eds.). Czechoslovak Academy of Sciences, Prague, CSSR, 23-44.
- [50] Herbert, D. 1964b. A theoretical analysis of continuous culture systems. *Soc. Chem. Ind. Monogr.* **12**: 21-53.
- [51] Hill, C.G. 1977. An introduction to chemical engineering kinetics and reactor design. Wiley, New York.
- [52] Hill, G.A.; Robinson, C.W. 1989. Minimum Tank Volumes for CFST Bioreactors

- in Series. *Can. J. Chem. Eng.* **67**: 818-824.
- [53] Holström, B.; Rose, J.K. 1964. Continuous two-stage culture of streptococci. In: *Proc. 2nd symp. contin. cult. microorganisms* (Malek, I., et al., Eds.). Czechoslovak Academy of Sciences, Prague, CSSR, 167-171.
- [54] Hospodka, J. 1966. Industrial application of continuous fermentation. In: *Theoretical and methodological basis of continuous culture of microorganisms* (Malek, I.; Fencel, Z. Eds.). Publishing house of the Czechoslovak Academy of Sciences, Prague, CSSR, 493-645.
- [55] Howgrave-Graham, A.G.; Jones, L.R.; James, A.G.; Terry, S.J.; Senior, E.; Watson-Craik, I.A. 1994. Microbial distribution throughout a cellobiose-supplemented three-stage laboratory-scale anaerobic digester. *J. Chem. Tech. Biotechnol.* **59**: 127-131.
- [56] Imanaka, T.; Kaieda, T.; Taguchi, H. 1973. Optimization of α -galactosidase production in multi-stage continuous culture of mold. *J. Ferment. Technol.* **51**: 431-439.
- [57] Karanth, N.G. 1979. Multiple continuous stirred tank reactors vs. batch reactors - some design considerations. *Biotechnol. Lett.* **1**: 139-144.
- [58] Kida, K.; Asano, S-I.; Yamadaki, M.; Iwasaki, K.; Yamaguchi, T.; Sonoda, Y. 1990. Continuous high-ethanol fermentation from cane molasses by a flocculating yeast. *J. Ferm. Bioeng.* **69**: 39-45.
- [59] Kitai, A.; Tone, H.; Ozaki, A. 1971. Mehrstufige Fermentationsvorrichtung und kontinuierliche Fermentationsverfahren unter Verwendung der Vorrichtung. German patent nr. 2037903, Sanraku-Ocean Co., Ltd, Tokio, Japan, (In German).
- [60] Klein, J.; Kressdorf, B. 1983. Improvement of productivity and efficiency in ethanol production with Ca-alginate immobilized *Zymomonas mobilis*. *Biotechnol. lett.* **5**: 497-502.
- [61] Klein, J.; Kressdorf, B. 1986. Rapid ethanol fermentation with immobilized *Zymomonas mobilis* in a three stage reactor system. *Biotechnol. Lett.* **8**: 739-744.
- [62] Kleinstreuer, C. 1987. Analysis of biological reactors. In: *Advanced Biochemical Engineering* (Bungay, H.R.; Belfort, G., Eds.). Wiley, New York, 33-78.
- [63] Klöppinger, M.; Fertig, G.; Fraune, E.; Miltenburger, H.G. 1990. Multistage production of *Autographa californica* nuclear polyhedrosis virus in insect cell cultures. *Cytotechnol.* **4**: 271-278.
- [64] Kompier, R.; Tramper, J.; Vlak, J.M. 1988. A continuous process for the production of baculovirus using insect cell cultures. *Biotechnol. Lett.* **10**: 849-854.

- [65] Kulozik, U.; Hammelehle, B.; Pfeifer, J.; Kessler, H.G. 1992. High reaction rate continuous bioconversion process in a tubular reactor with narrow residence time distributions for the production of lactic acid. *J. Biotechnol.* **22**: 107-116.
- [66] Kuriyama, H.; Ishibashi, H.; Miyagawa, H.; Kobayashi, H.; Mikami, E. 1993. Optimization of two-stage continuous ethanol fermentation using flocculating yeast. *Biotechnol. lett.* **15**: 415-420.
- [67] Lee, J.M.; Pollard, J.F.; Coulman, G.A. 1983. Ethanol fermentation with cell recycling : computer simulation. *Biotechnol. Bioeng.* **25**: 497-511.
- [68] Lelieveld, H.L.M. 1984. Mixed-strain continuous milk fermentation. *Process Biochem.* **19**: 112-113.
- [69] Lettinga, G.; Van Velsen, A.F.M.; Hobma, S.W.; De Zeeuw, W.; Klapwijk, A. 1980. Use of the upflow sludge blanket (USB) reactor concept for biological wastewater treatment, especially for anaerobic treatment. *Biotechnol. Bioeng.* **22**: 699-734.
- [70] Levenspiel, O. 1972. Chemical reaction engineering. 2nd ed., Wiley, New York.
- [71] Levenspiel, O. 1979. The chemical reactor omnibook. OSU, Corvallis.
- [72] Lo, S.N.; Marchildon, L.; Valade, J.L. 1983. Performance of two chemostats in series, when the values of the corresponding kinetic parameters in Monod's model being nonidentical. In: *Proc. third pacific chem. eng. Congr.* (Kim, C.; Ihm, S.K., Eds.). Korean institute of chemical engineers, Seoul, South Korea, **4**: 166-173.
- [73] Lopes, T.I.; Malcata, F.X. 1993. Optimal design of a series of CSTR's for biochemical reactions in the presence of enzyme deactivation. *J. Chem. Eng. Japan* **26**: 94-98.
- [74] Lumb, M.; Macey, P.E.; Wright, R.D.; Petchell, R.K. 1970. Fermentation processes. British patent nr. 1204486, Boots pure drug company, Nottingham, UK.
- [75] Luyben, K.Ch.A.M.; Tramper, J. 1982. Optimal design for a continuous stirred tank reactors in series using Michaelis-Menten kinetics. *Biotechnol. Bioeng.* **24**: 1217-1220.
- [76] Malcata, F.X. 1988. Optimal design on an economic basis for continuous stirred tank reactors in series using Michaelis-Menten kinetics for ping-pong reactions. *Can. J. Chem. Eng.* **66**: 168-172.
- [77] Malcata, F.X. 1989. A heuristic approach for the economic optimization of a series of CSTR's performing Michaelis-Menten reactions. *Biotechnol. Bioeng.* **33**: 251-255.
- [78] Malcata, F.X.; Cameron, D.C. 1992. Optimal design of a series of CSTR's performing reversible reactions catalyzed by soluble enzymes: a theoretical study. *Biocatalysis* **5**: 233-248.

- [79] Mitchell, D.W.; Shuler, M.L. 1978. Multistage continuous fermentation of poultry manure to a high protein feedstuff. *Food, Pharmaceut. Bioeng, AIChE symp. series* **172**: 182-188.
- [80] Molly, K.; Vande Woestyne, M.; Verstraete, W. 1993. Development of a 5-step multi-chamber reactor as a simulation of the human intestinal microbial ecosystem. *Appl. Microbiol. Biotechnol.* **39**: 254-258.
- [81] Moreno, M.; Goma, G. 1979. Alcohol fermentation in strict anaerobiosis in a plug-flow fermentor: effect of cell recycling. *Biotechnol. Lett.* **1**: 483-488.
- [82] Moser, A. 1988. Bioprocess technology. Springer, New York, 329-356.
- [83] Moser, A. 1985. General strategy in bioprocessing. In: *Biotechnology: a comprehensive treatise in 8 vol.: Fundamentals of biochemical engineering*. (Rehm, H.J., et al., Eds.). VCH, Weinheim, Federal Republic of Germany, **2**: 173-308.
- [84] Mulligan, C.N.; Safi, B.F.; Groleau, D. 1991. Continuous production of ammonium lactate by *Streptococcus cremoris* in a three-stage reactor. *Biotechnol. Bioeng.* **38**: 1173-1181.
- [85] Noworyta, A.; Bryjak, J. 1993. Process of penicillin G hydrolysis catalyzed by penicillin acylase immobilized on acrylic carrier. *Bioproc. Eng.* **9**: 271-275.
- [86] Ogbonna, J.C.; Amano, Y.; Nakamura, K.; Yokotsuka, K.; Shimazu, Y.; Watanabe, M.; Hara, S. 1989. A multistage bioreactor with replaceable bioplates for continuous wine fermentation. *Am. J. Enol. Vitic.* **40**: 292-298.
- [87] Ong, S.L. 1986. Optimization of CSTRs in series by dynamic programming. *Biotechnol. Bioeng.* **28**: 818-823.
- [88] Páca, J. 1980. Elimination of ethanol inhibition of yeast growth by a multistream ethanol feed in a multistage tower fermenter. *J. Chem. Tech. Biotechnol.* **30**: 764-771.
- [89] Páca, J. 1982. Multistream ethanol and oxygen supply to a multistage tower fermentor during continuous yeast cultivations. *J. Ferment. Technol.* **60**: 215-220.
- [90] Páca, J.; Grégr, V. 1979. Growth characteristics of *Candida utilis* in a multistage culture system. *Enzyme Microb. Technol.* **1**: 100-106.
- [91] Páca, J.; Grégr, V. 1979. Effect of interstage mixing in multistage culture systems on continuous biomass production. *Biotechnol. Bioeng.* **21**: 1809-1825.
- [92] Paiva, A.L.; Malcata, F.X. 1993. Optimal temperature and concentration profiles in a cascade of CSTR's performing Michaelis-Menten reactions with first order enzyme deactivation. *Bioproc. Eng.* **9**: 77-82.
- [93] Park, S.C.; Baratti, J.C. 1992. Continuous ethanol production from sugar beet

- molasses using an osmotolerant mutant strain of *Zymomonas mobilis*. *J. Ferment. Bioeng.* **73**: 16-21.
- [94] Pfaff, M.; Heald, S.C.; Jenkins, R.O. 1993. Trichloroethylene removal by a strain of *Pseudomonas putida*: kinetic modelling and bioprocess design. Poster presented at the sixth European Congress on Biotechnology, Florence, Italy.
- [95] Pirt, S.J. 1975. Principles of microbe and cell cultivation. Blackwell, Oxford, UK.
- [96] Pirt, S.J.; Callow, D.S. 1959. Continuous-flow culture of the filamentous mould *Penicillium chrysogenum* and the control of its morphology. *Nature* **184**: 307-310.
- [97] Plevako, E.A. 1964. Continuous two-stage cultivation of baker's yeast. In: *Proc. 2nd symp. contin. cult. microorganisms* (Malek, I., et al., Eds.). Czechoslovak Academy of Sciences, Prague, CSSR, 273-277.
- [98] Powell, E.O.; Lowe, J.R. 1964. Theory of multi-stage continuous cultures. In: *Proc. 2nd symp. contin. cult. microorganisms* (Malek, I., et al., Eds.). Czechoslovak Academy of Sciences, Prague, CSSR, 45-57.
- [99] Prokop, A.; Erickson, J.; Fernandez, J.; Humphrey, A.E. 1969. Design and physical characteristics of a multistage, continuous tower fermentor. *Biotechnol. Bioeng.* **11**: 945-966.
- [100] Qureshi, N.; Tamhane, D.V. 1986. Mead production by continuous series reactors using immobilized yeast cells. *Appl. Microbiol. Biotechnol.* **23**: 438-439.
- [101] Raba, J.; Mottola, H.A. 1994. Continuous-flow/stopped flow system incorporating two rotating bioreactors in tandem: application to the determination of alkaline phosphatase activity in serum. *Anal. Chem.* **66**: 1485-1489.
- [102] Reuveny, S.; Velez, D.; Miller, L.; Macmillan, J.D. 1986. Comparison of cell propagation methods for their effect on monoclonal antibody yield in fermentors. *J. Immunol. Meth.* **86**: 61-69.
- [103] Ricica, J. 1964. Study of the biosynthesis of 6-azauracil riboside by *Escherichia coli* B in a multi-stage continuous process. In: *Proc. 2nd symp. contin. cult. microorganisms* (Malek, I., et al., Eds.). Czechoslovak Academy of Sciences, Prague, CSSR, 153-165.
- [104] Ricica, J. 1969. Recent theoretical and practical trends in continuous cultivation. In: *Fermentation advances* (Perlman, D., Ed.). Academic Press, New York, 427-440.
- [105] Ryu, D.D.Y.; Lee, B.K. 1975. An example of process optimization of enzymatic transformation of steroids. *Process Biochem.* January/February, 15-19.
- [106] Ryu, Y.W.; Navarro, J.M.; Durand, G. 1982. Comparative study of ethanol production by an immobilized yeast in a tubular reactor and in a multistage reactor.

Eur. J. Appl. Microbiol. Biotechnol. **15**: 1-8.

- [107] Santos, V.A.; Tramper, J.; Wijffels, R.H. 1993. Simultaneous nitrification and denitrification using immobilized microorganisms. *J. Biomat. Art. Cells. Immob. Biotechnol.* **21**: 317-322.
- [108] Schügerl, K. 1982. Characterization and performance of single- and multistage tower reactors with outer loop for cell mass production. *Adv. Biochem. Eng.* **22**: 93-224.
- [109] Schügerl, K. 1987. *Bioreaction Engineering: reactions involving microorganisms and cells*. Wiley, Chichester, U.K., 68-73.
- [110] Shama, G. 1988. Developments in bioreactors for fuel ethanol production. *Process. Biochem.* **10**: 138-145.
- [111] Shimizu, K.; Matsubara, M. 1987. Product formation patterns and the performance improvement for multistage continuous stirred tank fermentors. *Chem. Eng. Comm.* **52**: 61-74.
- [112] Sikyta, B.; Daskocil, J.; Kasparova, J. 1959. Continuous streptomycin fermentation. *J. Biochem. Microbiol. Technol. Eng.* **1**: 379-392.
- [113] Takahashi, M.; Kyosai, S. 1991. Pilot plant study on microaerobic self-granulated sludge process (multi-stage reversing flow bioreactor: MRB) *Wat. Sci. Tech.* **23**: 973-980.
- [114] Taniguchi, N.; Koike, S.; Murakami, T.; Nakayama, S. 1988. High efficiency nitrogen removal using multi-stage air-lift recirculation for nitrogen and denitrification process. *WPCF Annual Conference*, Dallas, Texas.
- [115] Topiwala, H.H. 1974. The application of kinetics to biological reactor design. *Biotechnol. Bioeng. Symp.* **4**: 681-690.
- [116] Tramper, J. 1993. Critical problems in bioprocess engineering. In: *ECB6: Proc. 6th European Congress Biotechnol.* (Alberghina, L., et al., Eds.). Elsevier, Amsterdam, The Netherlands, 27-42.
- [117] Tramper, J.; Vlak, J.M. 1986. Some engineering and economic aspects of continuous cultivation of insect cells for the production of baculovirus. *Ann. N.Y. Acad. Sci.* **469**: 279-288.
- [119] Tyagi, R.D.; Ghose, T.K. 1980. Batch and multistage continuous ethanol fermentation of cellulose hydrolysate and optimum design of fermentor by graphical analysis. *Biotechnol. Bioeng.* **22**: 1907-1928.
- [120] Tzeng, J.W.; Fan, L.S.; Gan, Y.R.; Hu, T.T. 1991. Ethanol fermentation using immobilized cells in a multistage fluidized bed bioreactor. *Biotechnol. Bioeng.* **38**: 1253-1258.

- [121] Van Lier, F.L.J.; Van den End, E.J.; De Gooijer, C.D.; Vlak, J.M.; Tramper, J. 1990. Continuous production of baculovirus in a cascade of insect-cell reactors. *Appl. Microbiol. Biotechnol.* **33**: 43-47.
- [122] Van Lier, F.L.J.; Van der Meijs, W.C.J.; Grobben, N.G.; Olie, R.A.; Vlak, J.M.; Tramper, J. 1992. Continuous β -galactosidase production with a recombinant baculovirus insect-cell system in bioreactors. *J. Biotechnol.* **22**: 291-298.
- [123] Van 't Riet, K.; Tramper, J. 1991. Basic bioreactor design. Marcel Dekker, New York.
- [124] Venables, D.C.; Boraston, R.C.; Bushell, M.E. 1993. Two-stage chemostat studies of hybridoma growth, nutrient utilisation, and monoclonal antibody production. In: *Animal Cell technology; Basic and Applied aspects*, (Kaminogawa, S., Ed.). Kluwer, The Netherlands, **5**: 585-594.
- [125] Vos, H.J. 1990. Design of a continuous reactor for immobilized biocatalysts. PhD thesis, Delft University of Technology, The Netherlands.
- [126] Weuster, D.; Aivasidis, A.; Wandrey, Ch. 1990. Multistage ethanol fermentation of wastes in fluidized bed reactors - Operation in laboratory - and bench scale. In: *Dechema Biotechnologie Conferences*, (Behrens, D.; Krämer, P., Eds.). VCH-Weinheim, Frankfurt am Main, Federal Republic of Germany, **4B**: 721-728.
- [127] Yang, P.Y.; Chen, H.; Kongsricharoern, N.; Polprasert, C. 1993. A swine waste package biotreatment plant for the tropics. *Wat. Sci. Tech.* **28**: 211-218.
- [128] Yoon, S.K.; Yoo, Y.J.; Rhee, H.-K. 1989. Optimal temperature control in a multi-stage immobilized enzyme reactor system. *J. Ferment. Bioeng.* **68**: 136-140.
- [129] Zhang, J.; Kalogerakis, N.; Behie, L.A.; Iatrou, K. 1993. A two-stage bioreactor system for the production of recombinant proteins using a genetically engineered baculovirus/insect cell system. *Biotechnol. Bioeng.* **42**: 357-366.

This chapter 5 has been published as: Bakker, W.A.M.; Knitel, J.T.; Tramper, J.; De Gooijer, C.D. 1994. Sucrose conversion by immobilized invertase in a Multiple Air-lift Loop bioreactor. *Biotechnol. Prog.* **10**: 277-283.

CHAPTER 5

SUCROSE CONVERSION BY IMMOBILIZED INVERTASE IN THE MULTIPLE AIR-LIFT LOOP BIOREACTOR

SUMMARY

A new bioreactor series within one vessel, the Multiple Air-lift Loop reactor (MAL), is introduced. In the MAL, a series of air-lift loop reactors is incorporated into one vessel. From residence time distribution studies, it was shown that the three-compartment MAL behaves as a series of three ideal mixers. A continuously operated MAL, containing immobilized invertase as a model biocatalyst, was evaluated. The advantage of approaching plug flow by using a bioreactor cascade could be shown by comparing substrate conversion in the three-compartment MAL to that in a single vessel at the same overall dilution rate. This was done for two sets of experimental conditions, which were chosen by using a previously developed model. Intrinsic kinetic parameters of the immobilized enzyme, needed for the model calculations, were determined experimentally. Model calculations gave good approximations of the results. The model incorporates external mass-transfer resistance and diffusion and reaction in the biocatalyst beads.

INTRODUCTION

Cascades of continuously operated stirred-tank reactors can be flexible tools for the optimization of bioprocesses [Hill and Robinson, 1989; Luyben and Tramper, 1982; Malcata and Cameron, 1992; Pirt, 1975; Shimizu and Matsubara, 1987]. The Multiple Air-lift Loop reactor (MAL) is a new type of bioreactor consisting of a series of air-lift loop reactors (ALRs) within one vessel [De Gooijer, 1989]. With a series of ideal mixers, the behavior of a plug-flow reactor can be approximated [Levenspiel, 1972]. On a laboratory scale ($V \leq 0.01 \text{ m}^3$), and with a regular aspect ratio ($H/D \leq 13$), ALRs behave as nearly ideally mixed vessels [Chisti, 1989; Van 't Riet and Tramper, 1991]. Therefore, as a whole, the MAL is an approximation of an aerated plug-flow bioreactor when sufficient ALRs ($N \geq 20$) are placed in series. Thus, the advantages of both reactor types are combined in this reactor series: the possibility of improved substrate conversion in the plug-flow approximation, and suitable conditions for measurement and control in the nearly ideal mixers. The MAL can be used to study the applications of a reactor series in biotechnology.

In 1982, Luyben and Tramper derived an analytical expression for the optimal design of a cascade of continuous stirred-tank reactors, with the minimal overall reactor volume required for a specific substrate conversion as a criterion. They limited their design to biocatalytic reactions with suspended enzymes following Michaelis-Menten kinetics. This expression was extended to immobilized enzymes that obey intrinsic Michaelis-Menten kinetics and validated experimentally by De Gooijer *et al.* [1989] for reactors in series. Further studies on reactor series containing suspended enzymes were made by Malcata [1988; Malcata and Cameron, 1992] for different kinetics, taking minimal capital investment as the optimization criterion. These authors [Luyben and Tramper, 1982; Malcata, 1988; De Gooijer *et al.*, 1989] observed that the decrease in required overall reactor volume for a desired conversion is the largest when going from one to two reactors in series. Only slight improvement is found when going from two to three, and even more reactors in the cascade is economically not feasible [Malcata, 1988]. From these observations, it was decided that a MAL with three reactors in series incorporated in it would be used for this study.

Sucrose conversion by invertase was selected as a convenient and cheap biological model system to compare the performance of the MAL to that of a single vessel of the same volume. Obviously, there can be all kinds of other arguments, such as economic motives (not taken into account here), to select a different model system or to prefer the use of a single vessel.

In the present contribution, a MAL was operated continuously with invertase immobilized in gel beads as a biological model system. The gel beads moved freely and were kept fluidized and well-mixed in each MAL compartment. Substrate conversion in a three-compartment MAL was compared to that in a single vessel at the same overall dilution rate. This experimental comparison was not made by De Gooijer *et al.* [1989]. Statistically significant improvement (based on the difference in steady-state concentrations with no overlay of their 95% confidence intervals) of substrate conversion in the new bioreactor series over a single, nearly ideally mixed, vessel could be demonstrated. The theoretical development and the calculation procedures of De Gooijer *et al.* [1989] were used as a tool to choose the experimental conditions, using intrinsic kinetic parameters that were determined experimentally. With this model, the simultaneous diffusion and consumption of substrate in the biocatalyst bead are described, resulting in an estimation of the substrate concentration profile in the bead. The trend of the model estimations agreed with reality.

The assumption that the MAL behaves as a cascade of three nearly ideal mixers was validated by residence time distribution (RTD) measurements. The RTD of a tracer was determined in the effluent for various influent and gas flow rates. In all cases, the MAL could be described best as three mixers in series.

MULTIPLE AIR-LIFT LOOP REACTOR

The central MAL compartment is a conventional internal loop ALR with aeration in the annulus (Figure 1). Subsequent compartments in the MAL are concentric. The annular-shaped compartments have a circular baffle, which splits them into a riser section and a downcomer section.

Fresh medium is supplied to the central ALR; from there, it flows into the downcomer of the next compartment, where it is mixed with the down-flowing stream. In this way, medium travels through the cascade of ALRs. The MAL can

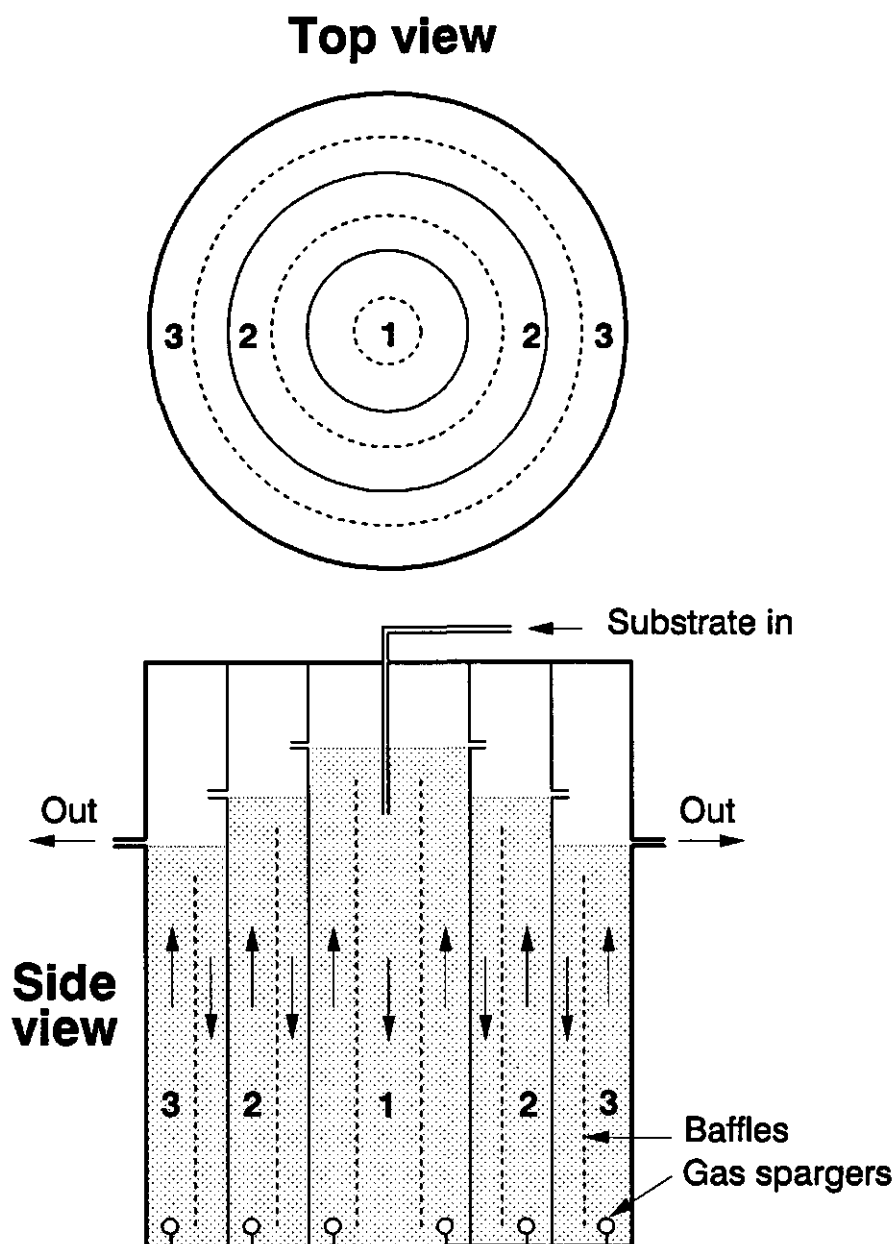


Figure 1. Three compartment Multiple Air-lift Loop bioreactor cross-sectional side and top view. Geometric data are given in Table I.

be constructed in many configurations for various applications [De Gooijer, 1989]. By supplying different gases to the subsequent compartments, for example, aerobic and anaerobic processes can be carried out in series within one reactor vessel.

The advantages of the MAL compared to single ALRs, or bubble columns, in series include the fact that no extra pumps or hoses are needed. Also, the reactor series can be sterilized as one reactor, and old reactor vessels can be reused and upgraded to a MAL. Disadvantages of the MAL in this comparison include that, on a lab scale, the compartments are narrow, which makes cleaning difficult. Further, the gas distributor is relatively complex.

Hydrodynamics and mixing are greatly influenced by reactor geometry; these subjects were investigated previously [Bakker *et al.*, 1993] in a MAL of a larger scale (0.034 m³ per compartment) than the MAL used in the present study. In that previous study, the second compartment of the MAL was used as a model for the new internal-loop reactor geometry. Liquid velocities, gas holdup, and mixing were comparable to those of conventional ALRs with an internal loop. Complete mixing was established within four liquid circulations ($\tau_m \leq 54$ s) for all gas flow rates applied. This implied that, also on this larger scale, the subsequent MAL compartments could be regarded as nearly ideally mixed.

MATERIALS AND METHODS

MAL

The vessel used in this study was a 0.022-m³ three-compartment MAL made of transparent perspex (Figure 1). Geometric data are given in Table I. The three compartments were arbitrarily chosen to be of nearly equal volumes. The circular sparger rings were constructed of porous Accurel polypropylene membrane tube (type V8/2, maximum pore size: 0.51 μm ; gift of AKZO, Obernburg, Germany). The spargers were positioned at the riser entrance to prevent entrainment of gas bubbles in the downcomer. Gas was distributed over the circular risers by the membrane spargers at a flow rate of 9.7×10^{-6} m³.s⁻¹ for each MAL compartment. The gas flow rate was kept low to prevent excessive foam formation.

Table I. Geometric data of the multiple air-lift loop reactor (MAL).

	MAL		
	compartment 1	compartment 2	compartment 3
Liquid volume [m ³]	8.07×10^{-3}	7.29×10^{-3}	6.89×10^{-3}
Working volume [†] [m ³]	7.71×10^{-3}	6.97×10^{-3}	6.57×10^{-3}
Liquid height [m]	2.97×10^{-1}	2.37×10^{-1}	1.65×10^{-1}
Diameter ^{††} [m]	1.99×10^{-1} (4)	3.0×10^{-1}	4.0×10^{-1} (4)
Baffle diameter ^{††} [m]	1.1×10^{-1}	2.4×10^{-1}	3.4×10^{-1}
Baffle height ^{†††} [m]	2.91×10^{-1}	2.31×10^{-1}	1.55×10^{-1}

[†] The working volume is the liquid volume corrected for gas holdup and foam formation during the experiments.

^{††} Outer diameters are given. The perspex wall thickness was 5 mm, except for the two tubes marked with (4) where it was 4 mm.

^{†††} The distance between the baffles and the bottom (1.5 cm) is included in the baffle height.

ENZYME IMMOBILIZATION

Microgranular anion exchanger (DE32-cellulose), sodium alginate, and other chemicals were described previously [De Gooijer *et al.*, 1989]. The invertase (Maxinvert P) was a gift of Gist-brocades, Delft, The Netherlands. Invertase was coupled to DE32-cellulose before immobilization in alginate [De Gooijer *et al.*, 1989]. DE32-cellulose (50 kg.m⁻³) was equilibrated for 48 h in sodium phosphate buffer (10 mol.m⁻³, pH 7.0). Invertase was added (5 kg.m⁻³) and stirred with the DE-32 particles for 3 h at room temperature. Non-adsorbed invertase was then removed by washing three times with the equilibrating sodium phosphate buffer and finally once with a sodium-acetate buffer (10 mol.m⁻³, pH 4.6). The latter wash liquid no longer showed enzymatic activity. The DE32-cellulose invertase was then added to a 2% (w/w) sodium-alginate solution in acetate buffer. In this way, a 35 kg.m⁻³ gel load, based on dry-complex weight, was obtained in the beads resulting from immobilization. This immobilization was performed with a resonance nozzle [Hulst *et al.*, 1985] at 35 °C. Alginate drops were collected in

200 mol.m⁻³ CaCl₂ at 5 °C. To obtain perfect spheres, decane was layered on the CaCl₂ solution [Wijffels *et al.*, 1991]. The decane-CaCl₂ was kept at 5 °C in order to initiate the gelation. After solidification for 2 h, the beads were kept in a 50 mol.m⁻³ CaCl₂ acetate buffer at 4 °C. The Sauter mean bead diameter d_{32} was 1.74 mm.

For the determination of intrinsic kinetic parameters, beads were prepared, in the same way as described above, with five different gel loads (9, 33, 69, 83 and 100 kg of dry enzyme complex per cubic meter of gel beads (kg.m⁻³)). To obtain those gel loads, the amount of DE32-cellulose invertase added to the sodium alginate solution in acetate buffer was changed. The beads were used directly for activity assays to determine apparent kinetic constants (*i.e.* including transport limitation).

ANALYSES

Glucose and sucrose concentrations were determined with a D-glucose kit and a sucrose kit, respectively (Boehringer, Germany). Sucrose concentrations were measured in the influent stream. Sucrose was found to be converted stoichiometrically into glucose and fructose. Reactor sucrose concentrations thus could be calculated from glucose analysis. Samples (1.5 cm³) were heated for 5 min at 100 °C to inactivate the freely suspended enzyme-DE32 complex used for the determination of the kinetic parameters. Consequently, this procedure was used for all samples to warrant uniform sample treatment. After heating, the samples were frozen at -20 °C until analysis to prevent microbial degradation of the sugars.

ACTIVITY ASSAYS

For all determinations of kinetic parameters (intrinsic and for freely suspended enzyme complex), substrate conversion was measured as a function of time until sucrose was completely converted. The initial sucrose concentration was 600 mol.m⁻³, and the batchwise experiments were done in acetate buffer at 30 °C in a stirred vessel. For the determination of a loss in enzyme activity with time, beads (gel load: 100 kg.m⁻³) were stored at 30 °C in acetate buffer between the determinations to obtain the same conditions as during the MAL experiment. Parameters were estimated by fitting the integrated Michaelis-Menten equation to

each set of experimental data with nonlinear regression [Van 't Riet and Tramper, 1991]. The 95% confidence intervals of the kinetic parameters were calculated with the use of the Student's *t*-test value from one set of experimental data (*i.e.*, substrate versus time) for the different measurements [Zwietering *et al.*, 1990].

MAL EXPERIMENTS

The MAL was operated continuously twice at 30 °C for several days. The substrate was 630 mol.m⁻³ sucrose in acetate buffer. In the two MAL experiments the reactor gel holdup, 6.3% and 9.1% (v/v), respectively, was equal for each of the three MAL compartments. Beads were kept in each compartment by a stainless steel sieve (hole diameter, 0.5 mm) at the overflows to the next compartment. After a change in substrate feed rate, steady-state conditions were established after four hydraulic residence times through the cascade of air-lift reactors. Subsequently, during three MAL volume changes, samples were taken regularly from all three MAL-compartments, and thus the attainment of a steady state was verified. Enzyme decay was assumed to be negligible during the short period (compared to the duration of the complete experiment) of a steady-state measurement. For the two MAL experiments at 6.3% and 9.1% gel holdup substrate was supplied at a constant rate of 2.65×10^{-6} and 2.4×10^{-6} m³.s⁻¹, respectively.

The central compartment of the MAL was used as a single-vessel reference. To this end, it was operated at a different substrate feed rate (0.94×10^{-6} and 0.85×10^{-6} m³.s⁻¹ for the two experiments at 6.3% and 9.1% gel holdup, respectively). Consequently, the overall residence time (2.2 and 2.5 h, respectively) in the comparison between the three-compartment MAL and the single compartment was equal. Here, residence times were arbitrarily based on the liquid volume plus beads, that is, without gas holdup and foam formation (Table I).

MIXING IN THE MAL

Macroscopic mixing in the MAL was investigated by measurement of the residence time distribution (RTD). For that, the MAL was operated continuously under various conditions as explained in the Results and Discussion section. The effluent response of an inlet salt pulse (30 cm³, 4000 mol.m⁻³ NaCl) was measured with a

conductivity electrode.

The RTD-curves were characterized by the mean $\bar{\theta}$ and variance σ^2 of the distribution [Levenspiel, 1972]. The distributions were normalized with respect to time (θ = time (s)/one hydraulic residence time (s)) and concentration (C = concn (kg.m^{-3})/initial concn (kg.m^{-3})) to make them comparable at different hydraulic residence times. The distribution curve was known at a number of discrete time values θ_i , from which the mean $\bar{\theta}$ and the variance σ_θ^2 were calculated as described by Levenspiel [1972]. From this, the theoretical number of equal-size ideal mixers N in the series could be derived from $N = 1/\sigma_\theta^2$. Finally, the area under the RTD curve represented the fraction of tracer recovered.

The conditions during the MAL experiments with the immobilized enzyme, as described above, were within the applied range with respect to the gas flow rate, and were lower for the liquid flow-rate.

MODEL PARAMETER VALUES

Parameter values used for the model calculations were as follows: maximum substrate consumption rate, V_m (at $t = 0$) = $0.10 \text{ mol.kg}^{-1}.\text{s}^{-1}$; Michaelis constant, $K_m = 310 \text{ mol.m}^{-3}$; gel load = 35 kg.m^{-3} ; effective diffusion coefficient [De Gooijer *et al.*, 1989], $D_e = 3.85 \times 10^{-10} \text{ m}^2.\text{s}^{-1}$; Sauter mean bead diameter, $d_{32} = 1.74 \text{ mm}$; inlet substrate concentration = 630 mol.m^{-3} ; substrate feed rate = $2.4 \times 10^{-6} \text{ m}^3.\text{s}^{-1}$ (MAL experiment) and $0.85 \times 10^{-6} \text{ m}^3.\text{s}^{-1}$ (single-vessel experiment); reactor gel holdup = 9.1%; liquid/solid mass-transfer coefficient, $k_{l,s} = 1 \times 10^{-5} \text{ m.s}^{-1}$, zero-order decay rate, $k_d = 4.0 \times 10^{-8} \text{ mol.kg}^{-1}.\text{s}^{-2}$. The first steady-state measurement was taken after the MAL was run continuously for 3.5 days ($t = 3.5 \text{ days}$), therefore, this time was used to make a correction for the enzyme decay in the model calculations.

RESULTS AND DISCUSSION

KINETIC PARAMETERS

Alginate beads with five different gel loads of enzyme complex (DE32-cellulose-invertase) immobilized therein were used to determine intrinsic kinetic parameters of the Michaelis-Menten equation:

$$V = \frac{V_m S}{S + K_m} \quad (1)$$

where V is the specific reaction rate ($\text{mol.kg}^{-1}.\text{s}^{-1}$), S is the substrate concentration (mol.m^{-3}), V_m is the maximum substrate consumption rate ($\text{mol.kg}^{-1}.\text{s}^{-1}$) and K_m is the Michaelis constant (mol.m^{-3}). Extrapolation to zero gel load gives the diffusion free, intrinsic, kinetic constants V_m and K_m [Van Ginkel *et al.*, 1983; Van 't Riet and Tramper, 1991]. Here, a linear relationship between the apparent kinetic constants V'_m and K'_m and gel load is assumed. The validity of this assumption was assessed statistically by using the Students t -test (Table II). For the intrinsic V_m (Figure 2), the slope coefficient was sufficiently different from zero to warrant a significant correlation (Table II). The intrinsic V_m , *i.e.*, the intercept of the linear regression line in Figure 2, was $0.10 \text{ mol.kg}^{-1}.\text{s}^{-1}$ (Table II). No statistically reliable intrinsic K_m could be determined in this way because the slope coefficient (Figure 3) was found to not differ significantly from zero (Table II).

Furthermore, the kinetic parameters V_m and K_m were also determined by using freely suspended DE32-cellulose-invertase complex, assuming negligible diffusion limitation. The average V_m obtained from six independent determinations was $0.10 \text{ mol.kg}^{-1}.\text{s}^{-1}$, and the $K_m = 310 \text{ mol.m}^{-3}$ (Table II). This average V_m agrees very well with the above intrinsic parameter obtained from the beads with different gel loads (Table II). Therefore, no effect due to immobilization in alginate, for example a change in conformation of the enzyme, on this kinetic parameter of the enzyme complex could be shown. The accuracy of the apparent constant K'_m was limited, as illustrated by the large 95% confidence intervals (Figure 3) and the rejection of the linear model (Table II). This limitation of accuracy is more often encountered in the determination of immobilized enzyme

Table II. Statistical evaluation of the linear regression analysis of the kinetic parameters determined from immobilized enzyme complex with five different gel loads, enzyme inactivation in time, and intrinsic kinetic data obtained from the immobilized enzyme complex and from the freely suspended enzyme complex.

Linear model statistics				Enzyme complex immobi- lized in gel beads		Freely suspended enzyme complex ^{††}	
Test on the slope coef- ficient	<i>t</i> - statistic [†]	<i>t</i> - table	Para- meter	Unit	Value	min ^{†††}	max ^{†††}
Figure 2	-7.43	-3.18	V_m	$\text{mol.kg}^{-1}.\text{s}^{-1}$	0.10	0.08	0.12
Figure 3	1.95	3.18	K_m	mol.m^{-3}	---	---	---
Figure 4	-8.72	-4.30	k_d	$\times 10^{-8} \text{ mol.kg}^{-1}.\text{s}^{-2}$	4.0	2.1	6.0
					---	---	---
					0.10	0.09	0.11
					310	205	415
					---	---	---

[†] Boldface data indicate acceptance of the linear model with the *t*-test.

^{††} Means and confidence intervals for the freely suspended enzyme complex were calculated from six independent experiments.

^{†††} Min and max are 95% confidence limits for the parameter values.

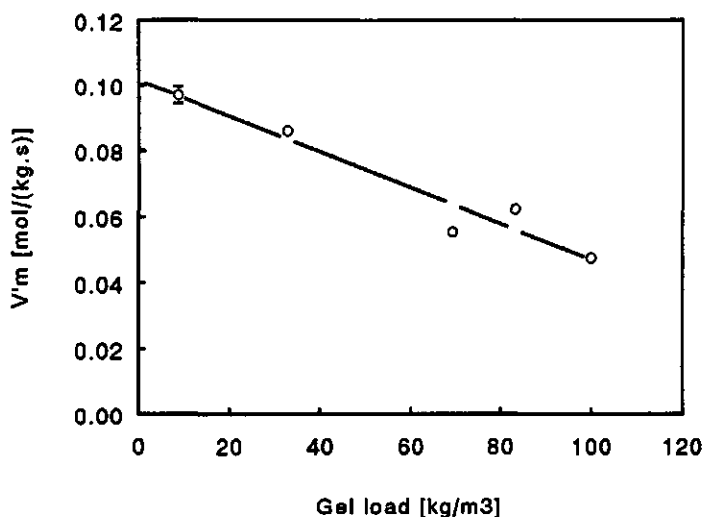


Figure 2. Apparent maximal substrate consumption rate V'_m as a function of the gel load. Bars give 95% confidence intervals; when invisible it is due to overlay by the data points. Solid line: linear regression line for extrapolation to the intrinsic V_m at zero gel load.

kinetics [Hooijmans *et al.*, 1992]. It was assumed that K_m was also left unaffected by the immobilization, and thus the average of 310 mol.m^{-3} for the freely suspended enzyme complex represented the intrinsic K_m . This K_m was on the same order of magnitude as the earlier reported 198 mol.m^{-3} for a different batch of enzymes [De Gooijer *et al.*, 1989] and other literature data. Typical values of K_m , for different binding methods and different invertase preparations, are in the range $50 - 270 \text{ mol.m}^{-3}$ [Johansen and Flink, 1986; Mansfeld and Schellenberger, 1987; Mansfeld *et al.*, 1991].

For all determinations of kinetic parameters, the initial substrate concentration was in the same range (600 mol.m^{-3}) as was applied during the MAL experiments (630 mol.m^{-3}). For those concentrations, possible effects of substrate or product inhibition on the reaction rate [Combes and Monsan, 1983; Mansfeld and Schellenberger, 1987; Mansfeld *et al.*, 1991] were found to be negligible, because all experimental results could be described well with the Michaelis-Menten equation.

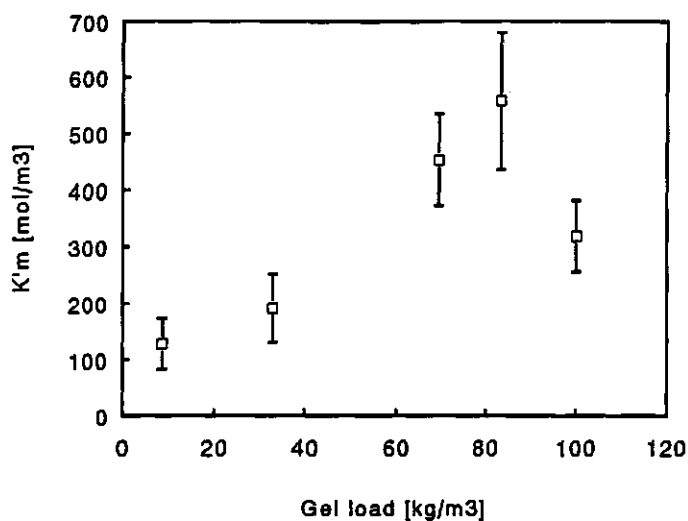


Figure 3. Apparent Michaelis-constant for the rate limiting substrate K'_m as a function of the gel load. Bars give 95% confidence intervals.

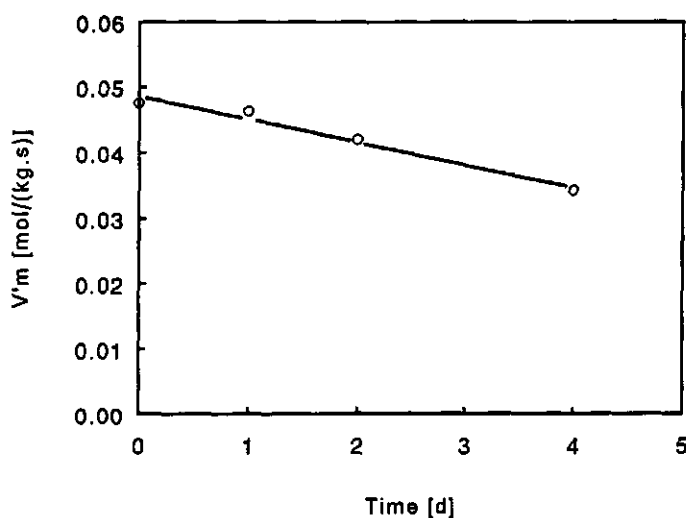


Figure 4. The apparent maximal substrate consumption rate V'_m as a function of time. Bars for the 95% confidence intervals are invisible because they are overlaid by the data points. Solid line: linear regression line giving the inactivation rate.

To make a correction for the loss of enzyme activity in time, the inactivation rate was measured by determining V'_m from the same beads for 4 days (gel load, 100 kg.m^{-3}). Figure 4 shows a linear loss of enzyme activity in 4 days. The zero-order decay rate k_d was $4.0 \times 10^{-8} \text{ mol.kg}^{-1}.\text{s}^{-2}$. This slope coefficient, k_d , was statistically significantly different from zero (Table II). The decay rate k_d was comparable to the 29% activity loss reported for invertase coupled to DE-cellulose after 4 days at 30°C [Suzuki *et al.*, 1966].

MIXING IN THE MAL

A model assumption for the prediction of substrate conversion was that the continuously operated MAL behaved as a series of three ideal mixers. This was validated experimentally by RTD measurements, as illustrated in Figure 5. The theoretical number of equal-size ideal mixers, N , was derived from the RTD curves and is given in Table III. Even under the extreme experimental conditions applied (low gas flow rates and, for biological systems, relatively short residence times),

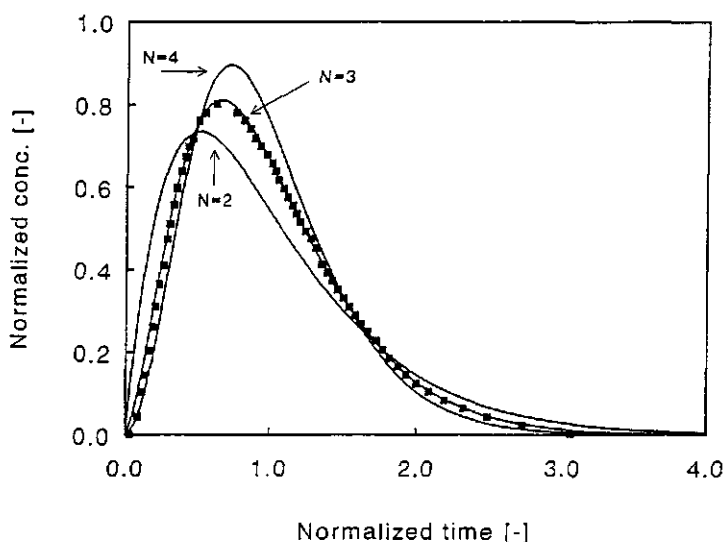


Figure 5. Normalized salt concentration C as a function of the normalized time θ , resulting in a typical residence time distribution (RTD) curve (exp. no. 1 in Table III). Solid lines: model calculations for two, three, and four ideal mixers in series.

the mixing in the MAL was like that in a series of three ideal mixers ($N = 3$, see Table III). To illustrate this, model calculations by mass-balance equations (at short time intervals of 0.1 s) for two, three, and four ideal mixers in series in the MAL are given in Figure 5. The model calculations for three ideal mixers in series were, as illustrated in Figure 5, also found to be in good agreement with the RTD curves obtained from the other experiments. From these results it was concluded that the mixing in the MAL during the sucrose conversion experiments indeed could be described as that in a series of three ideal mixers. Residence times applied there were an order of magnitude larger than those for the mixing experiments, thus allowing sufficient time for complete mixing in the MAL compartments.

Mixing per MAL compartment was also investigated during the MAL experiments with immobilized invertase. Samples were drawn at the same time at different places over the circle of each compartment. The low spread in the concentrations (Figure 6) indicated good mixing within the compartments. The aeration of the compartments resulted in hydrodynamic behavior such that all alginate beads were kept fluidized and circulating through the riser and the downcomer (visually observed) in the three well-mixed MAL compartments.

Table III. Results of the mixing studies by residence time distribution measurements.

No.	Overall liquid residence time [s]	Gas flowrate per MAL compartment [$\text{m}^3 \cdot \text{s}^{-1}$]	Mean $\bar{\theta}$ [-]	Var. σ_{θ}^2 [-]	$N = 1/\sigma_{\theta}^2$ [-]	NaCl recovery [%]
1	851	14×10^{-6}	0.93	0.34	2.98	96
2	851	42×10^{-6}	0.96	0.33	3.00	97
3	552	8.3×10^{-6}	0.97	0.31	3.24	96
4	556	14×10^{-6}	0.97	0.32	3.09	97
5	554	42×10^{-6}	0.98	0.32	3.11	99

SUCROSE CONVERSION IN THE MAL

Steady-state sucrose concentrations for the MAL and for a single vessel, both at 9.1% gel holdup, together with model calculations are given in Figure 6. For practical convenience, the same beads were used for several days, while substrate

conversion in the MAL was compared to that in a single vessel. Figure 6 clearly shows the advantage of using a MAL reactor series over a single vessel. Substrate conversion in the MAL improved to 83% compared to 73% in the single vessel. The difference in substrate concentrations was shown to be statistically significant (no overlay of the 95% confidence intervals). The single-vessel experiment was conducted one day before and one day after the MAL experiment. Both steady-state sucrose concentrations for the single vessel were averaged to account for enzyme inactivation.

For the model calculations shown in Figure 6, the working volumes of the MAL compartments given in Table I were used. A correction of the maximal substrate consumption rate V_m was made using the experimentally determined inactivation rate, taking into account the number of days between startup and steady-state measurement. The calculation procedures used were based on the work of De Gooijer *et al.* [1989] and incorporated internal diffusion and reaction in the

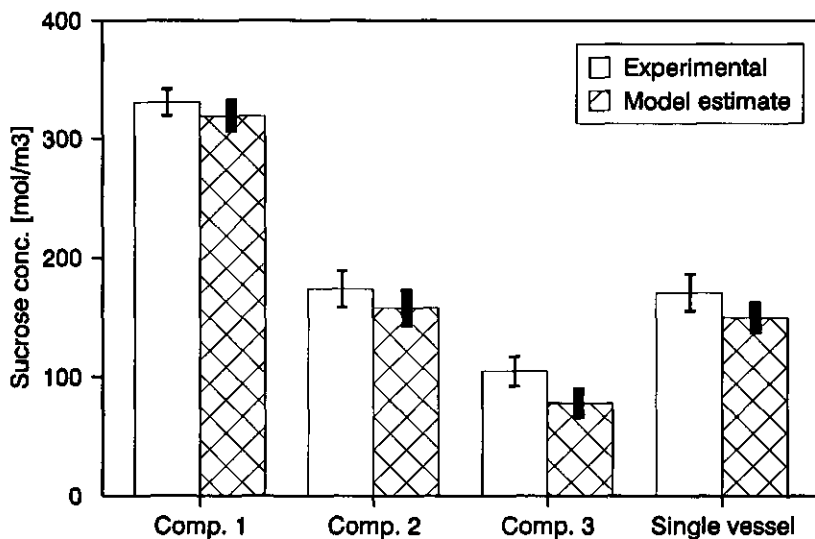


Figure 6. Results of the multiple air-lift loop reactor experiment per compartment and comparison with a single vessel (empty bars); line bars give 95% confidence intervals. Model estimates (cross-hatched bars): here the solid black bars give the range of model estimates using no film theory ($k_{l,s} = \infty$) and $k_{l,s} = 5 \times 10^{-6} \text{ m.s}^{-1}$.

beads and external mass-transfer resistance. Parameter values used for the calculations are given in the Materials and Methods section.

The contribution of the liquid/solid mass-transfer coefficient, $k_{l,s}$, to the total mass-transfer resistance can be estimated from the Biot number, which is defined as the ratio of the mass transfer resistance in the stagnant layer around the bead to that in the bead [De Gooijer *et al.*, 1989; Wijffels *et al.*, 1991]. The $k_{l,s}$ was very roughly estimated from the relation of Brian and Hales (1969), which was selected because the Reynolds number for the beads was estimated to be 20 (based on the particles moving at the rate of free fall). The resulting Biot number ($Bi = 26$) indicated that external mass-transfer resistance was nearly negligible compared to internal mass-transfer resistance. Therefore, $k_{l,s}$ was chosen to be infinite (*i.e.*, no stagnant layer present) and one-half the estimated value of $k_{l,s} = 1 \times 10^{-5} \text{ m.s}^{-1}$ to give a range of model estimates (Figure 6). This range is in agreement with estimations made for $k_{l,s}$ using recent correlations for ALRs proposed by Mao *et al.* [1992], $k_{l,s} = 2 \times 10^{-5} \text{ m.s}^{-1}$, and by Kushalkar and Pangarkar [1994], $k_{l,s} = 4 \times 10^{-6} \text{ m.s}^{-1}$. All other model parameters were determined experimentally and the calculations agreed well with experimental results (Figure 6).

MODEL CALCULATIONS

Model estimates of the sucrose conversion under various conditions were made to choose the experimental conditions, and thus the number of experiments needed could be reduced. The residence time and the gel holdup were selected as variables that can be easily adapted. The inlet sucrose concentration was chosen such that large absolute differences in the steady-state concentrations between both reactor configurations could be expected. From the model, those differences were found to increase with increasing inlet sucrose concentration. On the other hand, the influent concentration was chosen to be not too extreme, such that substrate and product inhibition were negligible. The gel load and bead diameter parameters were chosen arbitrarily. In Figure 7, model estimates are given for the relative conversion as a function of the overall residence time and gel holdup. Other parameter values were as mentioned before. The same relative conversion optimum can be reached under different conditions. For example, lowering the gel holdup requires increasing residence times (Figure 7). In this example, the sucrose conversion in both reactors

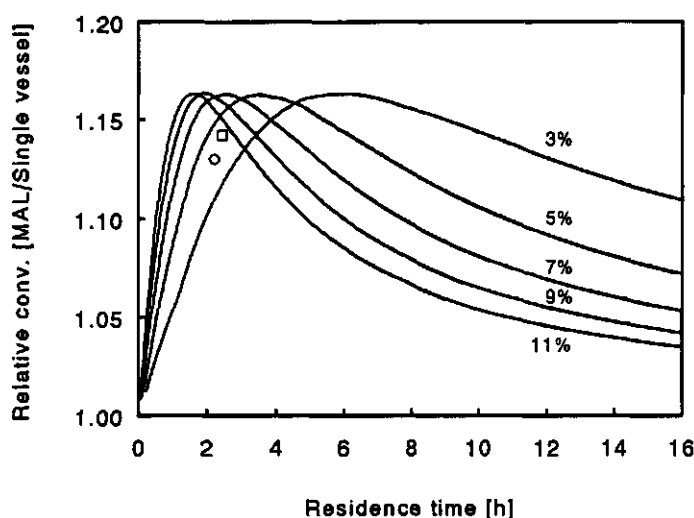


Figure 7. Model estimates for the relative conversion of sucrose in the MAL compared to a single vessel as a function of gel holdup (percentages shown in the graph) and overall residence time. Experimental results are for 6.3% gel holdup (○) and 9.1% gel holdup (□).

is low. This means that the absolute differences between the steady-state concentrations will be small and difficult to show experimentally. Figure 7 also shows the experimentally determined relative conversion at 6.3% and at 9.1% gel holdup. Both experimental results are in rather good agreement with the model estimates (Figure 7).

CONCLUSIONS

The novel multiple air-lift loop reactor was evaluated with immobilized invertase as a biological model system. The conversion of sucrose in the MAL reactor series was higher than that in a single vessel with the same overall residence time. The difference was statistically significant. From RTD measurements, it was found that the three-compartment MAL could be described as three ideal mixers in series. Thus, the MAL proved to be a suitable tool for the experimental evaluation of

reactor series in biotechnology.

No effect of the immobilization in alginate on the kinetics of the DE32-cellulose-invertase complex could be shown. The immobilized enzyme complex was observed to inactivate as a function of time, with a decay rate that was not negligible with respect to the duration of the experiment. Therefore, enzyme decay was incorporated in the model calculations.

Model estimations for the sucrose conversion based on the work of De Gooijer *et al.* [1989], incorporating internal diffusion and reaction in the beads and external mass-transfer resistance, were in good agreement with the experimental results.

ACKNOWLEDGEMENTS

The authors thank A.D. Hamming for his contribution to the experiments. H.H. Beeftink is thanked for carefully reading the manuscript. This work was partly supported by Applikon Dependable Instruments B.V., Schiedam, The Netherlands. The research was carried out in a PBTS project (No. 89069) initiated by the Dutch Ministry of Economic Affairs.

NOMENCLATURE

Bi	Biot number	[-]
C	normalized salt concentration	[-]
d_{32}	Sauter mean bead diameter	[m]
D	diameter	[m]
D_e	effective diffusion coefficient	[m ² .s ⁻¹]
H	height	[m]
k_d	zero-order decay rate	[mol.kg ⁻¹ .s ⁻²]
$k_{l,s}$	liquid/solid mass-transfer coefficient	[m.s ⁻¹]
K_m	Michaelis constant for the rate-limiting substrate	[mol.m ⁻³]
K'_m	apparent Michaelis constant for the rate-limiting substrate	[mol.m ⁻³]

N	theoretical number of equal-size ideal mixers	[-]
S	substrate concentration	[mol.m ⁻³]
V	volume	[m ³]
V_m	maximal substrate consumption rate	[mol.kg ⁻¹ .s ⁻¹]
V'_m	apparent maximal substrate consumption rate	[mol.kg ⁻¹ .s ⁻¹]

Greek symbols:

θ	normalized time	[-]
$\bar{\theta}$	mean normalized time	[-]
σ_θ^2	variance of the normalized distribution curve	[-]

REFERENCES

- [1] Bakker, W.A.M.; Van Can, H.J.L.; Tramper, J.; De Gooijer, C.D. 1993. Hydrodynamics and mixing in a Multiple Air-lift Loop reactor. *Biotechnol. Bioeng.* **42**: 994-1001.
- [2] Brian, P.L.T.; Hales, H.B. 1969. Effects of transpiration and changing diameter on heat and mass transfer to spheres. *AIChE J.* **15**: 419.
- [3] Chisti, M.Y. 1991. Airlift bioreactors. Elsevier, London, UK.
- [4] Combes, D.; Monsan, P. 1983. Sucrose hydrolysis by invertase. Characterization of products and substrate inhibition. *Carbohydr. Res.* **117**: 215-228.
- [5] De Gooijer, C.D. 1989. Dutch patent application. No. 89.01649. (In Dutch).
- [6] De Gooijer, C.D.; Hens, H.J.H.; Tramper, J. 1989. Optimum design for a series of continuous tank reactors containing immobilized biocatalyst beads obeying intrinsic Michaelis-Menten kinetics. *Bioproc. Eng.* **4**: 153-158.
- [7] Hill, G.A.; Robinson, C.W. 1989. Minimum tank volumes for CFST bioreactors in series. *Can. J. Chem. Eng.* **67**: 818-824.
- [8] Hooijmans, C.M.; Stoop, M.L.; Boon, M.; Luyben, K.C.A.M. 1992. Comparison of two experimental methods for the determination of Michaelis-Menten kinetics of an immobilized enzyme. *Biotechnol. Bioeng.* **40**: 16-24.
- [9] Hulst, A.C.; Tramper, J.; Van 't Riet, K.; Westerbeek, J.M.M. 1985. A new technique for the production of immobilized biocatalyst in large quantities. *Biotechnol. Bioeng.* **27**: 870-876.

- [10] Johansen, A.; Flink, J.M. 1986. Influence of alginate properties on sucrose inversion by immobilized whole cell invertase. *Enzyme Microb. Technol.* **8**: 485-490.
- [11] Kushalkar, K.B.; Pangarkar, V.G. 1994. Particle-liquid mass transfer in a bubble column with a draft tube. *Chem. Eng. Sci.* **49**: 139-144.
- [12] Levenspiel, O. 1972. Chemical reaction engineering. 2nd ed. Wiley, New York.
- [13] Luyben, K.Ch.A.M.; Tramper, J. 1982. Optimal design for continuous stirred tank reactors in series using Michaelis-Menten kinetics. *Biotechnol. Bioeng.* **24**: 1217-1220.
- [14] Malcata, F.X. 1988. Optimal design on an economic basis for continuous stirred tank reactors in series using Michaelis-Menten kinetics for ping-pong reactions. *Can. J. Chem. Eng.* **66**: 168-172.
- [15] Malcata, F.X.; Cameron, D.C. 1992. Optimal design of a series of CSTR's performing reversible reactions catalyzed by soluble enzymes: a theoretical study. *Biocatalysis* **5**: 233-248.
- [16] Mansfeld, J.; Schellenberger, A. 1987. Invertase immobilized on macroporous polystyrene: properties and kinetic characterization. *Biotechnol. Bioeng.* **29**: 72-78.
- [17] Mansfeld, J.; Förster, M.; Schellenberger, A.; Dautzenberg, H. 1991. Immobilization of invertase by encapsulation in polyelectrolyte complexes. *Enzyme Microb. Technol.* **13**: 240-244.
- [18] Mao, H.H.; Chisti, Y.; Moo-Young, M. 1992. Multiphase hydrodynamics and solid-liquid mass transport in an external-loop airlift reactor - a comparative study. *Chem. Eng. Comm.* **113**: 1-13.
- [19] Pirt, S.J. 1975. Principles of microbe and cell cultivation. Blackwell, Oxford, UK.
- [20] Shimizu, K.; Matsubara, M. 1987. Product formation patterns and the performance improvement for multistage continuous stirred tank fermentors. *Chem. Eng. Comm.* **52**: 61-74.
- [21] Suzuki, H.; Ozawa, Y.; Maeda, H. 1966. Studies on the water-insoluble enzyme hydrolysis of sucrose by insoluble yeast invertase. *Agr. Biol. Chem.* **30**: 807-812.
- [22] Van Ginkel, C.G.; Tramper, J.; Luyben, K.Ch.A.M.; Klapwijk, A. 1983. Characterization of *Nitrosomonas europaea* immobilized in calcium alginate. *Enzyme Microb. Technol.* **5**: 297-303.
- [23] Van 't Riet, K.; Tramper, J. 1991. Basic bioreactor design. Marcel Dekker, New York.

- [24] Wijffels, R.H.; De Gooijer, C.D.; Kortekaas, S.; Tramper, J. 1991. Growth and substrate consumption of *Nitrobacter agilis* cells immobilized in carrageenan: Part 2. Model evaluation. *Biotechnol. Bioeng.* **38**: 232-240.
- [25] Zwietering, M.H.; Jongenburger, I.; Rombouts, F.M.; Van 't Riet, K. 1990. Modeling of the bacterial growth curve. *Appl. Environ. Microbiol.* **56**: 1875-1881.

This chapter 6 has been submitted for publication as: Bakker, W.A.M.; Schäfer, T.; Beeftink, H.H.; Tramper, J.; De Gooijer, C.D. Hybridomas in a bioreactor cascade: modeling and determination of growth and death kinetics.

CHAPTER 6

HYBRIDOMAS IN A BIOREACTOR CASCADE: MODELING AND DETERMINATION OF GROWTH AND DEATH KINETICS

SUMMARY

Hybridomas were cultured under steady-state conditions in a series of two continuous stirred-tank reactors (CSTRs), using a serum-free medium. The substrate not completely converted in the first CSTR, was transported with the cells to the second one and very low growth rates, high death rates, and lysis of viable cells were observed in this second CSTR. These conditions are hardly accessible in a single vessel, because such experiments would be extremely time-consuming and unstable due to a low viability. In contrast to what is often observed in literature, kinetic parameters could thus be derived without the necessity for extrapolation to lower growth rates. Good agreement with literature averages for other hybridomas was found. Furthermore, showing that the reactor series is a valuable research tool for kinetic studies under extreme conditions, the possibility to observe cell death under stable and defined steady-state conditions offers interesting opportunities to investigate apoptosis and necrosis. Additionally, a model was developed that describes hybridoma growth and monoclonal antibody production in the bioreactor

cascade on the basis of glutamine metabolism. Good agreement between the model and the experiments was found.

INTRODUCTION

Series of bioreactors can be used in biotechnology for kinetic studies [Pirt, 1975]; they also offer the possibility for an overall volumetric productivity improvement, when compared to a single vessel [Shimizu and Matsubara, 1987; Hill and Robinson, 1989]. In literature many practical and theoretical studies are present [De Gooijer *et al.*, 1995]. Examples of successful applications are bioethanol [Shama, 1988] and lactic acid production [Aeschlimann *et al.*, 1990]. Also for monoclonal antibody (MAb) production by hybridomas a few studies are known [Reuveny *et al.*, 1986; Venables *et al.*, 1993].

Reuveny *et al.* [1986] cultured hybridomas semi-continuous and stage-wise in flasks, whereby additional substrates were added to the second stage. They found a doubling of the overall MAb productivity for two-stage operation when compared to a single flask. Later, Venables *et al.* [1993] used a chemostat cascade with no extra feed to the second stage. They also found increased MAb concentrations in the second stage and showed promising possibilities for kinetic studies at low growth rates.

The reactor series is indeed a valuable tool for kinetic studies under extreme conditions. In the research reported here, hybridoma growth and production kinetics were studied in a series of two continuous stirred-tank reactors (CSTRs, Figure 1), using a serum-free medium. Steady states were analysed at different dilution rates with respect to specific rates of growth, consumption, production, and cell death. At the relatively higher dilution rates, very low growth rates of the hybridomas were observed in the second CSTR. These conditions are hardly accessible in a single vessel, because such experiments would be extremely time consuming and unstable due to a low viability. At the lower dilution rates, high death rates could be studied under stable conditions in the second CSTR, which can not be done in a single vessel. This is because, in contrast to a single vessel, there is a continuous feed of biomass to the second CSTR of a reactor series. As such,

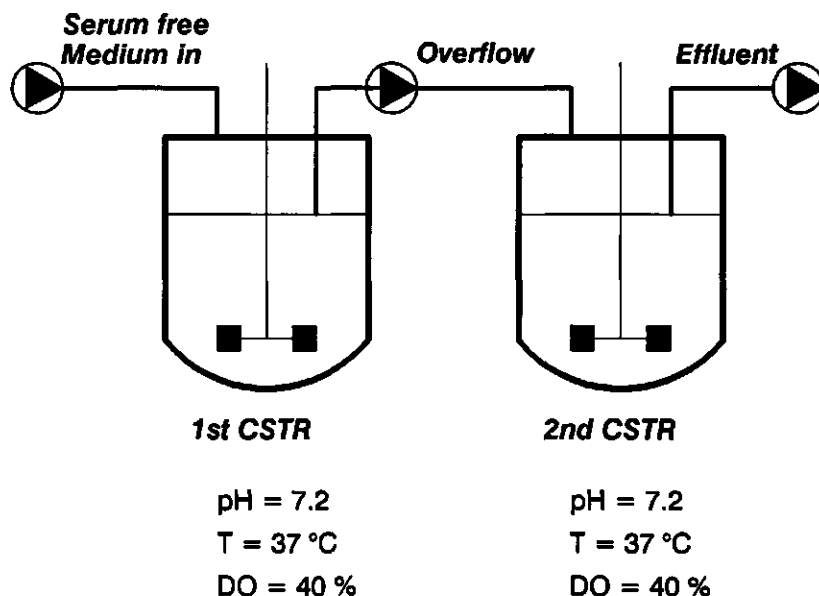


Figure 1. Scheme of the bioreactor cascade used for the hybridoma culture.

this experimental set-up offers interesting opportunities to study the different processes of cell death, like apoptosis (programmed cell death [Mercille and Massie, 1994]) and necrosis (passive, uncontrolled cell death [Mercille and Massie, 1994]), under steady-state conditions.

From the steady-state data, kinetic parameters were determined to use in a model that describes hybridoma growth and MAb production in a bioreactor cascade. Model estimates were in good agreement with the measurements.

MATERIALS AND METHODS

CELL LINE

The cell line, PFU-83, is a rat/mouse hybridoma suspension cell that produces monoclonal antibodies against rat/human corticotropin releasing factor [Van Oers *et al.*, 1989]. Every four months a sample from the same working cell bank was

thawed and used to inoculate the bioreactors.

MEDIUM

Serum-free culture medium, a 3:1 mixture of DMEM and Ham's F12 (both Gibco BRL, Life Technologies, U.K.) with additions, was described previously [Van der Pol *et al.*, 1992]. Transferrin (5 g.m^{-3} , human holo-form, Intergen, Belgium) was the only protein component. The initial glucose and glutamine concentrations were 21.3 and 7.35 mol.m^{-3} , respectively. The medium was kept at 4°C in order to avoid glutamine degradation.

CONTINUOUS CULTURES

The cells were grown in two standard 1 dm^3 unbaffled, round-bottomed bioreactors ($\varnothing = 10 \text{ cm}$; Applikon, The Netherlands) with a marine impeller ($\varnothing = 45 \text{ mm}$). Both reactors were operated continuously, either separately or in series, with a working volume of 0.615 dm^3 , at different dilution rates. Steady-state concentrations were analysed when four hydraulic residence times after a change had elapsed. Culture conditions were controlled at a dissolved-oxygen tension (DO) of $40 \pm 5 \%$ (air saturation), $\text{pH} = 7.2 \pm 0.1$, a temperature of $37.0 \pm 0.2^\circ\text{C}$, and a stirrer speed of 2.5 s^{-1} . Air and oxygen (for DO control), and CO_2 (for pH control) were supplied via the headspace. Cells were transported from the first to the second vessel via a hose with a pump. The residence time of the liquid in this hose was less than 60 s . Cell viability and concentration were unaffected by this pumping. Thirty-five steady-states were determined, of which 28 in the serial bioreactor (14 in the first and 14 in the second vessel), and 7 separately in a single vessel.

BATCH CULTURES

The inhibitory effect of ammonia (NH_4Cl , Merck) and lactate (lactic acid, Sigma) was investigated separately in batch cultures (T-flasks). Both components were added, in the desired amounts, to the medium before filtration. Lactic acid was neutralized by the addition of NaOH . The T-flasks were all inoculated from the same batch culture, in which the cells were growing exponentially. The flasks were aerated after taking samples. Samples were taken regularly to obtain complete S-

curves. All experiments were done in duplicate. To describe these growth curves uniformly, the modified Gompertz-equation was fitted to the data. This three-parameters Gompertz model describes the growth curves of many microorganisms adequately [Zwietering *et al.*, 1990]. The three parameters characterize the lag period, the maximum number of cells and the maximum specific growth rate μ_{max} .

ANALYSIS

Cell counts were done with a hemocytometer. Viability was determined by the trypan-blue-exclusion method. Samples from the cultures were centrifuged for 30 s at 450 g and the supernatant was frozen at -20 °C until analysis.

Substrates (glutamine and glucose) and metabolic by-products (ammonia and lactate) were determined enzymatically with an Analox GM-7 analyzer (Analox Instruments, UK). The monoclonal-antibody concentration in the supernatant of the samples was determined by a quantitative ELISA as described previously [Van der Pol *et al.*, 1990, 1992].

DEAD-CELL LYSIS AND APOPTOSIS

The specific dead-cell lysis rate was determined from a batch experiment which followed after a continuous culture ($D = 6.0 \times 10^{-6} \text{ s}^{-1}$). At steady state, medium supply was stopped and culture conditions were controlled at the same levels as in the continuous culture. Samples were taken in time during the death phase, and both viable and dead cells were counted.

During this batch experiment, the number of apoptotic cells among the dead cells was analysed by fluorescence microscopy [Mercille and Massie, 1994; Singh *et al.*, 1994]. Cells in a sample were fixed by the addition of an equal volume of 2% formaldehyde solution in phosphate-buffered saline (PBS). Then they were stained by the addition of an equal volume of 10 g.m^{-3} acridine orange (Sigma) solution in PBS. After that, apoptosis in the cells was shown by the appearance of condensed chromatin. This was done in the same way as described by Singh *et al.* [1994].

RESULTS AND DISCUSSION

CONTINUOUS CULTURES

Over a wide range of dilution rates the viable-cell concentration in the first stage of the reactor series was about $1.4 \times 10^{12} \text{ cell.m}^{-3}$ (Figure 2). At the highest dilution rates wash-out conditions, where cells grow at the maximal rate, were approached.

From the viable and dead-cell concentrations the viability (X_v/X_t , where $X_t = X_v + X_d$) was calculated, which is shown in Figure 3. Above dilution rates of $7.5 \times 10^{-6} \text{ s}^{-1}$ the viability in the first CSTR was higher than 0.95, while it starts to decrease with lower dilution rates. As the viable-cell concentration remains almost constant, this decrease in viability is caused by an increase in dead-cell concentrations. This indicated, as expected, that circumstances become more favourable for death at lower dilution rates.

During serial operation, the effluent of the first CSTR was transported to the

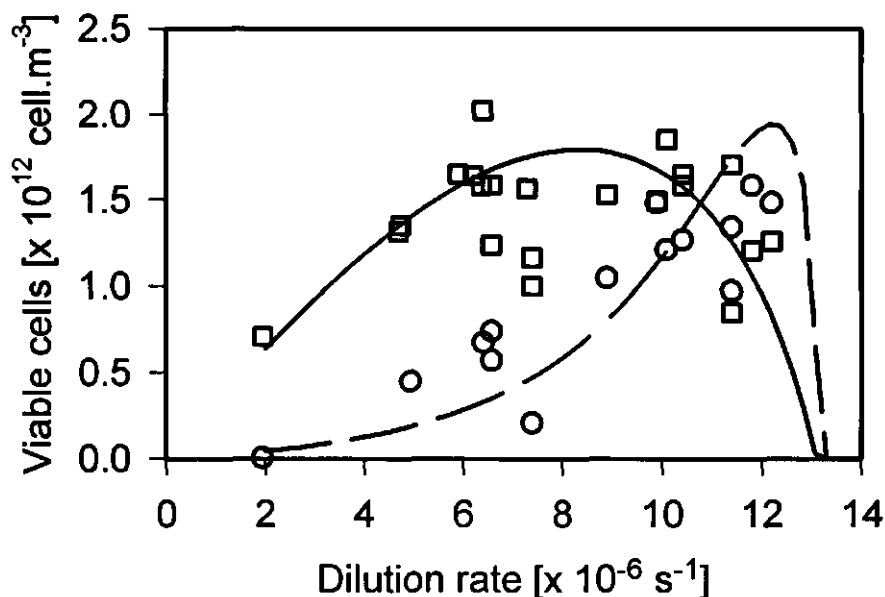


Figure 2. Viable-cell concentration of hybridomas in two CSTRs in series as a function of the dilution rate D in the first or the second CSTR. First stage (\square), second stage (\circ). Solid line: model estimates for the first stage, dashed line: model estimates for the second stage. These lines are discussed in the section 'Model estimates'.

second CSTR. Circumstances in that vessel were comparable to those in the first reactor, except that there was a continuous inflow of partially spent medium containing viable and dead biomass, and other products of hybridoma growth. In that second stage of the reactor cascade, the viable-cell concentration monotonously rose with increasing dilution rate (Figure 2). At higher dilution rates, substrate is used less complete by bioprocesses in a single CSTR [Pirt, 1975]. Therefore, more substrate will be left over for growth in the second reactor, giving rise to the higher viable-cell counts (Figure 2). Besides viable cells, also substantial amounts of dead cells were found in the second CSTR. This resulted in a viability that was lower than that in the first reactor at every dilution rate (Figure 3). Again, as in the first CSTR, the viability decreased with lower dilution rates (Figure 3).

At the lowest dilution rate ($D = 1.9 \times 10^{-6} \text{ s}^{-1}$), almost no viable cells were found in the second CSTR (Figs. 2 and 3). As a result, this gave inaccurate estimates of specific rates of growth, consumption and production, and therefore data from that experiment in the second CSTR were not used in further

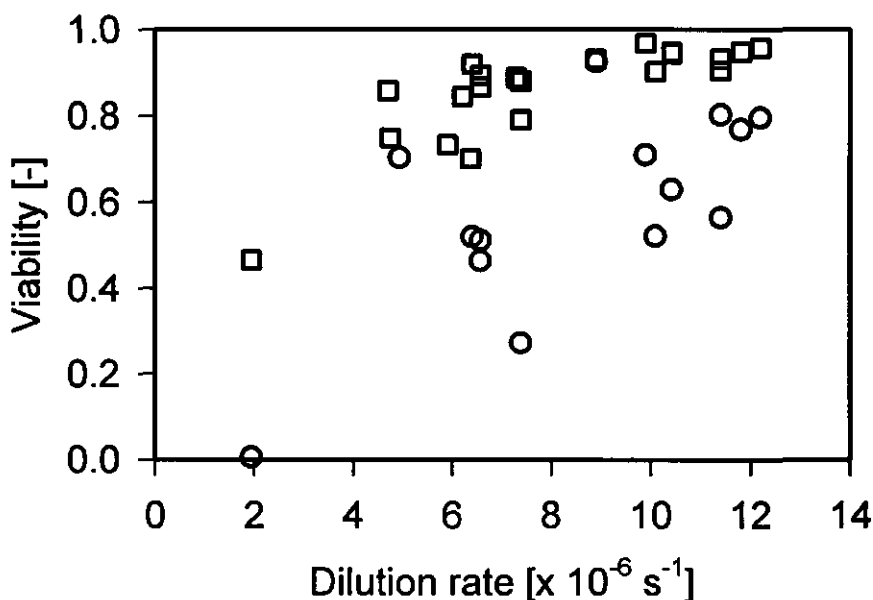


Figure 3. Viability of hybridomas in two CSTRs in series as a function of the dilution rate D in the first or the second CSTR. First stage (\square), second stage (\circ).

calculations.

MEASUREMENTS AND PRELIMINARY EXPERIMENTS

Rate-limiting substrate. Analogous to Frame and Hu [1991a], the rate-limiting substrate was determined from step-change experiments. Continuous experiments with different initial substrate concentrations were done at a low dilution rate ($6.6 \times 10^{-6} \text{ s}^{-1}$). At steady state the glutamine concentration in the feed was increased step-wise. After that a new steady state established. Going from a low to a high initial glutamine concentration (from 3.25 to 7.35 mol.m⁻³) a significant increase in viable-cell concentration (from 1.1×10^{12} to 1.6×10^{12} cell.m⁻³) was observed. This indicates that glutamine is the rate-limiting substrate. That not a doubling of the biomass concentration occurred, which might be expected when doubling the substrate concentration, can be explained by the increased biomass concentration, which requires more substrate for maintenance, especially at this low dilution rate.

Dead-cell lysis. At five dilution rates below $7.5 \times 10^{-6} \text{ s}^{-1}$, total cell counts ($X_t = X_v + X_d$) in the second CSTR were lower than those in the preceding first vessel. This means that either dead or viable cells disappear by lysis. In four of the five cases, there were more dead cells in the second CSTR than in the first reactor. This indicates that the dead cells did not lyse, which was verified in a batch-experiment (Figure 4). Lysis of dead cells could not be detected during 11 days after all cells had died in the batch. This is shown by the straight solid line from day 7 to day 18 in Figure 4. Thus the effect of dead cells which disappear by lysis was not taken into account in our calculations. The same result was obtained by Goergen *et al.* [1993]. Therefore, the only possible candidates for lysis were the viable cells, which was also observed by Goergen *et al.* [1993].

Growth inhibition. Hybridomas are often found to be inhibited in their growth by lactate and ammonia. Here, there was no need to account for inhibition. This was assessed by the following batch experiments and the analysis of the steady-state data from the continuous cultures.

From the batch experiments, no statistically significant effect (*t*-test) of added ammonia on the specific growth rate could be found for ammonia

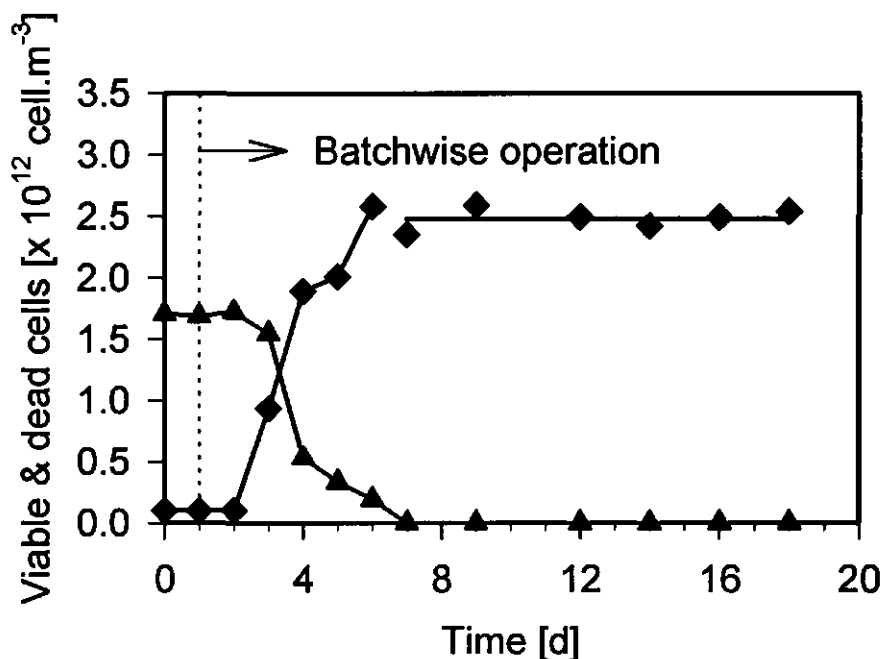


Figure 4. Viable (\blacktriangle) and dead-cell concentrations (\blacklozenge) in time in a batch under controlled conditions to determine the dead-cell lysis rate. Solid line: linear regression on the dead-cell concentration in time after all cells had died.

concentrations below 4 mol.m^{-3} . In the continuous experiments the ammonia concentration was always lower than 4.5 mol.m^{-3} . From the steady-state data, the true specific growth rate was observed to decrease with increasing ammonia concentration, thus suggesting inhibition. At the same time, however, the steady-state concentration of the growth-limiting substrate glutamine decreased. No discrimination between both effects could be made. Therefore, concluding from the batch and continuous experiments, growth inhibition by ammonia was assumed to be negligible. This result is in agreement with some findings in literature for ammonia, although others observed significant inhibition at lower concentrations; ammonia concentrations in the range of 2 to 10 mol.m^{-3} were observed to inhibit the growth rate by 50% [Ozturk *et al.*, 1992; Lüdemann *et al.*, 1994]. In both reviews it is suggested that inhibition can differ markedly between cell lines.

The same analysis was done for lactate. From the batch experiments no statistically significant effect (*t*-test) of added lactate on the specific growth rate could be found for lactate concentrations below 30 mol.m^{-3} . In the continuous

experiments the lactate concentration was always below this value. From the steady-state data no correlation between lactate concentration and the true specific growth rate was observed. Thus lactate did not inhibit growth, neither in the batch, nor in the continuous experiments. In literature the inhibitory concentration of lactate is at least one order of magnitude higher than that for ammonia [Ozturk *et al.*, 1992]. In several studies reviewed by those authors no significant lactate inhibition was observed at 40 mol.m⁻³ of lactate.

In conclusion, the inhibitory effects of both metabolic by-products (lactate and ammonia) were negligible, and therefore growth inhibition by these compounds was not taken into account in the further analysis.

Accuracy of the measurements. The accuracy of the measurements was assessed by determination of standard deviations. For each component analyzed in a steady state, which consisted of four or more samples taken in time, the standard deviation was expressed as a percentage of the mean. The averages of those percentages from all steady states were for viable cells 9%, dead cells 20%, glutamine 24%, glucose 10%, ammonia 15%, lactate 6% and for the monoclonal antibodies 13%.

Within the experimental error, no significant glutamine breakdown could be found when the medium (without cells) was stored for 200 h at 37 °C. Nevertheless, during the experiments the medium was kept at 4 °C to prevent non-specific chemical decomposition of glutamine such as has been found in literature [Glacken *et al.*, 1986; Ozturk and Palsson, 1990; Truskey *et al.*, 1990].

MODEL DEVELOPMENT

Net specific growth rate. In steady state, the net specific growth rate μ_{net} of viable cells is derived from the mass balance for viable cells:

$$\mu_{net,n} = \frac{D_n \cdot (X_{v,n} - X_{v,n-1})}{X_{v,n}} \quad (1)$$

Where D is the dilution rate, X_v is the viable-cell concentration and n the vessel number. Net specific growth rates were calculated from this Eq. (1). They are

shown, for both reactors in the series, as a function of the steady-state glutamine concentration in Figure 5. For cells in the second vessel, at lower glutamine concentrations between 2.5 and 1 mol.m⁻³, negative net specific growth rates are seen in this Figure 5. These negative growth rates are explained by viewing the net specific growth rate in more detail. In this net specific growth rate all processes, that describe the fate of the viable cells, are lumped together (see Appendix). Viable cells grow at a true specific growth rate μ_{true} , not only to overcome the dilution rate, but also to compensate for death and lysis. These three processes of which the net specific growth rate is composed are given by Eq. A2 in the Appendix.

The true specific growth rate is by definition positive. Therefore, negative net specific growth rates are caused by a substantial specific death rate, a high specific lysis rate of viable cells, or a combination of both. To gain insight in the net specific growth rate, the two loss terms in Eq. A2, μ_d and μ_b , are first discussed in more detail.

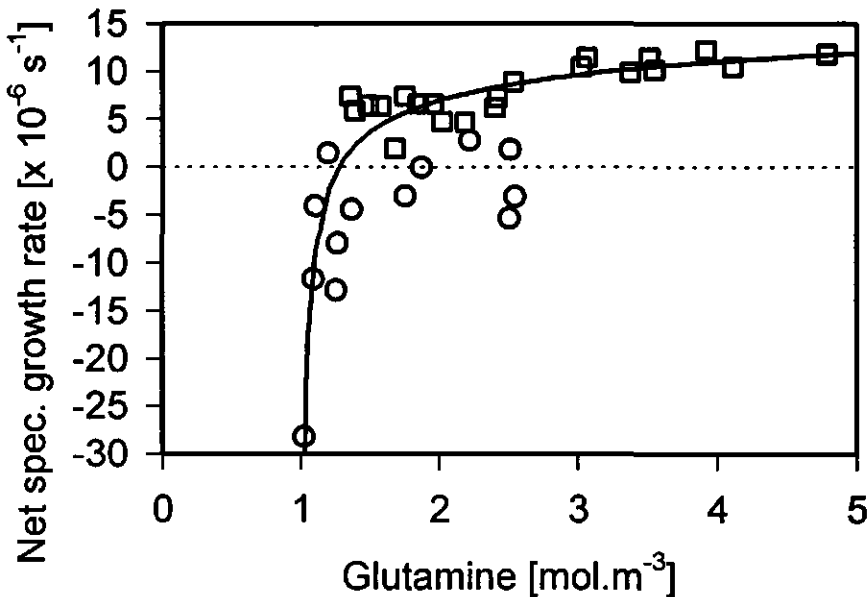


Figure 5. Net specific growth-rate μ_{net} for hybridomas in two CSTRs in series as a function of the glutamine concentration. First stage (□), second stage (○). Solid line: curve fit with Eq. A2 (discussed in the section 'true specific growth rate'), parameter values are given in Table I.

Specific death rate. The mass balance for dead cells, at steady state, gives an expression for the specific death rate μ_d :

$$\mu_{d,n} = \frac{D_n \cdot (X_{d,n} - X_{d,n-1})}{X_{v,n}} \quad (2)$$

Specific death rates were calculated from this Eq. (2). The curve for the specific death rate as a function of the glutamine concentration in Figure 6 appeared as an inverted Monod-curve:

$$\mu_d = \mu_{d,min} \cdot \frac{K_d + C_{gln}}{C_{gln}} \quad (3)$$

With $\mu_{d,min}$ being the minimum specific death rate and K_d a death-rate constant. This Eq. (4) was fitted to the measurements by non-linear regression. Both

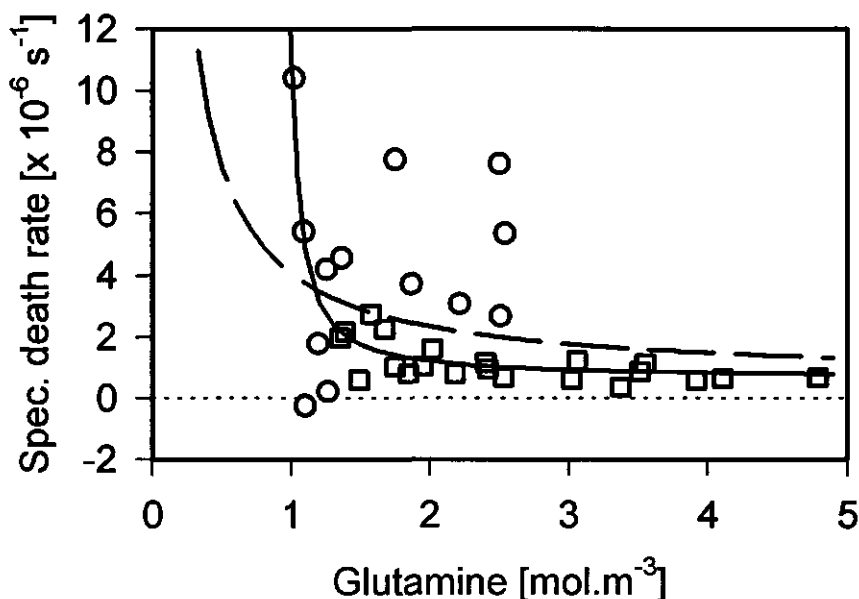


Figure 6. Specific death-rate μ_d for hybridomas in two CSTRs in series as a function of the glutamine concentration. First stage (\square), second stage (\circ). Dashed line: curve fit with Eq. (3). Solid line: curve fit with Eq. (4), parameter values are given in Table I.

parameters, $\mu_{d,min}$ and K_d , were statistically insignificant (*t*-test). Therefore $\mu_{d,min}$ was arbitrarily chosen $6.2 \times 10^{-7} \text{ s}^{-1}$, which is the average μ_d at the three highest glutamine concentrations (Figure 6). With the best fit now, the specific death rate was overestimated for the first CSTR at all glutamine concentrations (Figure 6), even when $\mu_{d,min}$ was chosen lower. To be able to describe the specific death rate better, an extra parameter was added to Eq. (3) as described below. At glutamine concentrations between 2 and 1 mol.m⁻³ the specific death rate mostly increased in both CSTRs (Figure 6). Also, the glutamine concentration was never lower than 1 mol.m⁻³ (Figure 6). This was described by an additional glutamine threshold concentration $C_{gln,th,d}$ to the reversed Monod model. This is the same approach as followed by Frame and Hu [1991a, 1991b] for other hybridomas:

$$\mu_d = \mu_{d,min} \cdot \frac{K_d + C_{gln} - C_{gln,th,d}}{C_{gln} - C_{gln,th,d}} \quad (4)$$

Such thresholds are rarely seen in literature about hybridomas, but in a review Button [1985] found that threshold concentrations are more often encountered, *e.g.* with micro-organisms. Hence, Eq. (4) was fitted to the measurements by non-linear regression, with $\mu_{d,min}$ fixed at $6.2 \times 10^{-7} \text{ s}^{-1}$ (Figure 6), and the resulting statistically significant (*t*-test) parameter values are given in Table I. Figure 6 shows that Eq. (4) fits the results of the first CSTR much better. Therefore Eq. (4) was used to describe the specific death rate in the model calculations. In the next section, the specific lysis rate of viable cells will be described by the same type of equation.

Table I. Kinetic constants with their source and, where possible, comparison to literature averages which were taken from Martens *et al.*, 1995.

Subject	Kinetic constant	Value	Literature average	Unit	Remarks / Source
Death rate	$\mu_{d,min}$	6.20 ± 3.09	--	$\times 10^{-7} \text{ s}^{-1}$	Curve fitting (Eq. 4, Figure 6)
	K_d	1.01 ± 0.90	--	mol.m^{-3}	Curve fitting (Eq. 4, Figure 6)
	$C_{gln,th,d}$	0.95 ± 0.08	--	mol.m^{-3}	Curve fitting (Eq. 4, Figure 6)
Lysis rate	$\mu_{l,min}$	2.00 ± 1.33	--	$\times 10^{-7} \text{ s}^{-1}$	Curve fitting (Eq. 6 in Eq. A2, Figure 5)
	K_l	8.52 ± 6.46	--	mol.m^{-3}	Curve fitting (Eq. 6 in Eq. A2, Figure 5)
	$C_{gln,th,l}$	0.95 ± 0.09	--	mol.m^{-3}	Curve fitting (Eq. 6 in Eq. A2, Figure 5)
True growth rate	μ_{max}	1.70 ± 0.26	--	$\times 10^{-5} \text{ s}^{-1}$	Washout experiments
	K_s	1.40 ± 0.29	--	mol.m^{-3}	Curve fitting (Eq. 7 in Eq. A2, Figure 5)
Glutamine	$Y_{x/gln}$	5.69 ± 1.32	7.68	$\times 10^{11} \text{ cell.mol}^{-1}$	Linear regression (Eq. 8, Figure 9)
	m_{gln}	4.07 ± 3.74	3.76	$\times 10^{-18} \text{ mol.cell}^{-1}.\text{s}^{-1}$	Linear regression (Eq. 8, Figure 9)
MAB's	q_{Mab}	2.68 ± 2.88	3.99	$\times 10^{-16} \text{ g.cell}^{-1}.\text{s}^{-1}$	Average at all growth rates

Values are expressed $\pm 95\%$ confidence limits.

Specific lysis rate of viable cells. The concentrations of lysed viable cells in the first reactor were unknown. For the second vessel in the series, the amount of lysed viable cells was estimated from the difference in total cell count between both reactors: $X_{l,2} = (X_{v,1} + X_{d,1}) - (X_{v,2} + X_{d,2})$. Assuming steady state, the mass balance for lysed viable cells gives an expression for the specific lysis rate of viable cells μ_l :

$$\mu_{l,n} = \frac{D_n \cdot (X_{l,n} - X_{l,n-1})}{X_{v,n}} \quad (5)$$

Specific lysis rates of viable cells in the second vessel in the reactor series were estimated from this Eq. (5). For that, as a first estimate, it was assumed that lysis of viable cells in the first reactor in the series was negligible. This assumption was made from the observations of Goergen *et al.* [1993], who found almost no lysis of viable cells in a continuous culture ($D = 4.7 \times 10^{-6} \text{ s}^{-1}$) at pH 7. However, at pH 6.8 they saw appreciable lysis of living cells ($\mu_l = 6.0 \times 10^{-6} \text{ s}^{-1}$). Our

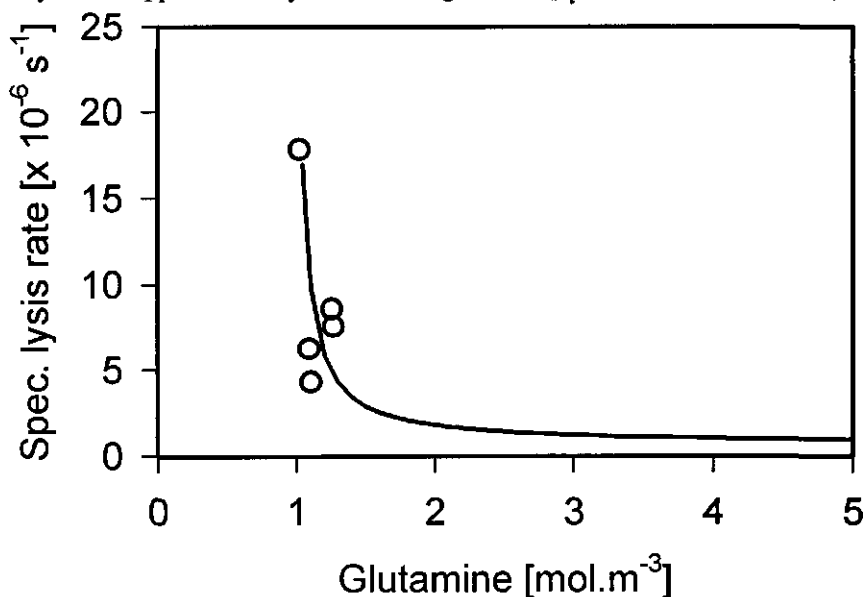


Figure 7. Estimated specific lysis rate of viable cells μ_l for hybridomas in the second vessel of the reactor series as a function of the glutamine concentration. Solid line: curve fit with Eq. (6).

experiments indicate that not only pH, but also the glutamine concentration can influence the specific lysis rate of viable cells. The estimated specific lysis rate of viable cells in the second CSTR is shown in Figure 7 as a function of the glutamine concentration. At low glutamine concentrations between 1 and 1.3 mol.m⁻³ lysis was not negligible (Figure 7), while at higher glutamine concentrations lysis was assumed to be negligible (mostly in the first reactor, see above). To describe this, the same reversed Monod kinetics with a glutamine threshold concentration was assumed as done for the specific death rate (see Eq. (4)):

$$\mu_l = \mu_{l,min} \cdot \frac{K_l + C_{gln} - C_{gln,th,l}}{C_{gln} - C_{gln,th,l}} \quad (6)$$

With $\mu_{l,min}$ being the minimum specific lysis rate of viable cells and K_l a lysis-rate constant. As a first impression, also in Figure 7, a fit by non-linear regression with Eq. (6) is shown. Here the $C_{gln,th,l}$ was taken the same as that for the death kinetics in Eq. (4). Determination of the actual parameter values in Eq. (6) (*i.e.* not fitted to the estimated specific lysis rate of viable cells as shown in Figure 7) will now be discussed in the following section about the true specific growth rate.

True specific growth rate. The true specific growth rate can not be calculated directly from the measurements with Eq. A2, because the concentrations of lysed viable cells are unknown. Therefore a Monod model was assumed to describe the true specific growth rate as a function of the glutamine concentration:

$$\mu_{true} = \mu_{max} \cdot \frac{C_{gln}}{K_s + C_{gln}} \quad (7)$$

where K_s is the Monod-constant. The maximal specific growth rate was determined to be $\mu_{max} = 1.7 \times 10^{-5} \text{ s}^{-1}$ from wash-out experiments. Substitution of Eqs. (4, 6 and 7) in Eq. A2 gives an expression for the net specific growth rate, with K_s , $\mu_{l,min}$, K_l and $C_{gln,th,l}$ being four unknown parameters since $\mu_{d,min}$, K_d and $C_{gln,th,d}$ were known from the previous (values in Table I). This expression was fitted to the net specific growth rate as a function of the glutamine concentration by non-linear

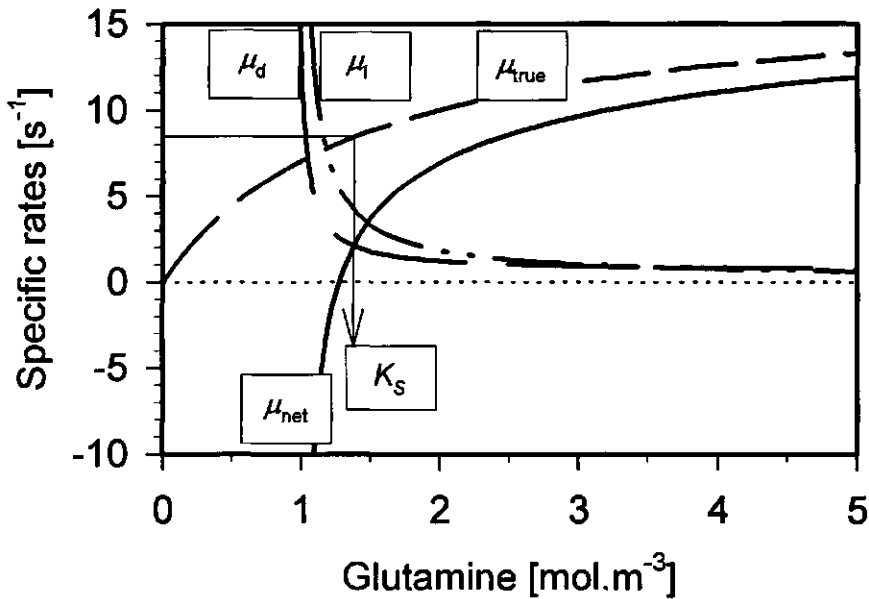


Figure 8. The net specific growth rate μ_{net} in Eq. A2 as a function of the glutamine concentration is the resultant of the three specific rates, μ_{true} from Eq. (7), μ_d from Eq. (4) and μ_l from Eq. (6). Straight solid lines indicate $0.5 \times \mu_{max}$ and K_s for the true specific growth rate curve. Parameter values are given in Table I.

regression, as shown in Figure 5. The resulting parameter values are given in Table I. From the overlay in 95%-confidence limits it was concluded that the threshold concentration $C_{gln,th,l}$ obtained here is comparable to that from the death rate equation (Eq. (4), Table I). All four rates discussed above are summarized in Figure 8. The net specific growth rate μ_{net} is the resultant of the three specific rates, μ_{true} , μ_d and μ_l (see Eq. A2 and Figure 8). At glutamine concentrations above 3.5 mol.m^{-3} the specific lysis rate of viable cells is lower than the specific death rate (Figure 8). But at low glutamine concentrations, approaching 1 mol.m^{-3} , the loss of viable cells by lysis dominates over the loss by death (Figure 8). From this, it was concluded that, under adverse conditions, lysis of viable cells can not be neglected and should be included in models describing hybridoma growth.

Glutamine consumption. To couple the glutamine consumption kinetics to the true specific growth rate, the following linear relation was assumed:

$$q_{gln} = \frac{\mu_{true}}{Y_{x/gln}} + m_{gln} \quad (8)$$

where $Y_{x/gln}$ is the yield factor of biomass on glutamine and m_{gln} is the maintenance coefficient for glutamine. The specific glutamine consumption rate q_{gln} was calculated from a general mass balance (see Eq. (A3) in the Appendix), assuming steady state:

$$q_{A,n} = \frac{D_n \cdot (C_{A,n} - C_{A,n-1})}{X_{v,n}} \quad (9)$$

In Figure 9 the specific glutamine consumption rate is shown as a function of the

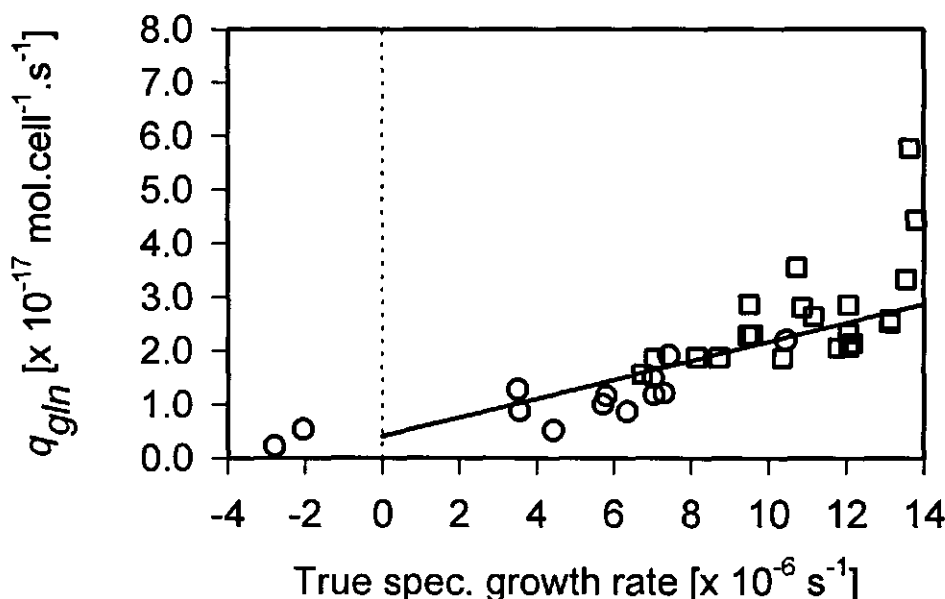


Figure 9. Specific glutamine consumption rate q_{gln} for hybridomas in two CSTRs in series as a function of the true specific growth rate μ_{true} for the determination of the kinetic parameters $Y_{x/gln}$ and m_{gln} in Eq. (8) by linear regression (solid line: parameter values given in Table I). In the linear regression the two observations above $q_{gln} = 4 \times 10^{-17} \text{ mol.cell}^{-1}.\text{s}^{-1}$ were omitted because they deviated statistically significant (t -test) from the linear model. First stage (\square), second stage (\circ).

true specific growth rate. The true specific growth rate was estimated with Eq. A2 by using μ_{net} and μ_d calculated with Eqs. (1) and (2) from the measurements, and μ_l calculated from Eq. (6) with parameter values from Table I. The yield factor of biomass on glutamine $Y_{x/gln}$ and the maintenance coefficient for glutamine m_{gln} were obtained from linear regression with Eq. (8) (Figure 9). The values are given in Table I, together with averages for other hybridomas. Although it should be realized that those parameters were determined for different hybridomas under often different process conditions, both parameters are in good agreement with values found in literature.

MAB production. In the same way as for glutamine, the specific MAB production rate q_{MAB} was analysed. The q_{MAB} , which was calculated from Eq. (9), appeared to be roughly constant with the true specific growth rate, or in other words it was non-growth associated (Figure 10, Table I). In literature both positive, negative and non-growth associated MAB production is observed in continuous cultures [Al-Rubeai *et al.*, 1992].

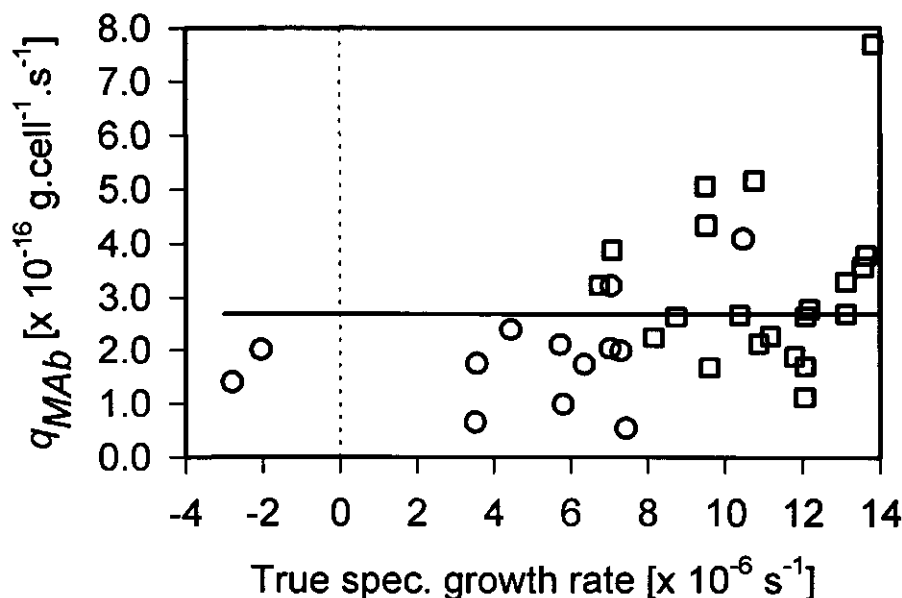


Figure 10. Specific MAB production rate q_{MAB} for hybridomas in two CSTRs in series as a function of the true specific growth rate μ_{true} . Solid line: average q_{MAB} independent of μ_{true} . First stage (\square), second stage (\circ).

Model estimates. Based on the steady-state viable-cell and glutamine balances, a model was developed. This steady-state model describes hybridoma growth, glutamine consumption, and their MAb production as a function of the dilution rate. By substitution of Eqs. A2, (4) and (6 - 9) in Eq. (1), an expression is obtained in which the steady-state glutamine concentration is the only unknown. Roots of this expression are found by a bisection method (RTBIS from Press *et al.* [1989]). When the steady-state glutamine concentration is known, other concentrations, like biomass and MAbs, can be estimated. In this way, using the above-mentioned parameter values given in Table I, model estimates were made for hybridoma growth and their MAb production in a reactor series. In Figure 2 the results for the viable cell concentrations are given. At higher dilution rates an increased maximal viable cell density was calculated in the serial bioreactor, when compared to a single vessel. The model estimates agree rather well with the experiments (Figure 2). Seeing the variance in experimental data for the specific MAb production rate in Figure 10, we can not expect much from the model

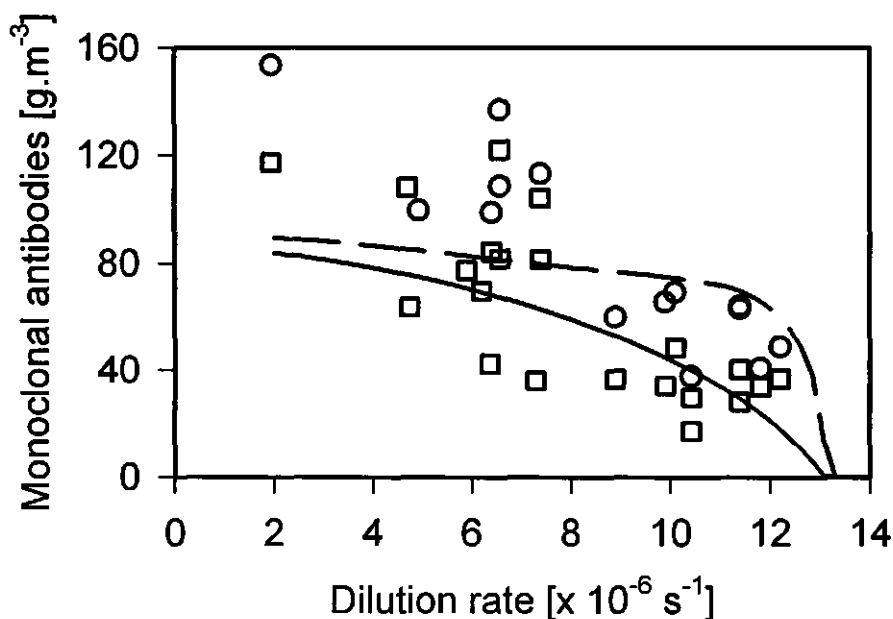


Figure 11. MAb concentration in two CSTRs in series as a function of the dilution rate D in the first or the second CSTR. First stage (\square), second stage (\circ). Solid line: model estimates for the first stage, dashed line: model estimates for the second stage.

estimates for the MAb concentrations. However, the model estimates for the first vessel agree reasonable well (Figure 11). For the second vessel there is still some, but less agreement, which could be expected as the estimations for the second vessel were made from the first one.

RESEARCH TOOL

Low growth rates. A main advantage of the reactor cascade, compared to a single CSTR, is that experimental results at very low and negative net specific growth rates can be obtained relatively fast and easy in the second CSTR. Thus very informative data for model development, regarding the metabolism as a function of the whole range of possible specific growth rates can be obtained (see Figs. 8, 9 and 10). These conditions are hardly accessible in a single vessel, because such experiments would be extremely time-consuming and unstable due to a low viability. This shortcoming in single-vessel experiments is often seen in literature where extrapolations to lower specific growth rates have to be made to obtain values for kinetic parameters [Hiller *et al.*, 1991; Linardos *et al.*, 1991; Miller *et al.*, 1988].

Further, in the steady states at lower dilution rates, dead and lysed cell concentrations increased to high levels in the second vessel. In contrast to a single vessel, a reactor cascade can easily supply these high concentrations because growth, death and lysis prolongate in the second vessel. As such, this offers interesting possibilities to study apoptosis and necrosis kinetics under stable conditions.

Apoptosis. Apoptotic cell death is commonly seen in hybridomas [Mercille and Massie, 1994; Singh *et al.*, 1994]. This was qualitatively assessed here. After 5 days in a batch (samples taken from the experiment shown in Figure 4) more than 80% of the cells were observed to have died of apoptosis, as shown by the appearance of condensed chromatin.

In literature it is observed that low substrate concentrations induce apoptosis [Mercille and Massie, 1994; Singh *et al.*, 1994]. It is illustrated in Figure 8 that the net specific growth rate starts to deviate from normal Monod kinetics (*i.e.* the curve for the true specific growth rate) at about $0.5 \times \mu_{max}$, where glutamine

concentrations are below the K_s -value. This indicates that there exists a 'critical growth rate' at low substrate concentrations below which apoptosis is induced [Martens *et al.*, 1995]. Therefore apoptosis may be seen as the process that mainly caused the sudden increase in the specific death rate at glutamine concentrations below the K_s -value (Figure 8).

CONCLUSIONS

In a bioreactor cascade experimental conditions were realized that are not accessible in a single vessel. Hybridoma metabolism was analyzed as a function of the whole range of possible growth rates. Thus, a major advantage of the reactor series over a single vessel is that no extrapolations to lower growth rates were needed to obtain values for kinetic parameters. Further, at low dilution rates the reactor series supplied high concentrations of dead cells. This can be used to study apoptosis and necrosis under stable conditions. Hence, the bioreactor cascade is a powerful research tool.

Growth was described with a Monod relation. Glutamine was the rate-limiting substrate. No inhibition by lactate or ammonia was observed. Death and lysis of viable cells were both described by reversed, and modified, Monod kinetics. At low glutamine concentrations the growth rate decreased rapidly, which indicates that there exists a critical growth rate below which apoptosis is induced. The specific MAb production rate was non-growth associated.

Based on glutamine metabolism, model estimates were made for the hybridoma growth in a bioreactor series, and their MAb production. The model estimates agree rather well with the experiments.

ACKNOWLEDGEMENTS

The serum-free cell line was kindly supplied by L. van der Pol of Bio-Intermediair B.V. (Groningen, The Netherlands). The authors are indebted to M.S.N. Bakker and M.C.J. van de Noort for their contributions to the experiments. Furthermore, D.E. Martens is thanked for carefully reading the manuscript. This work was partly supported by Applikon Dependable Instruments B.V., Schiedam, The Netherlands. The research was carried out in a PBTS project, nr. 89069, initiated by The Economic Affairs Ministry of The Netherlands.

NOMENCLATURE

C_A	Concentration of any component A	$[\text{mol.m}^{-3}]$
D	Dilution rate	$[\text{s}^{-1}]$
K_d	Death-rate constant	$[\text{mol.m}^{-3}]$
K_l	Lysis-rate constant	$[\text{mol.m}^{-3}]$
K_s	Monod constant	$[\text{mol.m}^{-3}]$
m	Maintenance coefficient	$[\text{mol.cell}^{-1}.\text{s}^{-1}]$
q	Specific consumption or production rate	$[\text{mol.cell}^{-1}.\text{s}^{-1}]$
t	Time	$[\text{s}]$
X	Cell concentration	$[\text{cell.m}^{-3}]$
Y	Yield coefficient	$[\text{cell.mol}^{-1}]$

Greek symbols

μ_d	Specific death rate	$[\text{s}^{-1}]$
μ_l	Specific lysis rate of viable cells	$[\text{s}^{-1}]$
μ_{net}	Net specific growth rate	$[\text{s}^{-1}]$
μ_{true}	True specific growth rate	$[\text{s}^{-1}]$

Subscripts

d	Dead cells
gln	Glutamine

l	Lysed viable cells
max	Maximum
min	Minimum
n	Vessel number in the reactor series
t	Total cells
th	Threshold
v	Viable cells

Abbreviation

MAB Monoclonal Antibody

APPENDIX

The net specific growth rate in Eq. (1) can be further specified. In hybridoma cultivation both viable and dead cells are being observed. From a continuous culture viable cells disappear in three ways: i) by death, ii) by lysis, and iii) by dilution.

Death of viable biomass gives dead biomass. Besides that, Goergen *et al.* [1993] described lysis of viable cells, which was also observed in this study. Therefore, in the mass balance viable biomass is removed by death, lysis and dilution. At dilution rate D , this gives for the viable cells X_v :

$$\frac{dX_{v,n}}{dt} = D_n \cdot X_{v,n-1} + \mu_{true,n} \cdot X_{v,n} - \mu_{d,n} \cdot X_{v,n} - \mu_{l,n} \cdot X_{v,n} - D_n \cdot X_{v,n} \quad (A1)$$

where μ_{true} is the true specific growth rate at which the cells grow to compensate for death, lysis and dilution; μ_d is the specific death rate and μ_l the specific lysis rate of viable cells. Hence, the net specific growth rate in Eq. (1) can be described by the rates of growth, death and lysis from Eq. (A1):

$$\mu_{net,n} = \mu_{true,n} - \mu_{d,n} - \mu_{l,n} \quad (A2)$$

For any substrate or product with concentration C_A that is respectively consumed or produced at rate q_A the mass balance yields:

$$\frac{dC_{A,n}}{dt} = D_n \cdot C_{A,n-1} - D_n \cdot C_{A,n} + q_{A,n} \cdot X_{v,n} \quad (A3)$$

Here q_A is positive for production and has a negative sign for consumption.

REFERENCES

- [1] Aeschlimann, A.; Di Stasi, L.; von Stockar, U. 1990. Continuous production of lactic acid from whey permeate by *Lactobacillus helveticus* in two chemostats in series. *Enzyme Microb. Technol.* **12**: 926-932.
- [2] Al-Rubeai, M.; Emery, A.N.; Chalder, S.; Jan, D.C. 1992. Specific monoclonal antibody productivity and the cell cycle-comparisons of batch, continuous and perfusion cultures. *Cytotechnology* **9**: 85-97.
- [3] Button, D.K. 1985. Kinetics of nutrient-limited transport and microbial growth. *Microbiol. Rev.* **49**: 270-297.
- [4] Dalili, M.; Sayles, G.D.; Ollis, D.F. 1990. Glutamine-limited batch hybridoma growth and antibody production: experiment and model. *Biotechnol. Bioeng.* **36**: 74-82.
- [5] De Gooijer, C.D.; Bakker, W.A.M.; Beftink, H.H.; Tramper, J. 1995. Bioreactors in series: an overview of design procedures and practical applications. *Enzyme Microb. Technol.* Accepted.
- [6] Frame, K.K.; Hu, W-S. 1991a. Kinetic study of hybridoma cell growth in continuous culture. I. A model for non-producing cells. *Biotechnol. Bioeng.* **37**: 55-64.
- [7] Frame, K.K.; Hu, W-S. 1991b. Kinetic study of hybridoma cell growth in continuous culture: II. Behavior of producers and comparison to nonproducers. *Biotechnol. Bioeng.* **38**: 1020-1028.
- [8] Glacken, M.W.; Fleischaker, R.J.; Sinskey, A.J. 1986. Reduction of waste

- product excretion via nutrient control: possible strategies for maximizing product and cell yields on serum in cultures of mammalian cells. *Biotechnol. Bioeng.* **28**: 1376-1389.
- [9] Goergen, J.L.; Marc, A.; Engasser, J.M. 1993. Determination of cell lysis and death kinetics in continuous hybridoma cultures from the measurement of lactate dehydrogenase release. *Cytotechnology* **11**: 189-195.
- [10] Hill, G.A.; Robinson, C.W. 1989. Minimum tank volumes for CFST bioreactors in series. *Can. J. Chem. Eng.* **67**: 818-824.
- [11] Hiller, G.W.; Aeschlimann, A.D.; Clark, D.S.; Blanch, H.W. 1991. A kinetic analysis of hybridoma growth and metabolism in continuous suspension culture on serum-free medium. *Biotechnol. Bioeng.* **38**: 733-741.
- [12] Linardos, T.I.; Kalogerakis, N.; Behie, L.A.; Lamontagne, L.R. 1991. The effect of specific growth rate and death rate on monoclonal antibody production in hybridoma chemostat cultures. *Can. J. Chem. Eng.* **69**: 429-438.
- [13] Lüdemann, I.; Pörtner, R.; Märkl, M. 1994. Effect of NH_3 on the cell growth of a hybridoma cell line. *Cytotechnology* **14**: 11-20.
- [14] Martens, D.E.; Sipkema, E.M.; De Gooijer, C.D.; Beuvery, E.C.; Tramper, J. 1995. A combined cell-cycle and metabolic model for the growth of hybridoma cells in steady-state continuous culture. *Biotechnol. Bioeng.* Accepted.
- [15] Mercille, S.; Massie, B. 1994. Induction of apoptosis in nutrient-deprived cultures of hybridoma and myeloma cells. *Biotechnol. Bioeng.* **44**: 1140-1154.
- [16] Miller, W.M.; Blanch, H.W.; Wilke, C.R. 1988. A kinetic analysis of hybridoma growth and metabolism in batch and continuous suspension culture: effect of nutrient concentration, dilution rate, and pH. *Biotechnol. Bioeng.* **32**: 947-965.
- [17] Ozturk, S.S.; Palsson, B.O. 1990. Chemical Decomposition of Glutamine in Cell Culture Media: Effect of Media Type, pH and Serum Concentration. *Biotechnol. Prog.* **6**: 121-128.
- [18] Ozturk, S.S.; Palsson, B.O. 1991. Growth, metabolic, and antibody production kinetics of hybridoma cell culture .1. Analysis of data from controlled batch reactors. *Biotechnol. Prog.* **7**: 471-480.
- [19] Ozturk, S.S.; Riley, M.R.; Palsson, B.O. 1992. Effects of ammonia and lactate on hybridoma growth, metabolism, and antibody production. *Biotechnol. Bioeng.* **39**: 418-431.
- [20] Pirt, S.J. 1975. Principles of microbe and cell cultivation. Blackwell, Oxford, UK.
- [21] Press, W.H.; Flannery, B.P.; Teukolsky, S.A.; Vetterling, W.A. 1989.

- Numerical recipes in Pascal. Cambridge university press, Cambridge.
- [22] Reuveny, S.; Velez, D.; Miller, L.; Macmillan, J.D. 1986. Comparison of cell propagation methods for their effect on monoclonal antibody yield in fermentors. *J. Immunol. Meth.* **86**: 61-69.
- [23] Shama, G. 1988. Developments in bioreactors for fuel ethanol production. *Process Biochem.* **10**: 138-145.
- [24] Shimizu, K.; Matsubara, M. 1987. Product formation patterns and the performance improvement for multistage continuous stirred tank fermentors. *Chem. Eng. Comm.* **52**: 61-74.
- [25] Singh, R.P.; Al-Rubeai, M.; Gregory, C.D.; Emery, A.N. 1994. Cell death in bioreactors: a role for apoptosis. *Biotechnol. Bioeng.* **44**: 720-726.
- [26] Truskey, G.A.; Nicolakis, D.P.; DiMasi, D.; Haberman, A.; Swartz, R.W. 1990. Kinetic studies and unstructured models of lymphocyte metabolism in fed-batch culture. *Biotechnol. Bioeng.* **36**: 797-807.
- [27] Van der Pol, L.; Bakker, W.A.M.; Tramper, J. 1992. Effect of low serum concentrations (0% - 2.5%) on growth, production, and shear sensitivity of hybridoma cells. *Biotechnol. Bioeng.* **40**: 179-182.
- [28] Van der Pol, L.; Zijlstra, G.; Thalen, M.; Tramper, J. 1990. Effect of serum concentration on production of monoclonal antibodies and on shear sensitivity of a hybridoma. *Bioproc. Eng.* **5**: 241-245.
- [29] Van Oers, J.W.A.M.; Tilders, F.J.H.; Berkenbosch, F. 1989. Characterization of a rat monoclonal to rat/human corticotropin releasing factor. *Endocrinology* **124**: 1239-1246.
- [30] Venables, D.C.; Boraston, R.C.; Bushell, M.E. 1993. Two-stage chemostat studies of hybridoma growth, nutrient utilisation, and monoclonal antibody production. In: S. Kaminogawa *et al.* (Eds.), *Animal cell technology; basic & applied aspects*. Kluwer academic publishers, The Netherlands, 5, pp. 585-594.
- [31] Zwietering, M.H.; Jongenburger, I.; Rombouts, F.M.; Van 't Riet, K. 1990. Modeling of the bacterial growth curve. *Appl. Environ. Microbiol.* **56**: 1875-1881.

INTRODUCTION

Multistage processes are commonly used in waste-water treatment. The subsequent conversion steps can be executed separately in a series of vessels. For example, nitrification (*i.e.* the oxidation of ammonia via nitrite to nitrate) is often followed by a denitrification step (*i.e.* the conversion of nitrate to nitrogen) for complete removal of nitrogenous compounds from wastewaters [Barnes and Bliss, 1983]. An alternative use of the reactor cascade is to approximate plug-flow behaviour. Here one reaction step is applied repeatedly in each compartment of a serial bioreactor. This may be done when optimal bioreactor design with respect to a minimal total residence time at a given substrate conversion is the goal [De Gooijer *et al.*, 1995]. Recently a compact reactor cascade, which can both be used for scale-up of multi-step waste-water treatment systems and for plug-flow approximations, was introduced [Bakker *et al.*, 1995]. This new reactor type consists of a series of internal-loop air-lift reactors within one vessel. To investigate the applicability of such a bioreactor for plug-flow approximations, nitrite conversion to nitrate (the second step in nitrification) by immobilized *Nitrobacter agilis* was studied on laboratory scale in a cascade of two air-lift loop bioreactors.

In literature serial bioreactors are claimed to be especially favourable over a single vessel of the same overall volume when product inhibition plays an important role [Shimizu and Matsubara, 1987; Hill and Robinson, 1989]. Theory is well developed for freely suspended cells [De Gooijer *et al.*, 1995]. However, with the exception of bioethanol production, little is known about optimal design of bioreactor cascades when using immobilized growing cells. Therefore, to gain more insight, the effects of substrate and product inhibition on the performance of a single vessel as compared to a reactor series with immobilized *N. agilis* cells were studied. For that, high substrate (nitrite, NO_2^-) and, as a result of substrate conversion, high product (nitrate, NO_3^-) concentrations were applied; concentration levels which can be expected in waste streams from industry, agriculture or landfills [Hunik *et al.*, 1993].

In the experiments, the combined effect of substrate and product inhibition was investigated. For that, steady states at different dilution rates were analysed with respect to substrate and product concentrations. A statistically significant

improvement of substrate conversion by using the bioreactor cascade over a single vessel of the same overall volume was found. The experiments agreed with simulations by a dynamic model [Hunik *et al.*, 1994] that estimates biomass growth and concentration profiles across gel beads in time. The model incorporates the effects of diffusion limitation and substrate and product inhibition.

MATERIALS AND METHODS

CELL LINE AND MEDIUM

Nitrobacter agilis (ATCC 14123) was precultured at 30 °C in a 5-dm³ batch. The medium contained per dm³ demineralized water: 0.68 g KH₂PO₄; 0.87 g K₂HPO₄; 0.052 g MgSO₄·7H₂O; 0.052 mg FeSO₄·7H₂O; 0.026 mg CuSO₄; 0.74 mg CaCl₂·2H₂O; 0.24 mg Na₂MoO₄·2H₂O and 4.3 mg ZnSO₄·7H₂O [Hunik *et al.*, 1994; Wijffels *et al.*, 1991]. The pH was adjusted to 7.8 with 2 mol.m⁻³ KOH. Nitrite and nitrate concentrations were measured regularly and KNO₂ was added to 20 mol.m⁻³. Furthermore, the suspension was diluted every 2 days to avoid product inhibition. All chemicals were obtained from Merck.

IMMOBILIZATION

After centrifugation (20 min at 16300 g and 5 °C) the cells were immobilized in a 2.6% (w/w) κ -carrageenan solution as described by Wijffels *et al.* [1991]. The immobilization yielded gel beads with an average diameter of 1.99 ± 0.20 mm. An initial biomass concentration of 7.0 g.m⁻³ gel was estimated from the specific oxygen consumption rate of the cell suspension before immobilization. This estimation was made in the same way as described by Wijffels *et al.* [1991].

BIOREACTOR-CASCADE OPERATION

The beads with the immobilized cells were cultivated for 134 days in a cascade of two air-lift reactors with an external loop (ALRs, Figure 1). The continuous bioreactors were operated in series, both with a working volume of 2.4 dm³, at different dilution rates. Steady-state concentrations were analysed when at least four hydraulic residence times had elapsed, and reasonable stable maximum oxygen

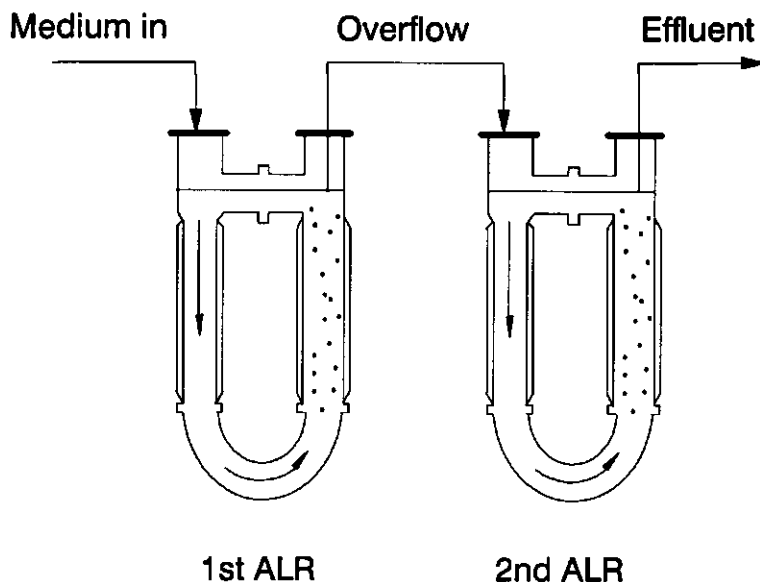


Figure 1. Scheme of the air-lift loop reactor (ALR) series used for the culture of immobilized *Nitrobacter agilis*.

consumption rates were observed, after a change had been made. Air, oxygen and nitrogen (for oxygen concentration control) were supplied via mass flow controllers to obtain a constant gas flow rate of $5.0 \text{ cm}^3 \cdot \text{s}^{-1}$ (superficial gas velocity = $0.18 \text{ cm} \cdot \text{s}^{-1}$). The oxygen concentration was maintained at $0.119 \pm 0.006 \text{ mol} \cdot \text{m}^{-3}$, and the temperature at $30.0 \pm 0.2 \text{ }^\circ\text{C}$. Medium was transported within 20 s from the first to the second vessel via a hose with a pump. The gel beads were kept in the reactors with sieve screens. The same medium as for the precultivation was used, but the pH was adjusted to 8.0 with $2 \text{ mol} \cdot \text{m}^{-3}$ KOH. The medium contained variable amounts of KNO_2 . A bead hold up of 20% (v/v) was used in both reactors. Steady-state concentrations were analysed five times, representing a total of 10 steady states (5 in the first and 5 in the second ALR) in the reactor series.

ANALYSIS

The NO_2^- and NO_3^- concentrations were measured daily with a Skalar autoanalyser, as described by Hunik *et al.* [1994]. Biomass activity was estimated

from the maximum oxygen consumption rate, as described by Wijffels *et al.* [1991]. For that, 100 beads and 4 cm³ fresh medium (pH 8.0) were transferred to a closed stirred vessel at 30 °C with an oxygen electrode in it. The oxygen consumption rate was measured in time after substrate (KNO₂) addition to a final concentration of 20 mol.m⁻³.

MODEL CALCULATIONS

Model estimates were made with the dynamic model validated by Hunik *et al.* [1994] because, in contrast to that used by Wijffels *et al.* [1991], this model incorporates the effects of both non-competitive substrate and product inhibition (see Appendix). The model described by Hunik *et al.* [1994] was for two microbial species co-immobilized in gel beads. For our purposes, only the part describing *N. agilis* growth was used. Input parameters were as in Hunik *et al.* [1994], except for the maximum biomass concentration. Here 11 kg.(m gel)⁻³ was used, which was determined experimentally by Wijffels *et al.* [1991]. This value was used, even though Hunik *et al.* [1994] observed lower maximum biomass concentrations for *N. agilis*, but this was for the case when co-immobilized with *N. europaea*. Further, the current experimental gel bead radius of 1.0 mm was used.

RESULTS AND DISCUSSION

SUBSTRATE AND PRODUCT INHIBITION

The immobilized *N. agilis* cells were cultured continuously for 134 days in a series of two ALRs. This is illustrated by the course of the maximum oxygen consumption rate given in Figure 2. Analogous to Wijffels *et al.* [1991], the maximum oxygen consumption rate was used as an estimate for the activity of the viable biomass. The first 70 days were intended to study product inhibition by applying high inlet substrate concentrations (up to 400 mol.m⁻³ of NO₂⁻). In this way, when substrate is almost completely converted into equimolar amounts of product, high product concentrations were expected. The first part of Figure 2 (day 1 - 70) is discussed separately below.

In a second period (day 70 - 134, Figure 2) changes in the dilution rate were

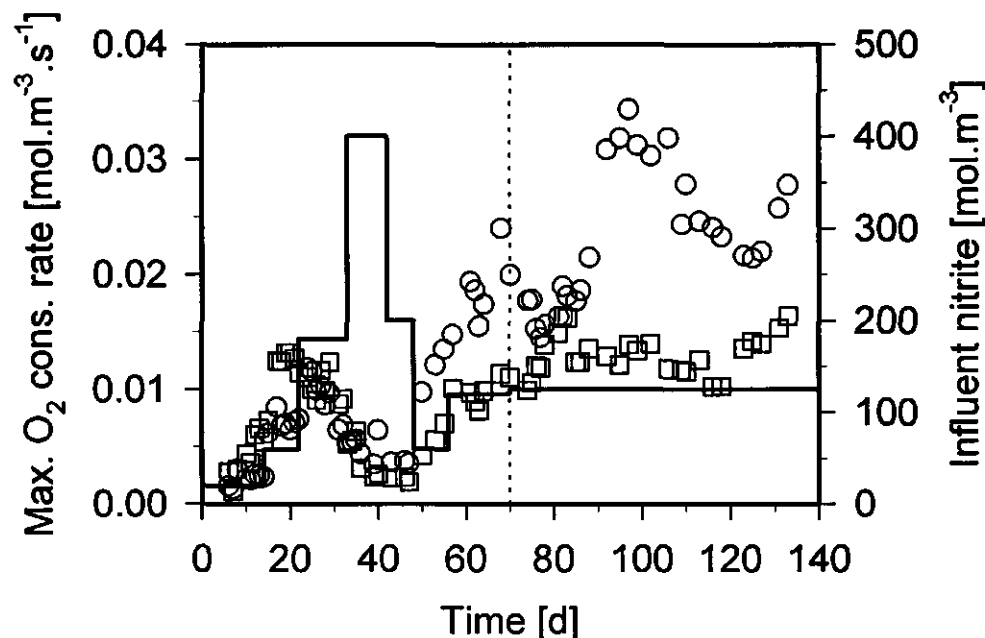


Figure 2. Overview of the biomass activity (expressed as maximum oxygen consumption rate) during 134 days of continuous culture in a bioreactor cascade. First reactor (\square), second reactor (\circ). Before day 70 (dashed line) the effects of high product concentrations were studied, and after that day the reactor series was operated at different dilution rates. Solid line: influent substrate (NO_2^-) concentration. Liquid residence times are given in the text.

made to compare the substrate conversion in a reactor series to that in a single vessel. In this period more moderate inlet substrate concentrations were used. This second period will be discussed in more detail in the next section.

From a preliminary continuous run for 60 days in the ALR train (results not shown), it was seen that biomass in both reactors remained active when the inlet substrate (NO_2^-) concentration was increased up to 200 mol.m^{-3} . Therefore, the feed substrate concentration was increased rapidly to this level in the current experiment. The reactor cascade was started at low, non-inhibitory inlet substrate (NO_2^-) concentrations to obtain high concentrations of immobilized biomass (day 1 - 22, Figure 2). A stepwise increase of the inlet substrate concentration from 20 to 60 mol.m^{-3} at day 14 roughly gave a doubling of the biomass activity in both reactors (Figure 2). Subsequently, the substrate concentration was further increased

stepwise, via 180 mol.m^{-3} (day 22), up to 400 mol.m^{-3} at day 33 to obtain high product concentrations, and thus facilitating observation of the effects of product inhibition. At first, with 180 mol.m^{-3} substrate in the inlet, an increase in the biomass activity in the second vessel was seen (days 24 and 25, Figure 2). However, later it was seen at this same inlet substrate concentration and a residence time of 6 h that the activity started to decrease somewhat in both reactors (day 23 - 33, Figure 2). For this situation it was estimated from the model that the steady-state substrate concentration would be about 60 mol.m^{-3} in the first reactor, i.e. almost 120 of the 180 mol.m^{-3} of substrate in the influent would have been converted into nitrate. Under these conditions, the effects of substrate inhibition were still assumed to be negligible. This assumption was made on the basis of the work of Hunik *et al.* [1993]. At pH 8.0, which was also applied in the current experiments, they found no substrate inhibition for freely suspended cells with substrate (NO_2^-) concentrations up to 100 mol.m^{-3} . Therefore, when assuming thus no substrate inhibition at pH 8.0, the results obtained in the first reactor until day 33 (Figure 2) could indicate that the decrease in biomass activity was caused by product inhibition. However, as conversion proceeds in the second vessel, even higher product concentrations were found in that reactor. Therefore, in the second ALR a lower activity than in the first was to be expected due to increased product inhibition. But adversely, the activities in both reactors were about the same (day 23 - 33, Figure 2). This low activity in the first ALR therefore indicates that, in contrast to what was found by Hunik *et al.* [1993] at pH 8.0, substrate inhibition has to be accounted for even below 100 mol.m^{-3} .

To study these effects further, the dilution rate was lowered to a residence time of 20 h and the inlet substrate concentration was further increased to 400 mol.m^{-3} to obtain high product concentrations (day 33 - 42, Figure 2). Now activity dropped even further, probably due to the increased substrate concentration which caused still more severe substrate inhibition. The circumstances with high product concentrations that were aimed at could thus not be attained in this way because the substrate conversion was too low. Then, high activity was regained by lowering the inlet substrate concentration to 125 mol.m^{-3} , and decreasing the residence time back to 6 h again (day 43 - 70, Figure 2).

NO_2^- CONVERSION IN A BIOREACTOR CASCADE

The second part of Figure 2 (day 70 - 134) shows the operation of the bioreactor cascade at different dilution rates and a constant inlet substrate concentration of 125 mol.m^{-3} . From day 81 on, steady states were analysed at different dilution rates in the reactor series with respect to specific rates of consumption and production. In this whole period biomass activity in the second ALR was higher than in the first (Figure 2). The biomass activity in both reactors varied with the changes in the dilution rate (day 70 - 134, Figure 2).

In Figure 3 the substrate concentrations in the influent and in both reactors are shown, together with the variations in the dilution rate. Also shown in this Figure 3 are estimates from a model that is discussed later. At residence times of 12 and 8 h all substrate is converted in the second vessel (day 81 - 89 and day

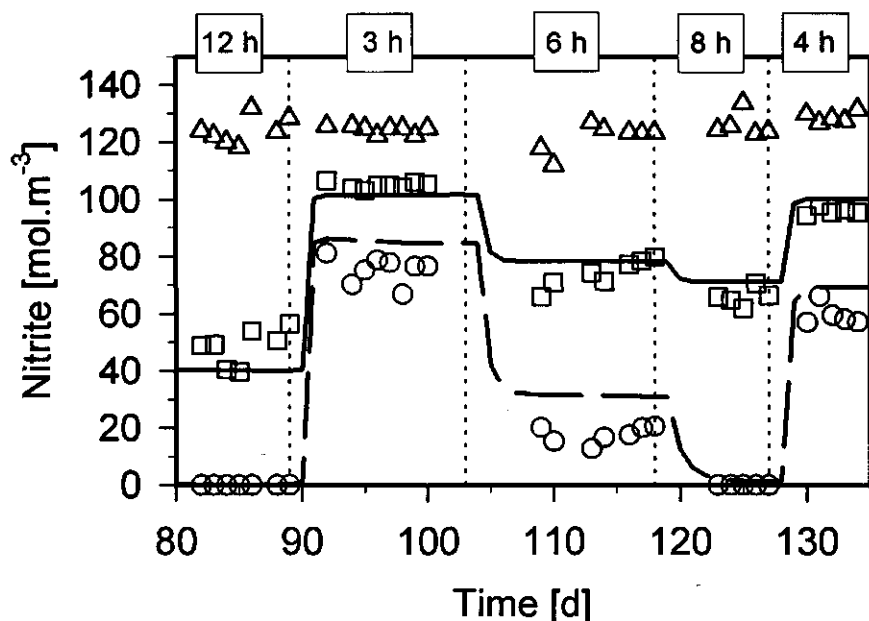


Figure 3. Substrate concentrations in the influent (Δ), the first reactor (\square), and the second reactor (\circ) at different dilution rates (periods separated by vertical dashed lines). Liquid residence times in the first reactor are given at the top of the graph. The residence time in the second reactor is the same because reactor volumes are equal. Model estimates for the steady-state substrate concentrations in the first reactor (solid line), and the second reactor (fat dashed line).

123 - 127, Figure 3), while at 3 h residence time about 70 of 125 mol.m⁻³ in the inlet is still unconverted in the second vessel (day 93 - 101, Figure 3). The steady-state concentrations at residence times of 6 and 4 h (day 109 - 118 and day 130 - 134, Figure 3) lie between those extremes. Substrate (NO₂⁻) was converted into equimolar amounts of product (NO₃⁻) with a maximum standard deviation of 6% in the steady-state concentrations. Here the combined effects of substrate and product inhibition were studied. The chosen residence times make a comparison between substrate conversion in the reactor series and that in a single vessel of the same overall volume possible.

For this comparison, substrate conversion in the ALR cascade and in a single vessel (i.e. the first ALR) was viewed at the same overall residence time. Conditions were thus chosen such that both reactor configurations could be compared at three different overall residence times (6, 8 and 12 h). For example, 3 h in the first ALR gave an overall residence time of 6 h in the reactor series (both ALRs were of equal volume), which was compared to the experiment where the residence time in the first vessel was 6 h (Figure 3). Substrate conversions at these three overall residence times, for both reactor configurations, are shown in Figure 4. As can be expected at higher overall residence times more substrate is converted (Figure 4). Figure 4 also shows that with higher overall residence times, substrate is converted increasingly better in the reactor series when compared to the single vessel. At the highest overall residence time (12 h), substrate conversion in the ALR series is statistically significant (no overlay of the 95%-confidence limits) better than that in one reactor (i.e. 86% conversion compared to 61%, Figure 4). For an explanation of this improvement no differentiation in the effects of substrate and product inhibition can be made because both effects occur simultaneously. Inspection of Eq. (1) (see Appendix) reveals that three terms can influence the growth rate, and thus substrate conversion. The affinity for the substrate (K_s) plays no role since $K_s = 0.36$ mol.m⁻³ [Hunik *et al.*, 1994], which value is low compared to the substrate concentrations. At pH 8.0 no substrate inhibition was to be expected [Hunik *et al.*, 1993], whereas the product inhibition term I_{NO_3} is 188 mol.m⁻³, which is in the same order of magnitude of the product concentrations observed. Hence, the improved substrate conversion at higher residence times is probably mainly caused by the effects of product inhibition.

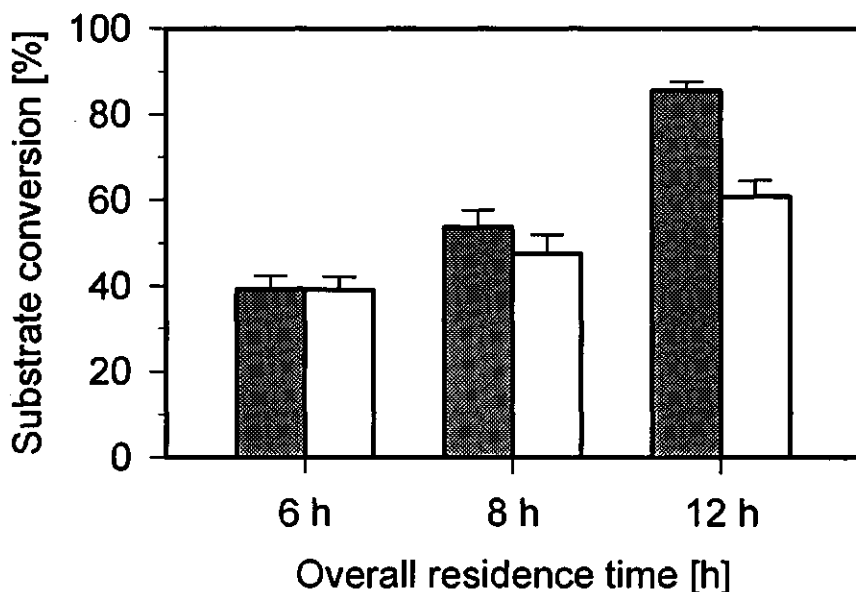


Figure 4. Substrate conversion in the reactor series (cross-hatched bars) compared to that in a single vessel (empty bars) at the same overall liquid residence time. Error bars give 95%-confidence intervals.

MODEL ESTIMATES

For product inhibition, Hunik *et al.* [1993] give an inhibition constant for freely suspended cells ($I_{NO_3} = 188 \text{ mol.m}^{-3}$). Substrate inhibition was reported to be pH-dependent, and no substrate inhibition was found at pH 8.0 [Hunik *et al.*, 1993]. For the model estimates to agree with our experiments in the first ALR, both inhibition constants had to be adapted by trial and error to more severe inhibition ($I_{NO_2} = 50 \text{ mol.m}^{-3}$ and $I_{NO_3} = 48 \text{ mol.m}^{-3}$). The model estimates thus obtained agree well with the trend in the experiments in both reactors in series (Figure 3). The adaptation of the substrate inhibition constant is in agreement with the observation here that not only product inhibition, but also substrate inhibition very likely plays a role.

CONCLUSIONS

In a bioreactor cascade improved nitrite conversion by immobilized *N. agilis* was shown, when compared to a single vessel with the same overall volume. With higher overall residence times, substrate is converted increasingly better in the reactor series when compared to a single vessel. This is probably mainly caused by product inhibition. At extreme conditions, not only product inhibition but also substrate inhibition played a role. Model estimates agreed well with the trends in the experiments. For that, the inhibition constants for both substrate and product had to be adapted to more severe inhibition than that reported in literature.

ACKNOWLEDGEMENTS

The authors thank M. Karadima for her contributions to the experiments and R.H. Wijffels for carefully reading the manuscript and for fruitful discussions. This work was partly supported by Applikon Dependable Instruments B.V., Schiedam, The Netherlands. The research was carried out in a PBTS project, nr. 89069, initiated by The Economic Affairs Ministry of The Netherlands.

APPENDIX

In the model calculations non-competitive substrate and product inhibition is described by:

$$\mu = \mu_{max} \cdot \frac{S}{(K_s + S) \cdot K_I} \quad (1)$$

where μ is the specific growth rate (s^{-1}), μ_{max} is the maximum specific growth rate (s^{-1}), S is the substrate concentration ($mol.m^{-3}$), K_s is the affinity constant for the

substrate (mol.m^{-3}), with:

$$K_I = \left(1 + \frac{S}{I_{NO_2}}\right) \cdot \left(1 + \frac{P}{I_{NO_3}}\right) \quad (2)$$

where P is the product concentration (mol.m^{-3}), I_{NO_2} is the nitrite (substrate) inhibition constant (mol.m^{-3}) and I_{NO_3} is the nitrate (product) inhibition constant (mol.m^{-3}).

REFERENCES

- [1] Barnes, D.; Bliss, P.J. 1983. Biological control of nitrogen in wastewater treatment. E.&F.N. Spon, London, UK.
- [2] Bakker, W.A.M.; Den Hertog, M.; Tramper, J.; De Gooijer, C.D. 1995. Oxygen transfer in a Multiple Air-lift Loop reactor. *Bioproc. Eng.* **12**: 167-172.
- [3] De Gooijer, C.D.; Bakker, W.A.M.; Beeftink, H.H.; Tramper, J. 1995. Bioreactors in series: an overview of design procedures and practical applications. *Enzyme Microb. Technol.* Accepted.
- [4] Hill, G.A.; Robinson, C.W. 1989. Minimum tank volumes for CFST bioreactors in series. *Can. J. Chem. Eng.*, **67**: 818-824.
- [5] Hunik, J.H.; Meijer, H.J.G.; Tramper, J. 1993. Kinetics of *Nitrobacter agilis* at extreme substrate, product and salt concentrations. *Appl. Microbiol. Biotechnol.* **40**: 442-448.
- [6] Hunik, J.H.; Bos, C.G.; Van den Hoogen, M.P.; De Gooijer, C.D.; Tramper, J. 1994. Co-immobilized *Nitrosomonas europaea* and *Nitrobacter agilis* cells: validation of a dynamic model for simultaneous substrate conversion and growth in κ -carrageenan gel beads. *Biotechnol. Bioeng.* **43**: 1153-1163.
- [7] Shimizu, K.; Matsubara, M. 1987. Product formation patterns and the performance improvement for multistage continuous stirred tank fermentors. *Chem. Eng. Comm.* **52**: 61-74.
- [8] Wijffels, R.H.; De Gooijer, C.D.; Kortekaas, S.; Tramper, J. 1991. Growth and substrate consumption of *Nitrobacter agilis* cells immobilized in carrageenan: Part 2. Model evaluation. *Biotechnol. Bioeng.* **38**: 232-240.

This chapter 8 has been submitted for publication as: Bakker, W.A.M.; Overdeest, P.E.M.; Beertink, H.H.; Tramper, J.; De Gooijer, C.D. 1995. Serial air-lift bioreactors for the approximation of aerated plug-flow.

CHAPTER 8

SERIAL AIR-LIFT BIOREACTORS FOR THE APPROXIMATION OF AERATED PLUG-FLOW

INTRODUCTION

Reactor series find their application not only in chemical engineering, but also in food and bioprocess engineering. Multistep processes are not an uncommon feature in biotechnology. The subsequent conversion steps can be executed separately in a series of vessels. An alternative use of the reactor cascade is to approximate plug-flow behaviour. Here, the design and applicability of a new type of serial bioreactor for aerated plug-flow approximations was studied. In general, with aeration, mixing is induced and thus a true plug-flow reactor can not be obtained with aeration. This lacuna is overcome with a new serial air-lift bioreactor.

SERIAL BIOREACTORS

Traditionally a bioreactor consists of a well-mixed single vessel, which is operated

continuous or batchwise [Van 't Riet and Tramper, 1991]. The single vessel is convenient with regard to *e.g.* measurement, control, sterilization, and medium supply. However, an interesting alternative is the cascade of continuous stirred-tank reactors. Namely, with a series of ideal mixers, a plug-flow reactor can be approximated. Such flexible reactor systems can be helpful tools for the optimization of bioprocesses with respect to different objectives like *e.g.* substrate conversion, product formation, or biomass production [Herbert, 1964; Bischoff, 1966; Pirt, 1975; Luyben and Tramper, 1982; Schügerl, 1987; Shimizu and Matsubara, 1987; Hill and Robinson, 1989; Malcata and Cameron, 1992; De Gooijer *et al.*, 1995].

Recently, a new type of serial bioreactor was introduced: the Multiple Air-lift Loop reactor (MAL: see description and figure in chapter 1) [Bakker *et al.*, 1993; 1994; 1995a]. In the patent application [De Gooijer, 1989], where the MAL was first described, many possible configurations for different biotechnological applications were suggested. Initially attention was focussed to one of the possible applications of the MAL, *i.e.* the possibility to approach an aerated plug-flow reactor. The first design considerations for a MAL were derived from a physical characterization [Bakker *et al.*, 1993; 1995a] and a study with several biological model systems [Bakker *et al.*, 1994; 1995b; 1995c]. From the knowledge thus obtained, new questions and interesting fields of further study were identified. These items are discussed in this article.

FLUID DYNAMICS AND DESIGN

With the outer compartments of the MAL, a new type of geometry for air-lift reactors with an internal loop was introduced. This new geometry was characterized with respect to hydrodynamics (*i.e.* liquid velocities and gas holdup), mixing and oxygen transfer. From these studies [Bakker *et al.*, 1993; 1995a], estimations of the hydrodynamic behaviour in a new design of a MAL can be made. Thus insight can be obtained in properties important to bioprocesses like mixing, mass and heat transfer, and shear forces, which are all affected by the fluid dynamics.

It was found that the outer compartments of the MAL behave like normal air-lifts with an internal loop. This means that, besides gas holdup in the riser, there was

also a considerable gas holdup in the downcomer. At all gas flow rates, and in different reactor configurations, the gas holdup in the downcomer was as high as 0.88 times that in the riser. Experiments in a conventional internal-loop air-lift reactor gave 0.86 for this ratio. This certainly is a substantial amount that is not negligible in internal-loop air-lift design. Others found a comparable value of 0.89 for this holdup ratio in conventional internal-loop air-lift reactors [Bello *et al.*, 1985; Chisti, 1989], although the latter author also reported 0.997, which is very high. Here, it should be noted that an exception to the constant holdup ratio exists. At sufficiently low gas flow rates, the induced liquid circulation is too low to drag gas into the downcomer [Chisti *et al.*, 1995]. This situation, with no gas holdup in the downcomer, may cause the gentle hydrodynamic environment needed for large scale animal cell culture in air-lift bioreactors [Ganzeveld *et al.*, 1995].

The hydrodynamics were described by adaptation of an existing model for air-lift reactors with an external loop [Verlaan *et al.*, 1986]. The only difference was that gas holdup in the downcomer was accounted for, which has a large influence on the hydrodynamic behaviour. Good agreement between the measurements and the model estimates was found [Bakker *et al.*, 1993]. Mixing and oxygen transfer in the new reactor configuration were comparable to that in conventional air-lifts with an internal loop. Further, oxygen transfer was measured by means of a steady-state method and a dynamic method. Both methods gave comparable results [Bakker *et al.*, 1995].

At high gas flow rates gas bubbles circulated through the downcomer back to the riser. Interestingly, at low gas flow rates, stagnant gas bubbles were observed in the downcomer. The bubbles may be seen as obstacles that obstruct the fluid flow in the downcomer [Bakker *et al.*, 1993; Chisti and Moo-Young, 1988; Ishii and Zuber, 1979; Patel *et al.*, 1986; Young *et al.*, 1991]. As such, they can influence the hydrodynamics to a large extent. With the general drag-force relations for bubble, droplet and particle flow, developed by Ishii and Zuber [1979], a mechanistic explanation for the interfacial drag effects between gas bubbles and the surrounding liquid in the riser and in the downcomer can be given. Young *et al.* [1991] adopted the Ishii and Zuber relations successfully for the estimation of the frictional losses in the riser of their air-lift loop reactor with an external loop.

Gas holdup in the downcomer of air-lifts with an internal loop had not much attention until now, and further study can certainly contribute to the knowledge of the

fluid dynamics in air-lift reactors. Recently, Chisti *et al.* [1995] addressed this subject. They described the relationship between the gas holdups in the riser and downcomer of internal-loop air-lift reactors based on mechanistic principles. However, the frictional loss coefficient in their model was estimated from a, non mechanistic, empirical correlation, which was reported to be uncertain [Chisti *et al.*, 1995], and shown to be invalid for general application [Bakker *et al.*, 1993].

BIOLOGICAL MODELS AND CASCADE OPTIMIZATION

Reactor cascades, like the MAL, can be used to approximate plug-flow behaviour. In that case one reaction step is applied repeatedly in each compartment of a serial bioreactor. This may be done when optimal bioreactor design is the goal. The optimal

Box 1. General optimization scheme for a serial bioreactor.

In a reactor series the subsequent vessels can be chosen of a different volume. The best solution of all possible configurations of a reactor series was found numerically by searching the optimum, according to the chosen optimization criteria. For that, the reactor configurations that were compared were all assumed to be of the same overall volume ($V = V_1 + V_2$; for a single vessel and a series of two reactors, respectively, see Figure 1). Then the range of possible feed rates F was determined from the kinetic expressions for growth in the same way as described by Pirt [1975], which is from zero until wash-out of the cells occurred. This is equivalent to the whole range of possible overall dilution rates $D_{ov} = 1/\Sigma_{n=1}^n (1/D_n)$, with $D_n = F/V_n$.

This range of dilution rates is then divided in many (about 100 - 200) small steps. At every step in this range of overall dilution rates the set of balance equations, for cells, substrate and product (with the appropriate kinetic expressions), is solved for the unknown substrate concentration by a zero-point finding bisection routine (RTBIS from Press *et al.* [1989]) for every vessel in the series. To find the optimum configuration of a serial reactor, the whole range of possible volume ratios for the reactors in the cascade is evaluated now at this same overall dilution rate (see Figure 1), also in small steps. According to the optimization criteria chosen, the optimal configuration is stored, and subsequently the next step in the overall dilution rate can be evaluated in the same way. Analogous, this procedure can be extended to more than two reactors in the series.

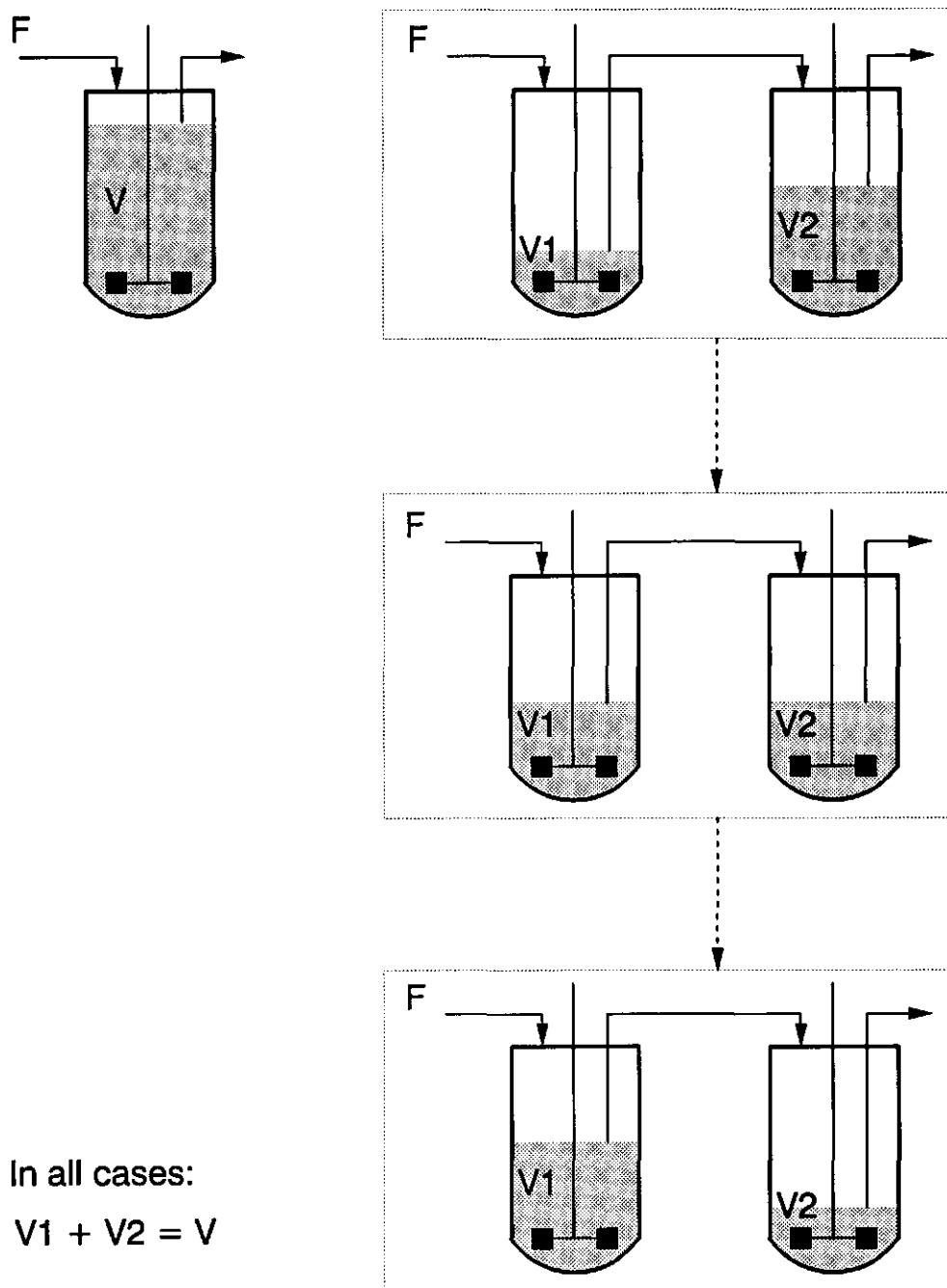


Figure 1. General optimization scheme for serial bioreactors.

design is defined as the minimal total residence time needed to reach a given goal. This goal can, for example, be a given substrate conversion [De Gooijer *et al.* 1995]. For this application of reactor cascades the design and use of the MAL was studied. For that several biological model systems were used to compare a reactor series with a single vessel of the same overall volume. These model systems included immobilized invertase for sucrose conversion [Bakker *et al.*, 1994] and immobilized growing cells

Box 2. Bioethanol fermentation.

In this example a constant overall reaction stoichiometry is assumed, thus substrate conversion is described by a single kinetic equation. Under these conditions, substrate conversion is equivalent to cell growth or product formation. Therefore, in the following attention can be focussed to the product production instead of substrate conversion.

This example (without taking maintenance into account) is adopted from the study of Shimizu and Matsubara [1987]. They showed that reactor series can be favourable for bioethanol production by yeasts. Here, the Monod growth kinetics is extended with absolute inhibition by the product ($1-P/P_m$), where P_m is the maximum attainable product concentration.

The overall volumetric productivity (PD = product concentration $P \times$ overall dilution rate D) was calculated at all possible dilution rates, until wash-out occurred. This overall volumetric productivity was plotted as a function of the product concentration (see Figure 2). At the higher dilution rates, product concentrations were low, while product concentrations became high at the lowest dilution rates. At about 45 kg ethanol per m^3 a maximum productivity is seen for a single vessel (Fig. 2). Shimizu and Matsubara [1987], saw that this optimum can not be improved by using more than one vessel. But, they also observed that, at higher product concentrations, a relatively improved volumetric productivity is possible by using more than one reactor. For example, at a product concentration of about 75 $kg \cdot m^{-3}$, productivity is almost 1.5 times higher (going from 0.7 to $1.1 \times 10^{-3} kg \cdot m^{-3} \cdot s^{-1}$) when using an optimized series of two reactors instead of a single one (Fig. 2). Optimization of the reactor series was done as described in the text of box 1.

Hill and Robinson [1989] argue that, with a reactor series, absolute improvement of the volumetric productivity is possible (*i.e.* above the maximum in Fig. 2). But, from Fig. 2 it is seen that, for the kinetic expressions used here, only a relative improvement can be obtained when an additional criterium, like a higher product concentration, is formulated. Therefore, to obtain relative improvements, a combination of at least two optimization criteria has to be chosen [Shimizu and Matsubara, 1987].

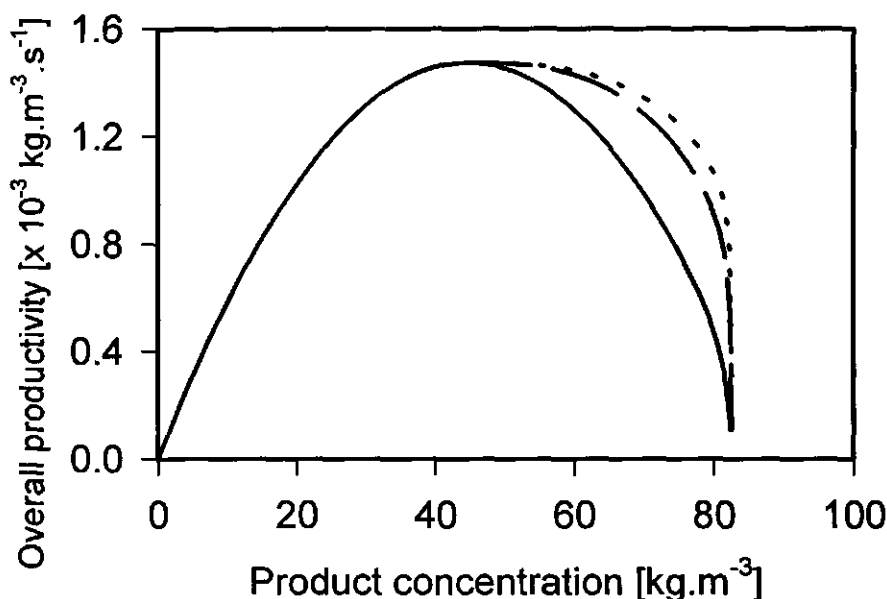


Figure 2. Volumetric productivity of an ethanol fermentation versus product concentration. Solid line = 1, dashed line = 2, dotted line = 3 reactors in series, respectively. Parameter values were as used by Shimizu and Matsubara [1987], with $K_s = 1.6 \text{ kg.m}^{-3}$, $\mu_m = 6.7 \times 10^{-5} \text{ s}^{-1}$, $Y_{xs} = 0.06$, $Y_{xp} = 0.16$, $P_m = 90 \text{ kg.m}^{-3}$, and $S_0 = 220 \text{ kg.m}^{-3}$. Note that at a product concentration of 82.5 kg.m^{-3} all substrate is converted.

(nitrifying bacteria for nitrite conversion) [Bakker *et al.*, 1995b]. In both cases, the advantage of using a reactor cascade over a single vessel was shown by an improved substrate conversion. Sucrose conversion in a three compartment MAL improved to 83% compared to 73% in the single vessel. Further, nitrite conversion in a cascade of two air-lift reactors was 86% compared to 61% in the single vessel.

Until now, the volumes of the reactors in the series were arbitrarily chosen to be the same, which is a sub-optimal design. The differences in substrate conversion between the series and the single vessel could have been even bigger when the reactor cascade had been designed optimally. Such optimal designs have been discussed extensively in the literature [for a review see: De Gooijer *et al.*, 1995], but the optimization has only once been carried out in practice [De Gooijer *et al.*, 1989]. A possible explanation for this omission for other applications can be that a detailed kinetic model should be available, which is almost always more complicated than the situations for which convenient mathematical expressions can be found, such as

described by De Gooijer *et al.* [1995]. This practical evaluation is certainly a challenge for future research with the MAL, or with reactor cascades in general, with regard to plug-flow approximations. To overcome the forementioned mathematic complexity, a general procedure for choosing the optimal bioreactor-cascade configuration for any application is outlined here (see text box 1).

Before such experiments are done, however, one should realize that advantages can only be found under certain conditions, *e.g.* beyond a given substrate conversion [De Gooijer *et al.*, 1995]. Further, sometimes the differences that can be found theoretically are too small to show a significant difference between the reactor series and a single vessel in practice. This was observed for monoclonal antibody production by hybridomas [Bakker *et al.*, 1995c], where the accuracy of the measurements was too low to show statistically significant differences between the cascade and a single vessel. For cells in suspension, like hybridomas, interesting complications arise when a more detailed description of the kinetics is used for bioreactor cascade optimization. Also here lies an opportunity for future research, which is now discussed in more detail.

CELLS IN SUSPENSION

Recently the design rules and applications of bioreactor series were reviewed [De Gooijer *et al.*, 1995]. In that paper, among others, design procedures for autocatalytic processes (cells in suspension) with a constant overall reaction stoichiometry were discussed extensively. In this context 'constant overall reaction stoichiometry' means that a single reaction is involved which can be described by a single kinetic equation. However, for more complex situations, where for example the maintenance requirement of the cells, or cell death has to be accounted for, no design rules exist [De Gooijer *et al.*, 1995]. Until now, for the sake of simplicity, this second situation was neglected in several theoretical studies [Bischoff, 1966; Schügerl, 1987; Hill and Robinson, 1989; De Gooijer *et al.*, 1995]. In reality this simplification can lead to sub-optimal design of bioreactor series. This was illustrated first by Shimizu and Matsubara [1987], who found that the maximum product concentration can be improved when the maintenance requirement of the cells is accounted for in optimal

Box 3. Monoclonal antibody production by hybridomas.

From continuous cultures it was seen that viable hybridoma cells not only grow to compensate for dilution, but also for death and lysis [Bakker *et al.*, 1995c]. Hence, the net specific growth rate μ_{net} can be described by the rates of growth μ_{true} , death μ_d and lysis μ_l : $\mu_{net} = \mu_{true} - \mu_d - \mu_l$. Kinetic expressions used in this equation were adaptations of the Monod growth kinetics. Further, the maintenance requirements for substrate were not negligible. Thus a complex kinetic expression described the hybridoma growth, from which the possible advantage of using a reactor cascade for MAb production can not be seen directly.

Model estimates for a single vessel and an optimized series are given in Figure 3. In this Fig. 3 the possibility of a relative improvement of the overall MAb productivity at higher MAb concentrations can be observed (e.g. about 1.9 times higher overall productivity at $C_{MAb} = 83 \text{ g.m}^{-3}$). Also in this Fig. 3 it should be noted that in contrast to the bioethanol production example, an absolute improvement of the maximum in the overall MAb productivity can be seen when using more than one optimally sized vessels in series. Although only a slight improvement is seen in this example, differences can become more pronounced when other kinetic expressions, or other parameter values, are used. The improvement seen in Fig. 3 is possible because the product formation is not directly related to the substrate converted, but to the amount of biomass produced. Therefore, increased biomass concentrations along the reactor series can enhance the overall productivity.

serial bioreactor design. They also showed, like Herbert [1964], that the maximum attainable overall volumetric product productivity ($\text{kg.m}^{-3}.\text{s}^{-1}$) is realizable in a single vessel (see text box 2). Further, they found that the relation between product formation and cell growth can influence this maximum in the attainable overall product productivity when using an optimally designed series of bioreactors (see text box 3). However, no general method for choosing the optimal bioreactor cascade was given.

Finally, for the hybridomas, it was seen that serial bioreactors can not only be used for bioprocess optimization, but also as a powerful research tool for kinetic studies. In the second vessel in a series stable conditions can be obtained that can hardly be reached in a single vessel. This means, for example, that not only growth, but also death (apoptosis and necrosis in case of hybridomas) can be studied under stable conditions in a bioreactor cascade. Further, experiments can be done at very low growth rates, which eliminates the need for extrapolations to low growth rates when determining kinetic parameters like yield factors and maintenance coefficients

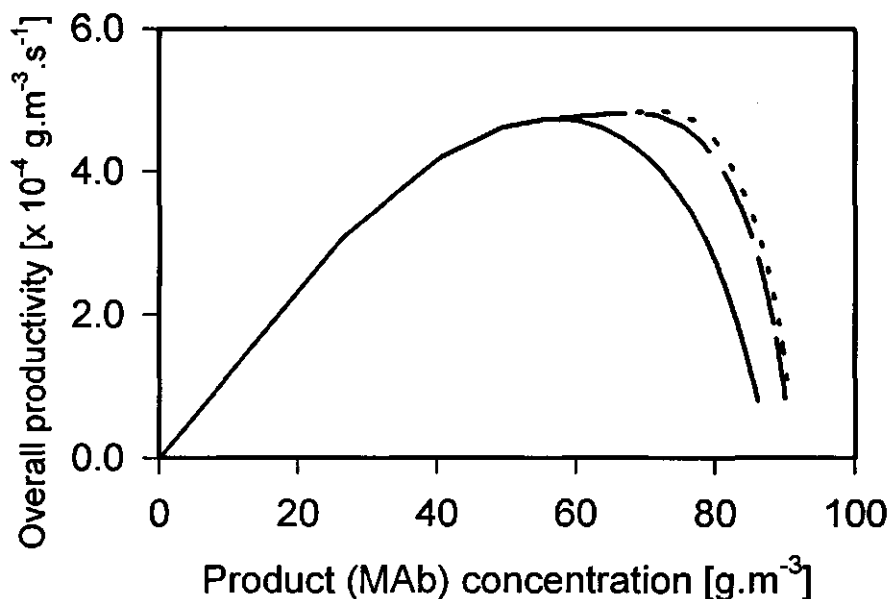


Figure 3. Model estimates for the overall MAb productivity by hybridomas as a function of the product concentration for one (solid line), two (dashed line) and three (dotted line) optimized reactors in series. Parameter values were as used by Bakker *et al.* [1995c].

[Bakker *et al.*, 1995c]. Of course this is also applicable to other cells or micro-organisms.

CONCLUSIONS

Several interesting topics for future research with regard to serial air-lift bioreactors, that can be used for the approximation of an aerated plug-flow reactor, were identified. For the design of air-lifts with an internal loop gas holdup in the downcomer can be studied for a more detailed description of the fluid-dynamics. The practical evaluation of optimal serial bioractor designs for plug-flow approximations is a challenge for future research. For cells in suspension, like hybridomas, interesting complications arise when a more detailed description of the kinetics is used for bioreactor cascade optimization.

REFERENCES

- [1] Bakker, W.A.M.; Van Can, H.J.L.; Tramper, J.; De Gooijer, C.D. 1993. Hydrodynamics and mixing in a multiple air-lift loop reactor. *Biotechnol. Bioeng.* **42**: 994-1001.
- [2] Bakker, W.A.M.; Knitel, J.T.; Tramper, J.; De Gooijer, C.D. 1994. Sucrose conversion by immobilized invertase in a multiple air-lift loop bioreactor. *Biotechnol. Prog.* **10**: 277-283.
- [3] Bakker, W.A.M.; Den Hertog, M.; Tramper, J.; De Gooijer, C.D. 1995a. Oxygen transfer in a multiple air-lift loop reactor. *Bioproc. Eng.* **12**: 167-172.
- [4] Bakker, W.A.M.; Kers, P.; Beftink, H.H.; Tramper, J.; De Gooijer, C.D. 1995b. Nitrification by immobilized *Nitrobacter Agilis* cells in an air-lift loop bioreactor cascade: effects of combined substrate and product inhibition. Submitted for publication.
- [5] Bakker, W.A.M.; Schäfer, T.; Beftink, H.H.; Tramper, J.; De Gooijer, C.D. 1995c. Hybridomas in a bioreactor cascade: modeling and determination of growth and death kinetics. Submitted for publication.
- [6] Bello, R.A.; Robinson, C.W.; Moo-Young, M. 1985. Gas holdup and overall volumetric oxygen transfer coefficient in airlift contactors. *Biotechnol. Bioeng.* **27**: 369-381.
- [7] Chisti, M.Y.; Moo-Young, M. 1988. Gas holdup in pneumatic reactors. *Chem. Eng. J.* **38**: 149-152.
- [8] Chisti, M.Y. 1989. Airlift bioreactors. Elsevier, London, UK.
- [9] Chisti, Y.; Wenge, F.; Moo-Young, M. 1995. Relationship between riser and downcomer gas hold-up in internal-loop airlift reactors without gas-liquid separators. *Chem. Eng. J.* **57**: B7-B13.
- [10] Bischoff, K.B. 1966. Optimal continuous fermentation reactor design. *Can. J. Chem. Eng.* **50**: 281-284.
- [11] De Gooijer, C.D. 1989. Werkwijze voor het uitvoeren van biotechnologische processen in meer-traps loopreactoren. Dutch patent application. No. 89.01649. (In Dutch).
- [12] De Gooijer, C.D.; Hens, H.J.H.; Tramper, J. 1989. Optimum design for a series of continuous stirred tank reactors containing immobilized biocatalyst beads obeying intrinsic Michaelis-Menten kinetics. *Bioproc. Eng.* **4**: 153-158.
- [13] De Gooijer, C.D.; Bakker, W.A.M.; Beftink, H.H.; Tramper, J. 1995. Bioreactors

- in series: an overview of design procedures and practical applications. *Enzyme Microb. Technol.* Accepted for publication.
- [14] Ganzeveld, K.J.; Chisti, Y.; Moo-Young, M. 1995. Hydrodynamic behaviour of animal cell microcarrier suspensions in split-cylinder airlift bioreactors. *Bioproc. Eng.* **12**: 239-247.
- [15] Herbert, D. 1964. Multi-stage continuous culture. In: *Proc. 2nd symp. contin. cult. microorganisms* (Malek, I., et al., Eds.). Czechoslovak Academy of Sciences, Prague, CSSR, 23-44.
- [16] Hill, G.A.; Robinson, C.W. 1989. Minimum tank volumes for CFST bioreactors in series. *Can. J. Chem. Eng.* **67**: 818-824.
- [17] Ishii, M.; Zuber, N. 1979. Drag coefficient and relative velocity in bubbly, droplet or particulate flows. *AIChE. J.* **25**: 843-855.
- [18] Luyben, K.Ch.A.M.; Tramper, J. 1982. Optimal design for continuous stirred tank reactors in series using Michaelis-Menten kinetics. *Biotechnol. Bioeng.* **24**: 1217-1220.
- [19] Malcata, F.X.; Cameron, D.C. 1992. Optimal design of a series of CSTR's performing reversible reactions catalyzed by soluble enzymes: a theoretical study. *Biocatalysis* **5**: 233-248.
- [20] Patel, S.A.; Glasgow, L.A.; Erickson, L.E.; Lee, C.H. 1986. Characterization of the downflow section of an airlift column using bubble size distribution measurements. *Chem. Eng. Comm.* **44**: 1-20.
- [21] Pirt, S.J. 1975. Principles of microbe and cell cultivation. Blackwell, Oxford, UK.
- [22] Press, W.H.; Flannery, B.P.; Teukolsky, S.A.; Vetterling, W.A. 1989. Numerical recipes in Pascal. Cambridge university press, Cambridge, U.K.
- [23] Schügerl, K. 1987. Bioreaction engineering: reactions involving microorganisms and cells. John Wiley & Sons, Chichester, U.K, p. 68-73.
- [24] Shimizu, K.; Matsubara, M. 1987. Product formation patterns and the performance improvement for multistage continuous stirred tank fermentors. *Chem. Eng. Comm.* **52**: 61-74.
- [25] Van 't Riet, K.; Tramper, J. 1991. Basic bioreactor design. M. Dekker, New York.
- [26] Verlaan, P.; Tramper, J.; Van 't Riet, K.; Luyben, K.Ch.A.M. 1986. A hydrodynamic model for an airlift-loop bioreactor with external loop. *Chem. Eng. J.* **33**: B43-B53.
- [27] Young, M.A.; Carbonell, R.G.; Ollis, D.F. 1991. Airlift bioreactors: analysis of local two-phase hydrodynamics. *AIChE. J.* **37**: 403-428.

SUMMARY

A new type of bioreactor is introduced: the Multiple Air-lift Loop reactor (MAL). The MAL consists of a series of air-lift loop reactors within one vessel. The central MAL compartment is a conventional internal loop air-lift reactor with aeration in the annulus. Subsequent compartments in the MAL are concentric. The annular-shaped compartments have a circular baffle which splits them into a riser and a downcomer section. With the outer compartments of the MAL, a new type of geometry for air-lift reactors with an internal loop is introduced. This new geometry was characterized with respect to hydrodynamics (liquid velocities and gas holdup), mixing and oxygen transfer; all these properties are important in the design of bioreactors like the MAL. The formulation of design rules for a MAL, and bioreactor series in general, was also the goal of this research.

The outer compartments of the MAL behave like normal air-lifts with an internal loop. This means that, besides gas holdup in the riser, there was also a considerable gas holdup in the downcomer. At all gas flow rates, and in different reactor configurations, the gas holdup in the downcomer was 0.88 times that in the riser. Only at very low gas flow rates no gas holdup is found in the downcomer. The hydrodynamics were described by adaptation of an existing model for air-lift reactors with an external loop. The only difference was that gas holdup in the downcomer was accounted for, which has a large influence on the hydrodynamic behaviour, and should always be considered in internal-loop air-lift reactor design. Good agreement between the measurements and the model estimates was found. Mixing and oxygen transfer in the new reactor configuration were comparable to that in conventional air-lifts with an internal loop. Further, oxygen transfer was measured by means of a steady-state method and a dynamic method. Both methods gave comparable results.

Reactor cascades can be used to approximate plug-flow behaviour. Here one reaction step is applied repeatedly in each compartment of a serial bioreactor. This may be done when optimal bioreactor design is the goal. The optimal design is defined as the minimal total residence time needed to reach a given goal. This goal can, for example, be a given substrate conversion. For this application of reactor cascades the design and use of the MAL was studied. For that several biological model systems were used to compare the reactor series with a single vessel of the same overall volume. These model systems included immobilized invertase for sucrose conversion and immobilized growing cells (nitrifying bacteria for nitrite conversion). With the

immobilized invertase it was shown in practice that a three-compartment MAL gives an improved substrate conversion when compared to a single vessel of the same overall volume. This could be described with a previously developed model. Also for the immobilized nitrifying bacteria improved substrate conversion was shown in the comparison of a reactor series to a single vessel.

Further, freely-suspended hybridoma cells were used for monoclonal-antibody production. The hybridomas were grown in a series of two continuously operated stirred vessels, instead of using a MAL, for practical reasons. Here, it was shown that bioreactor series can also be useful research tools for kinetic studies. In the second vessel in a series stable conditions can be obtained that can hardly be reached in a single vessel. This means, for example, that not only growth, but also death can be studied under stable conditions in a bioreactor cascade. Further, kinetic parameters could be derived without the necessity for extrapolation to lower growth rates. A model was derived that describes hybridoma growth and their monoclonal-antibody production on the basis of glutamine consumption. The model can be used for further bioreactor-cascade optimization.

Vessels in a series can be of equal volume, but very often unequal reactor volumes can be more advantageous when compared to a single vessel. Therefore, choosing the appropriate reactor volumes is an important design step, which is discussed for different applications. Finally, a general procedure for choosing the optimal bioreactor-cascade configuration for any application is given.

SAMENVATTING

In dit proefschrift wordt een nieuw type bioreactor geïntroduceerd: de Multiple Air-lift Loop reactor (MAL). De MAL bestaat uit een serieschakeling van air-lift loop reactoren in een vat. Het centrale MAL compartiment is een conventionele air-lift reactor met een interne lus (= 'loop'), welke in de binnenbuis wordt belucht. De volgende compartimenten in de MAL zijn concentrisch daaromheen geplaatst. In de schilvormige compartimenten bevindt zich een cirkelvormig keerschot waardoor ze in een stijgbuis en een daalbus worden verdeeld. Met de buitenste compartimenten van de MAL wordt een nieuw type geometrie voor air-lift reactoren met een interne lus geïntroduceerd. Deze nieuwe geometrie werd gekarakteriseerd met betrekking tot de hydrodynamica (vloeistofstroomsnelheid en gas holdup), menging en zuurstof overdracht; al deze grootheden zijn belangrijk voor het ontwerpen van een bioreactor zoals de MAL. Het opstellen van ontwerpregels voor een MAL, en serieschakelingen van bioreactoren in het algemeen, was tevens het doel van dit onderzoek.

De buitenste compartimenten van de MAL gedragen zich als normale air-lift reactoren met een interne lus. Dit betekent dat, naast gas holdup in de stijgbuis, ook een aanzienlijke hoeveelheid gas holdup in de daalbus werd waargenomen. Bij alle gas debieten, en in verschillende reactor configuraties, was de gas holdup in de daalbus 0.88 maal de hoeveelheid in de stijgbuis. Alleen bij zeer lage gasdebieten wordt geen gas holdup in de downcomer gevonden. De hydrodynamica werd beschreven met een aangepaste versie van een bestaand model voor air-lift reactoren met een externe lus. Het enige verschil was dat de gas holdup in de daalbus werd meegenomen in de berekeningen. Deze gas holdup in de daalbus heeft een grote invloed op de hydrodynamica, en behoort altijd te worden meegenomen in het ontwerp van air-lift reactoren met een interne lus. De overeenstemming tussen de metingen en de schattingen met het model was goed. Ook de menging en zuurstofoverdracht in de nieuwe reactor configuratie waren vergelijkbaar met die in conventionele air-lift reactoren met een interne lus. Verder werd de zuurstofoverdracht gemeten door middel van een stationaire en een dynamische methode. Beide methodes leverden vergelijkbare resultaten.

Serieschakelingen van reactoren kunnen worden gebruikt om propstroomgedrag te benaderen. Hierbij wordt een reactiestap herhaaldelijk uitgevoerd in elk compartiment van een serieschakeling van bioreactoren. Dit kan worden gedaan als optimaal ontwerp van de bioreactor het doel is. Het optimale ontwerp is gedefinieerd

als de minimaal benodigde verblijftijd om een bepaald doel te bereiken. Dit doel kan bijvoorbeeld een bepaalde graad van substraat omzetting zijn. Voor deze toepassing van serieschakelingen van reactoren werden ontwerp en gebruik van de MAL bestudeerd. Daartoe werden verschillende biologische modelsystemen gebruikt om de serieschakeling van reactoren te vergelijken met een enkelvoudig vat. De serieschakeling en het enkelvoudige vat hadden in deze vergelijking beide eenzelfde totaalvolume. De modelsystemen waren geïmmobiliseerde invertase voor het omzetten van sucrose en geïmmobiliseerde groeiende cellen (nitrificerende bacteriën voor de omzetting van nitriet). Met de geïmmobiliseerde invertase werd in de praktijk aangetoond dat een MAL met drie compartimenten een verbeterde substraat conversie gaf ten opzichte van een enkelvoudig vat met eenzelfde totaalvolume. Dit werd beschreven met een model dat eerder was ontwikkeld. Ook voor de geïmmobiliseerde nitrificerende bacteriën werd een verbeterde substraat conversie gevonden in de vergelijking tussen een serieschakeling van reactoren en een enkelvoudig vat.

Verder werden vrije, gesuspendeerde, hybridoma cellen gebruikt voor de productie van monoklonale antilichamen. De hybridoma's werden, om praktische redenen, niet in de MAL gekweekt maar in een serieschakeling van geroerde vaten, die continu werden bedreven. Hier werd aangetoond dat serieschakelingen van bioreactoren bruikbare gereedschappen zijn voor onderzoek naar kinetiek. In het tweede vat in een serieschakeling kunnen stabiele omstandigheden worden verkregen die nauwelijks in een enkelvoudig vat kunnen worden bereikt. Hierdoor kan bijvoorbeeld niet alleen groei, maar ook sterfte onder stabiele omstandigheden worden onderzocht. Verder konden kinetische parameters worden afgeleid zonder dat het nodig was te extrapoleren naar lagere groeisnelheden. Een model werd opgesteld dat de hybridoma groei en hun monoklonale antilichamen productie beschrijft op basis van glutamine verbruik. Het model kan worden gebruikt voor verdere optimalisatie van de serieschakeling van bioreactoren.

In serie geschakelde vaten kunnen een gelijk volume hebben, maar vaak zijn ongelijke volumes voordeliger in de vergelijking met een enkelvoudig vat. Daarom is het kiezen van de geschikte reactor volumes een belangrijke ontwerpstep. Dit werd besproken voor verschillende toepassingen. Afsluitend is een algemene methode gegeven waarmee de optimale serieschakeling van reactoren voor een willekeurige toepassing kan worden gekozen.

CURRICULUM VITAE

Wilfridus Adrianus Maria Bakker werd op 26 maart 1965 geboren te Alkemade, in het dorp Oud-Ade. In 1982 behaalde hij het HAVO diploma aan het Bonaventura college te Leiden. Vervolgens werd, door dezelfde scholengemeenschap, in 1984 het VWO diploma aan hem uitgereikt.

In 1984 begon hij met de studie Levensmiddelentechnologie aan de Landbouw-universiteit. Afstudeeronderzoeken werden gedaan in de Proceskunde en de Informatica. Stages in dezelfde richtingen werden uitgevoerd bij Bio-Intermediair B.V. in Groningen, en bij AKZO Systems B.V. in Velp en Ede. Op 27 augustus 1990 werd het ingenieursdiploma behaald.

Van september 1990 tot en met augustus 1994 was de auteur werkzaam als Assistent In Opleiding bij de Vakgroep Levensmiddelentechnologie, Sectie Proceskunde aan de Landbouwuniversiteit Wageningen. De resultaten van het daar uitgevoerde onderzoek, op het gebied van de Bioprocestechnologie, staan beschreven in dit proefschrift. Van november 1994 tot en met januari 1995 werkte hij, op dezelfde plaats, als toegevoegd onderzoeker voor het verzorgen van het werkcollege Procesontwerpen.

Vanaf september 1995 is de auteur werkzaam aan de Universiteit Utrecht als toegevoegd onderzoeker bij de Vakgroep Voedingsmiddelen van Dierlijke Oorsprong, Sectie Technologie, van de Faculteit Diergeneeskunde.

BIBLIOGRAPHY

- [1] Van der Pol, L.; Bakker, W.A.M.; Tramper, J. 1992. Effect of low serum concentrations (0% - 2.5%) on growth, production, and shear sensitivity of hybridoma cells. *Biotechnol. Bioeng.* **40**: 179-182.
- [2] Bakker, W.A.M.; Tramper, J.; De Gooijer, C.D. 1993a. Hydrodynamics, mixing and oxygen transfer in a multiple air-lift loop reactor. In: *3rd Int. Conf. on Bioreactor and Bioprocess Fluid Dynamics* (Nienow, A.W., Ed.), Mechanical Eng. Publ., London, UK, 49-60.
- [3] Bakker, W.A.M.; Van Can, H.J.L.; Tramper, J.; De Gooijer, C.D. 1993b. Hydrodynamics and mixing in a multiple air-lift loop reactor. *Biotechnol. Bioeng.* **42**: 994-1001.
- [4] Bakker, W.A.M.; Beftink, H.H.; Tramper, J.; De Gooijer, C.D. 1994a. Hybridomas in a bioreactor cascade for kinetic parameter determination. *Cytotechnol.* **14**: Suppl. 1: Proceedings of the ESACT/JAACT Meeting 1994, Veldhoven, The Netherlands.
- [5] Bakker, W.A.M.; Knitel, J.T.; Tramper, J.; De Gooijer, C.D. 1994b. Sucrose conversion by immobilized invertase in a multiple air-lift loop bioreactor. *Biotechnol. Prog.* **10**: 277-283.
- [6] De Gooijer, C.D.; Bakker, W.A.M.; Beftink, H.H.; Tramper, J. 1995. Bioreactors in series: an overview of design procedures and practical applications. *Enzyme Microb. Technol.* Accepted for publication.
- [7] Bakker, W.A.M.; Den Hertog, M.; Tramper, J.; De Gooijer, C.D. 1995a. Oxygen transfer in a multiple air-lift loop reactor. *Bioproc. Eng.* **12**: 167-172.
- [8] Bakker, W.A.M.; Kers, P.; Beftink, H.H.; Tramper, J.; De Gooijer, C.D. 1995b. Nitrification by immobilized *Nitrobacter Agilis* cells in an air-lift loop bioreactor cascade: effects of combined substrate and product inhibition. Submitted for publication.
- [9] Bakker, W.A.M., Overvest, P.E.M., Beftink, H.H., Tramper, J., De Gooijer, C.D. 1995c. Serial air-lift bioreactors for the approximation of aerated plug-flow. Submitted for publication.
- [10] Bakker, W.A.M.; Schäfer, T.; Beftink, H.H.; Tramper, J.; De Gooijer, C.D. 1995d. Hybridomas in a bioreactor cascade: modeling and determination of growth and death kinetics. Submitted for publication.